NUREG/IA-0023
Vol.1

International Agreement Report

Assessment of TRAC-PF1/MOD1 Version 14.3 Using Separate Effects Critical Flow and Blowdown Experiments

Volume 1: Text and Tables

Prepared by
B. Spindler, M. Pellissier

Commission of Atomic Energy
CENG/SETH
85X - 38041 Grenoble CEDEX
France

Office of Nuclear Regulatory Research
U.S. Nuclear Regulatory Commission
Washington, DC 20555

January 1990

Prepared as part of
The Agreement on Research Participation and Technical Exchange
under the International Thermal-Hydraulic Code Assessment
and Application Program (ICAP)

Published by
U.S. Nuclear Regulatory Commission

NOTICE

This report was prepared under an international cooperative agreement for the exchange of technical information. Neither the United States Government nor any agency thereof, or any of their employees, makes any warranty, expressed or implied, or assumes any legal liability or responsibility for any third party's use, or the results of such use, of any information, apparatus product or process disclosed in this report, or represents that its use by such third party would not infringe privately owned rights.

Available from

Superintendent of Documents
U.S. Government Printing Office
P.O. Box 37082
Washington, D.C. 20013-7082

and

National Technical Information Service
Springfield, VA 22161

NUREG/IA-0023
Vol.1

International Agreement Report

Assessment of TRAC-PF1/MOD1 Version 14.3 Using Separate Effects Critical Flow and Blowdown Experiments

Volume 1: Text and Tables

Prepared by
B. Spindler, M. Pellissier

Commission of Atomic Energy
CENG/SETH
85X - 38041 Grenoble CEDEX
France

Office of Nuclear Regulatory Research
U.S. Nuclear Regulatory Commission
Washington, DC 20555

January 1990

Prepared as part of
The Agreement on Research Participation and Technical Exchange
under the International Thermal-Hydraulic Code Assessment
and Application Program (ICAP)

Published by
U.S. Nuclear Regulatory Commission

NOTICE

This report is based on work performed under the sponsorship of the Commissariat a l'Energie Atomique (CEA) of France. The information in this report has been provided to the USNRC under the terms of an information exchange agreement between the United States and France (Agreement on Thermal-Hydraulic Research between the United States Nuclear Regulatory Commission and the Commissariat a l'Energie Atomique of France, September 1986). France has consented to the publication of this report as a USNRC document in order that it may receive the widest possible circulation among the reactor safety community. Neither the United States Government nor France nor any agency thereof, nor any of their employees, makes any warranty, expressed or implied, or assumes any legal liability of responsibility for any third party's use, or the results of such use, or any information, apparatus, product or process disclosed in this report, or represents that its use by such third party would not infringe privately owned rights.

ABSTRACT

Independent assessment of the TRAC code was conducted at the Centre d'Etudes Nucleaires de Grenoble of the Commissariate a l'Energie Atomique (France) in the frame of the ICAP.

This report presents the results of the assessment of TRAC-PF1/MOD1 version 14.3 using critical flow steady state tests (MOBY-DICK, SUPER-MOBY-DICK), and blowdown tests (CANNON, SUPER-CANNON, VERTICAL-CANON, MARVIKEN, OMEGA-TUBE, OMEGA-BUNDLE).

EXECUTIVE SUMMARY

1 Objectives

Independent assessment of the TRAC code was performed using the critical flow steady state tests MOBY-DICK and SUPER-MOBY-DICK, and the blowdown tests CANON, SUPER-CANON, VERTICAL-CANON, MARVIKEN, OMEGA-TUBE and OMEGA-BUNDLE. The assessment studies include base case simulation and sensitivity studies (among others nodalization sensitivity, and runs with the choked flow model and with natural choking).

These experiments are devoted to phenomena that occur during blowdown transients in a nuclear power plant, but are not representative of a power plant like plant subscale test facilities. The objective of the assessment of the code using separate effects experiments is then rather to derive conclusions concerning the models and constitutive laws of the code, than conclusions concerning directly plant accident analysis.

2 Run Statistics

All the runs were performed on a CRAY-XMP-2200 computer with the code TRAC-PF1/MOD1 version 14.3.

The extremum CPU time per cell per time step are given hereafter for each experiment (in CPU s *10+3).

MOBY-DICK	: 1.1 - 1.4
SUPER-MOBY-DICK	: 0.6 - 1.2
CANON	: 1.7 - 2.5
SUPER-CANON	: 1.7 - 2.8
VERTICAL-CANON	: 1.1 - 1.2
MARVIKEN	: 1.6 - 1.9
OMEGA-TUBE	: 1.3 - 1.6
OMEGA-BUNDLE	: 1.4 - 1.6

The largest CPU times per cell per time step correspond to the CANON and SUPER-CANON tests with a break equal to the pipe diameter, for which the blowdown transients are very fast (about 1 s from the opening of the break until the atmospheric pressure is reached).

3 Conclusions

3.1 General Agreement

The general agreement between the critical flow and blowdown tests and TRAC is moderate: the major trends are correctly predicted, and the thermal hydraulic phenomena are rather properly modelled. However, TRAC values are frequently outside the data uncertainties.

3.2 Critical Flow

The use of the choked flow model is convenient for fast transient tests, like CANON, SUPER-CANON, VERTICAL-CANON, OMEGA-TUBE and OMEGA-BUNDLE tests, for which it works well.

Similar results are obtained with natural choking and the choked flow model for steady state or low transient tests without interphase desequilibrium (part of MOBY-DICK, SUPER-MOBY-DICK and MARVIKEN tests).

The predictions with natural choking are far from the data for fast transients tests with two phase flow at the break (CANON, SUPER-CANON, OMEGA-TUBE, OMEGA-BUNDLE). When the break flow rapidly becomes single phase vapor flow, the discrepancy with the data is smaller than for the other tests (CANON-VERTICAL). The lack of a virtual mass term in natural choking probably takes part in the bad prediction of fast transients.

The lack of a thermal desequilibrium model in the choked flow model yields a worse agreement with data than natural choking for steady state or low transients tests with interphase desequilibrium (part of MOBY-DICK, SUPER-MOBY-DICK and MARVIKEN tests).

3.3 Constitutive Laws

No irremediable failure in the constitutive laws of TRAC was found. However some improvements should be made, concerning the CHF correlation, the boiling inception model and the interfacial shear stress coefficient.

4 Recommended Code Improvements

4.1 Critical Heat Flux Correlation

The Biasi CHF correlation used in TRAC is not suitable for low qualities and for large mass flow rates. Too early boiling crisis are then obtained for OMEGA-TUBE tests.

A CHF correlation more suitable for low qualities and large mass flow rates is needed.

4.2 Break Flow

The use of the choked flow model gives poor agreement between TRAC and data for steady state and low transient tests with significant interphase thermal desequilibrium. On the other hand, too fast transients are predicted with natural choking for fast blowdown transients, and the lack of a virtual mass term probably takes part in this discrepancy.

Improvements are needed in order to predict break flows without the help of any model. The addition of a virtual mass term may give better agreements. Meanwhile an improvement of the choked flow model is needed in order to take into account the interphase thermal desequilibrium.

4.3 Delayed Boiling Model

The predicted boiling inception corresponds to the saturation pressure. The inception of boiling is then predicted too early in the simulation of quite all the tests.

A delayed boiling model is needed.

4.4 Bernoulli Equation

In case of flow area variations, the predicted pressure drops do not follow the Bernoulli equation in liquid single phase flow. The discrepancy between the predicted and measured pressure drops is embarrassing in the simulation of some tests.

The adequacy between the predicted pressure drops in single phase flow and the Bernoulli equation, in case of flow area variations, is needed.

4.5 Interfacial Shear Stress

The sharp decrease of the interfacial shear stress coefficient at the transition between bubble-slug and annular flow yields large void fraction oscillations at low pressure (less than 1 Mpa), in case of vertical upflow. In the same conditions, but at the transition between bubble and slug flow regime, where the interfacial shear stress coeeficient also decreases, low void fraction oscillations may occur. However, these oscillations are reduced when large cell sizes are used.

More smooth decreases of the interfacial shear stress coefficient at the transitions between bubble and slug flow, and between bubble-slug and annular flow, for low pressures, are needed.

4.6 Rod Wall Thickness

An axially varying rod wall thickness model is needed, in order to obtain more realistic rod wall temperatures in the simulation of the OMEGA-BUNDLE tests.

4.7 Time Step

In the simulation of fast transients with fine mesh at the break (little cell sizes and large velocities), a Courant stability criterion calculated in subroutine TF1DS1 becomes very limitative. This was not found in the runs performed with version 13.0 of the code, where the value of parameter CSF1D was 1*10+6, instead of 1*10+3 in version 14.3.

The value of parameter CFS1D in subroutine TF1DS1 is questionable.

TABLE OF CONTENTS

LIST OF TABLES

LIST OF FIGURES

Figure No. Page of Volume 2

Figure No. Page of Volume 2

Figure No. Page of Volume 2

Figure No. Page of Volume 2

Figure No. Page of Volume 2

Figure No. Page of Volume 2

Figure No. Page of Volume 2

1 INTRODUCTION

1.1 Background

The **International Code Assessment and Applications Program** (ICAP) is an international cooperative reactor safety research program organized by the Office of Nuclear Regulatory Research, United States Nuclear Regulatory Commission (USNRC) in 1985 to provide an independent assessment of USNRC sponsored thermal-hydraulic codes. The codes are developed for analysing nuclear power plant response to postulated transients and loss of coolant accidents in light water reactors. The assessment results from the ICAP are used to qualitatively evaluate the code, and also to quantify code uncertainty. The ultimate goal of the code assessment program is to use the quantification of code uncertainty for scaled applications of the code to determine the accuracy of the code for nuclear power plant application.

The **Commissariat à l'Energie Atomique** of France has joined the ICAP in september 1986. The code assessment program of the CEA in the frame of the ICAP includes mainly separate effects tests conducted in the Centre d'Etudes Nucléaires de Grenoble.

Since there is a scarcity of plant transient or accident data, the code assessment has to rely heavily on simulation of the transients conducted in plant subscale test facilities. It is also important to determine wether the thermal-hydraulic phenomena that are expected to control the transients in a nuclear power plant can be properly modelled, and to assess the constitutive laws of the codes. This is achieved by conducting separate effect experiments, focusing on a particular phenomenon and performed in a reduced or full scale.

1.2 Tests Selection

1.2.1 Experiments

The CEA supported continuous efforts to provide comprehensive separate effects experiments. Many of them are devoted to phenomena that occur during postulated blowdown transients in a nuclear power plant, and were conducted in the Centre d'Etudes Nucléaires de Grenoble: the MOBY-DICK and SUPER-MOBY-DICK steady state critical flow tests, the CANON, SUPER-CANON, VERTICAL-CANON, OMEGA-TUBE and OMEGA-BUNDLE blowdown tests. The CEA was also participant in the MARVIKEN full scale critical flow tests international program, conducted in the Marviken power station in Sweden.

The succession of these experiments corresponds to an increasing complexity and representativity of a nuclear power plant. The simpler experiments (MOBY-DICK, SUPER-MOBY-DICK, CANON, SUPER-CANON, VERTICAL-CANON) are adiabatic tests in order to deal only with hydrodynamic phenomena, and the test sections of these experiments have not been designed to be representative of whatever may exist in a nuclear power plant, but essentially to allow accurate and significant measurements, in order to obtain a better understanding of the basic phenomena that occur during a blowdown. The more complex experiments (OMEGA-TUBE, OMEGA-BUNDLE) include an heated tube or rod bundle, simulating the core, and capacities simulating the primary circuit volume.

The **MOBY-DICK** tests are devoted to steady state low pressure and low quality critical flows, whereas the **SUPER-MOBY-DICK** tests are devoted to steady state high pressure and high velocity critical flows, both in vertical tubes of 14 or 20 mm inside diameter.

The **CANON** and **SUPER-CANON** tests are devoted to adiabatic blowdown transients in a simplified geometry consisting in a horizontal tube of 0.1 m inside diameter. The CANON tests are conducted with an initial pressure of 3.2 MPa, and the SUPER-CANON tests with an initial pressure of 15 MPA corresponding to the pressure in the primary system of a PWR.

The **VERTICAL-CANON** tests are devoted to adiabatic blowdown transients in a simplified geometry consisting in a vertical tube of 0.1 m inside diameter, with a small break at the top. The VERTICAL-CANON tests are conducted with initial pressures of 5 through 15 MPa.

The **MARVIKEN** Critical Flow Tests are devoted to adiabatic blowdown transients in a reactor vessel followed by a discharge pipe and a nozzle, which supports rupture discs. The tests are conducted with an initial pressure of 5 MPa, with subcooled conditions in the vessel and different nozzle lengths and diameters.

The **OMEGA-TUBE** tests are devoted to blowdown transients in a simplified geometry consisting in a vertical heated tube of 0.012 m inside diameter and 3.66 m length simulating the reactor core, connected upstream and downstream to capacities which simulate the primary circuit volume, and support the nozzles preceeding the breaks. The OMEGA-TUBE tests are conducted with an initial pressure of 16 MPA corresponding to the pressure in the primary system of a PWR.

The **OMEGA-BUNDLE** tests are devoted to blowdown transients in a simplified geometry consisting in a vertical bundle of 36 electrically heated rods in full length simulating the reactor core, connected upstream and downstream to capacities which simulate the primary circuit volume, and support the nozzles preceeding the breaks. The OMEGA-BUNDLE tests are conducted with an initial pressure of 13 MPA representative of the pressure in the primary system of a PWR.

1.2.2 Criteria for Tests Selection

Among the numerous tests performed for each experiment, some were selected for code assessment. The criteria for selection are stated hereafter.

Thermohydraulic conditions of the test are as close as possible of the anticipated conditions to be encountered during an accident on reactor. The range of parameters is as large as possible; the values of the parameters of all the tests of a facility are inside the range of the parameters of the selected tests. Tests have significant features: that is to say, regarding some special effects, they are illustrated by the selected tests. Experimental results, i.e. measurements, are accurate enough, and reliable. Tests are choosen in such a way that as few tests as possible are needed to achieve the previous goals.

1.3 Objectives

The objective of this report is to present the results of the code simulations and the comparisons with the experimental data for tests selected from the MOBY-DICK and SUPER-MOBY-DICK critical flow tests, the CANON, SUPER-CANON, VERTICAL-CANON, MARVIKEN, OMEGA-TUBE and OMEGA-BUNDLE blowdown tests.

The experiments are devoted to phenomena that occur during blowdown transients in a nuclear power plant, but are not representative of a power plant like plant subscale test facilities. The objective of the assessment of the code using separate effects experiments is then rather to draw conclusion concerning the models and constitutive laws of the code, than to derive conclusions concerning plant accident analysis.

1.4 Report Outline

Chapters 2 through 9 present the bulk of the assessment work, each chapter corresponding to a single experiment, in the following succession: MOBY-DICK, SUPER-MOBY-DICK, CANON, SUPER-CANON, VERTICAL-CANON, MARVIKEN, OMEGA-TUBE and OMEGA-BUNDLE.

Each chapter opens with the test section description, including a description of the measurements performed. It is followed by the code input model, and then by the base case calculation results and run statistics. Sensitivity studies are then presented, including always nodalization sensitivity and results obtained with natural choking and with the choked flow model, and finally the conclusion derived from the code assessment using the considered experiment. The tables, including typical input data decks, are inserted after each chapter. The figures are

presented in volume 2 of this report, in order to provide a better reading of together the text and the figures. Overall summary, conclusions and recommendations are presented in chapter 10.

2 MOBY-DICK CRITICAL FLOW EXPERIMENTS

2.1 Test Description

The MOBY-DICK critical flow steady state tests were conducted in the Service des Transferts Thermiques of the Centre d'Etudes Nucléaires de Grenoble (France), during the years 1971 through 1975 (test section 1: Réocreux, 1974, test sections 2 and 3: Guizouarn et al., 1975).

2.1.1 Test Sections

The MOBY-DICK tests were conducted with three different test sections, each for vertical upflow.

The lower part of **test section 1** consists of a vertical straight pipe of 20 mm inside diameter and 2.160 m length, including 5 pressure taps. The upper part of test section 1 consists of a vertical straight pipe section of 20 mm inside diameter and 0.285 m length, followed by a 7 degrees diverging nozzle 0.327 m long, and another straight pipe of 60 mm inside diameter and 0.208 m length. The upper part is instrumented with 35 pressure taps.

The lower part of **test section 2** consists of a vertical straight pipe of 14 mm inside diameter and 2.426 m length, including 4 pressure taps. The upper part of test section 2 consists of a vertical straight pipe of 14 mm inside diameter and 0.245 m length, followed by a 7 degrees diverging nozzle 0.2536 m long, and another straight pipe of 45 mm inside diameter and 0.2816 m length. The upper part is instrumented with 22 pressure taps.

The lower part of **test section 3** consists of a vertical straight pipe of 29.5 mm inside diameter and 2.227 m length, followed by a converging nozzle 0.130 m long, and a straight pipe of 14 mm inside diameter and 0.069 m length. The lower part is instrumented with three pressure taps. The upper part of test section 3 is the same as the upper part of test section 2.

The two parts of test sections 2 and 3 have not the same roughness (the upper part is smooth).

2.1.2 Measurements

The diametral **density** is measured at several locations along the test section by the X-rays absorption technique, for test section 1 only. The measurement error is evaluated to 5 %.

The **pressure** is measured by pressure taps implemented along the test sections. Results are given with an accuracy of 50 Pa for the measurements in test section 1, and with an accuracy of 500 Pa for the measurements in test section 2 and 3.

The fluid **temperature** at the inlet and outlet of the test sections is measured by chromel-alumel thermocouples, with an uncertainty of 0.1 K.

The **mass flow rate** is measured by a turbine flow meter with an uncertainty of 1 %.

2.1.3 Test Matrix

The tests with section 1 were conducted for three pressures (0.150, 0.175 and 0.200 MPa) and four mass flow rates (4.2, 6.5, 8.7 and 10.3 Mg/m2.s).

The tests with section 2 were conducted for one pressure (0.20 MPa) and four mass flow rates (6.5, 8.5, 10.2 and 11.9 Mg/m2.s). The tests with section 3 were conducted for four mass flow rates (5.4, 6.9, 7.5 and 10.2 Mg/m2.s) at the pressure of 0.35 MPA, and for four mass flow rates (9.0, 11.7, 13.3 and 14.7 Mg/m2.s) at the pressure of 0.7 MPa. For each fixed value of the critical pressure and mass flow rate, two through five tests are conducted, with a reduction of the outlet pressure. If the inlet pressure remains the same, then the flow is under critical conditions.

The following tests were selected for TRAC simulation in the frame of the ICAP:

Test section 1:
Test 403: P=0.15 MPa, G= 4 Mg/m2.s, T=390 K.
Test 408: P=0.15 MPa, G=10 Mg/m2.s, T=389 K.
Test 455: P=0.20 MPa, G=10 Mg/m2.s, T=398 K.

Test section 2:
Test 79: P=0.20 MPa, G=10 Mg/m2.s, T=398 K.

Test section 3:
Test 172: P=0.70 MPa, G=13 Mg/m2.s, T=447 K.

2.2 Input Model

Tables 2.1 give typical input data decks used for the MOBY-DICK simulations.

2.2.1 Components

The test section is modelled with a PIPE component.

Two BREAK components, one at the entrance and the other at the exit of the test section, are used to impose the pressure boundary conditions. The temperature is imposed at the entrance in the BREAK component.

The entrance and exit BREAK lengths are equal respectively to the first and last cell length, in order to impose the entrance and exit pressure at the exact location where they are measured.

2.2.2 Modalization

In order to compare predictions with data near the throat, where the pressure and void fraction variations are very large, a fine mesh is used at the throat (0.02 m). Simulations are made without the choked flow model (option ICFLOW=0).

The size of the cells is increasing from the throat to the ends of the tube, until 0.45 m or 0.50 m at the inlet, and 0.08 or 0.09 at the outlet. Twenty-six cells are used to model test section 1, and twenty-five for tests sections 2 and 3 (fig. 2.1).

In order to obtain a valuable comparison between tests, the same inlet position for each test must be used, as explained in paragraph 2.5.1. The inlet pressure at position ZA (ZA=-2.395 m with Z=0 at the throat) is therefore extrapolated from the other experimental pressures for test 455, where experimental pressure PA at ZA is missing. In the same way, an inlet pressure PA1 at position ZA1 (ZA1=-2.395 m) is extrapolated from pressures PA at ZA (ZA=-2.433 m) and PD at ZD (ZD=-0.723 m) for test 79 performed with test section 2. The value PA1=0.378 MPa is obtained.

For test 172 performed with test section 3 only the measured pressure PD at ZD (ZD=-0.327 m) is available. The lower part of test section 3 is therefore modelled as the lower part of test section 2 (14 mm diameter, same friction factor). The inlet pressure PA1 at ZA1 is extrapolated from the experimental pressure PD at ZD and the calculated pressure drop between ZA1 and ZD. The value PA1=1.078 MPa is obtained.

2.2.3 Friction Factor

Pressure measurements located before the boiling inception point, in the lower part of the test sections, give informations to fit the wall friction factor. Neglecting the acceleration term and the variation of the physical properties of the fluid gives the following pressure gradient (with TRAC nomenclature):

DP/DZ = rho * g + 2 * f * rho * V * V / Dh,

where

f = a / Re**0.2 and Re = rho * V *Dh / mu

are the friction factor and Reynolds number.

Measurements give DP, DZ and V; the physical properties rho and mu are taken from the code. The value of the coefficient a fitted from the experimental results are presented in table 2.2.

The experimental value of the coefficient **a** is compared to the standard value of the code, which is 0.046. The conclusion is that for test section 1 and the upper part of test section 2, the experimental value corresponds to the standard value (smooth tube). For the lower part of test section 2 the standard value is too low: an additional friction factor is used (FRIC option). The value of FRIC is calculated from the following equation:
FRIC = 2 * (**f**exp - **f**code).
For test 79 (with the measured value of V), the value FRIC=1.7*10-3 is obtained. For test 172, conducted with test section 3, no sufficiently pressure measurements exist to fit the coefficient, and the same values as for test 79 are used.

2.2.4 Initial Conditions

The following initial conditions are imposed in each cell of the PIPE component: void fraction is zero, vapor and liquid velocity are 0.1 m/s, vapor and liquid temperature are the inlet temperature, pressure is 0.2 greater as the saturation temperature corresponding to the inlet temperature.

The time step is free, with an initial value of 1*10-3 s. The code is run with fixed boundary conditions to reach a steady state for each test.

2.3 Code Predictions and Comparisons with Data

2.3.1 Oscillations

The run are pursued until 20, 40 or 60 seconds real time without obtaining a steady state because oscillations occur (fig. 2.2). For tests 403, 406 and 79, the amplitude of the mass flow rate oscillations is lower than the data uncertainty (1 %). For test 455, the amplitude of the oscillations is 2.5 %, and for test 172, it is 5.5 %.

These oscillations are due to the small length of the cells at the throat on one hand (see the nodalization sensitivity study paragraph 2.5.2), and to the abrupt decrease of the interfacial shear stress for a void fraction of 0.75, corresponding to the transition between bubble -slug flow and annular flow regime, on the other hand (for test 403 only).

2.3.2 Boiling Inception

In the code predictions, boiling begins when the pressure becomes lower than the saturation pressure, whereas in the experimental data boiling begins with a liquid overheating of 2 through 3 K. A delayed boiling model is missing in the code.

2.3.3 Critical Flow

Table 2.3 compares the measured and calculated values (relative to the position ZAi) of the critical mass flow rate for each test. Test 403 at low mass flow rate gives the worst results. For this test, the calculated void fraction at the throat is large, and very different from the measured void fraction, which explains a different behavior from the other tests.

It has to be noticed that these critical flow results are relative to a given inlet position, as explained in paragraph 2.5.1.

2.3.4 Pressure and Void Fraction Profiles

The pressure and void fraction profiles are drawn at a given real time of 20, 40 or 60 seconds, depending on the test (fig. 2.3). Their time variations due to the oscillations are weak.

The measured and calculated pressure lines coincide at the inlet position ZAi, and then diverge in proportion of the difference between the measured and calculated mass flow rates (the slope of the pressure line in the single phase region is proportional to the squared mass flow rate).

The boiling inception leads to an inflexion of the pressure line, which is predicted at a too high pressure (lack of a delayed boiling model), but at positions not far from the experimental ones (except for test 403): the calculated pressure difference between the inlet and the boiling inception point is lower than the measured pressure difference, with a discrepancy which roughly corresponds to the difference between the measured and calculated boiling inception pressures. The measured and predicted void fraction lines are then not far one from the other. For test 403 at lower mass flow rate, the pressure differences have not the same order of magnitude than for the other tests, and the boiling inception point is predicted far from the experimental one. The void fraction lines are then very different.

2.4 Run Statistics

The runs are performed on a CRAY-XMP-2200 computer with TRAC-PF1/MOD1 version 14.3. The run statistics are given on table 2.4, and figures 2.4 and 2.5 show typical plots of the time step and CPU time versus real time.

For test 403, the time step is lower than for the other tests: void fraction oscillations, corresponding to the transition between bubble-slug flow and annular flow in the interfacial shear stress, occur in addition to the oscillations that exist for the other tests.

2.5 Sensitivity Studies

2.5.1 Entrance Location

Two simulations of test 408 are compared, the first corresponding to the reference run (inlet position ZA = - 2.395 m), and the other performed with a shortened test section, with experimental pressure PD imposed at inlet position ZD = - 0.825 m). The results are given on table 2.6 and figure 2.6.

The two simulations lead to very different results in terms of critical mass flow rates, corresponding to very different pressure line slopes. If the pressure line obtained with the run performed with pressure PD imposed at position ZD is extended until position ZA, a pressure PA' is obtained, lower of 0.327 MPa from the experimental pressure PA. In other words, imposing the experimental pressure at one or another location is equivalent to impose one or another pressure at the same location. Hence it is seen that the predicted critical flow depends on the inlet position choosen by the code user, or on the pressure taps position choosen by the experimentators.

The comparison is made for test 408, with a high mass flow rate, and with two positions ZA and ZD far one from the other, two conditions which enlarge the differences between the results of the two runs. Nevertheless, the entrance location sensitivity is high, and the predicted mass flow rates are relative to a given entrance position, and are not absolute ones. Comparisons between tests have then to be made with the same entrance location for each test, wich is choosen to be -2.395 m upstream the throat.

The MOBY-DICK experiments are useful to assess the boiling model at low pressure. The more interesting part in the tests is the region after the boiling inception point, where a two phase flow exists. The more the single phase inlet region is long, the few the two phase region is significant, with regard to the entire pressure drop between entrance and exit, the best seems to be the predicted flow rate.

2.5.2 Nodalization

Runs were performed with a cell size at the throat of 0.005, 0.04 or 0.08 m instead of 0.02 m for the reference runs.

The results show that for sufficiently large cells at the throat, a steady state is obtained, except for test 403, for which void fraction oscillations still remains (fig. 2.7). The pressure lines are few sensitive to the meshing. The void fraction lines are more sensitive: a fine mesh is needed to track the boiling inception point (fig. 2.8). The mass

flow rates are sensitive to the size of the throat cells (table 2.7), hence the throat cells must be sufficiently small.

2.5.3 Choked Flow Model

Runs were performed with the choked flow model (option ICFLOW = 2, with choked flow at the throat) instead of natural choking.

For the tests with weak interphase thermal desequilibrium, the results are the same as those obtained with natural choking, with the same nodalization sensitivity.

For test 172, the differences between the two runs are sensitive (fig. 2.9): the discrepancy with the data of the mass flow rate predicted with the choked flow model is -11 %, instead of -7 % for the reference run.

2.6 Summary and Conclusions

The simulation of five MOBY-DICK steady state critical flow tests was performed with the code TRAC-PF1/MOD1 version 14.3. The test sections are modelled with 25 or 26 cells, with throat cells of 0.02 m length, and natural choking is used.

For all the tests, a steady state is not reached, due to the small size of the throat cells, and, in addition for one test, to the abrupt decrease of the interfacial shear stress for a void fraction corresponding to the transition between bubble-slug and annular flow. However, the amplitude of the mass flow rate oscillations is sufficiently low to allow comparisons between tests and data.

The pressure at the boiling inception is overpredicted, due to the lack of a delayed boiling model. The experimental liquid overheating is 2 through 3 K at the boiling inception, which is significant at the low pressures of the tests.

For the runs performed with an inlet position located 2.395 m before the throat, the predicted critical mass flow rates are underpredicted, with deviations of -7 through -15 % for high mass flow rates, and of -39 % for the test at low mass flow rate, for which the void fraction line is far from the data.

The results are very sensitive to the inlet location with regard to the throat, or to the single phase flow length with regard to the total length, and the predicted mass flow rates are therefore relative to a specified inlet location.

The runs performed with different cell sizes at the throat show that the oscillations vanish with sufficiently large cells (0.08 m), except for the test with a void fraction corresponding to the abrupt decrease

of the interfacial shear stress at the transition between the bubble -slug and annular flow regimes. The predicted mass flow rates are sensitive to the cell size.

The runs performed with the choked flow model show a worse agreement with the data only for the test with a significant interphase thermal desequilibrium.

Table 2.1a: MOBY-DICK, typical input data deck for test section 1.

```
FREE
*NUMTCR  IEOS  INOPT  NMAT
6        0     1      0
TRAC-PF1/MOD1 14.3 MD488   ZA 11/5/89

MD488 ZA
ZA * 2D
403 * 408 * 488

************************************************
                    *NAMELIST DATA
 $INOPTS  ICFLOW=0  $END
                    *MAIN CONTROL CARDS
*  DSTEP   TIMET
   0       0.0
*  STDYST  TRANSI  NCOMP  NJUN  IPAK
   1       0       3      2     0
*  EPSO    EPSI    EPSS
   1.0E-3  1.0E-5  1.0E-4
*  OITMAX  IITMAX  SITMAX  ISOLUT
   10      0       10      0
*  NTSV  NTCB  NTCF  NTRP  NTCP
   0     0     0     0     0
*   COMPONENT
     1    5    *  BREAK: INLET
     2    5    *  PIPE
     3    6    *  BREAK : OUTLET
* ()()()()()()()()()()()()()()()()()()()()()()()
   BREAK    1   1             INLET
*  JUN1  IBTY  ISAT  IVOV  IOFF
   1     0     0     0     0
*  DXIN   VOLIN     ALFIN  TIN     PIN
*  ZA                      403
*  0.480  1.41E-4   0.     300.8   0.1900E+6
*  ZA                      406
*  0.480  1.41E-4   0.     300.0   0.2632E+6
*  ZA   PA'                406
*  0.480  1.41E-4   0.     300.0   0.2300E+6
*  ZA   P                  406
*  0.480  1.41E-4   0.     300.0   0.2633E+5
*  ZA   TE                 406
*  0.480  1.41E-4   0.     300.1   0.2632E+6
*  2D                      406
*  0.290  0.70E-6   0.     300.0   0.1930E+6
*  ZA                      488
   0.480  1.41E-4   0.     300.1   0.3141E+6
*  PAIN  CONCIN  RBMX  POFF  BELV
   0.    0.      0.    0.    J.
*  ::::::::::::::::::::::::::::::::::::::::::::::::::
   BREAK   3   3             OUTLET
*  JUN  IBTY  ISAT  IVOV  IOFF
   2    0     0     0     0
*  DXIN   VOLIN    ALFIN  TIN    PIN
* 403
*   .0084  2.70E-4  1.     370.8  0.1180E+6
* 408
*   .0084  2.70E-4  1.     377.8  0.1102E+6
* 408 P OUTLET
*   .0084  2.70E-4  1.     377.8  0.1400E+6
* 488
    .0084  2.70E-4  1.     387.6  0.1050E+6
*  PAIN  CONCIN  RBMX  POFF  BELV
   0.0   0.      0.    0.    0.
*  ::::::::::::::::::::::::::::::::::::::::::::::::::
```

```
   PIPE  2   2                   TEST SECTION
*  NCELLS  NODES  JUN1  JUN2  MAT
*  ZA
   28      0      1     2     0
*  2D
*  22      0      1     2     0
*  ICHF  ICONC  IACC  IPOW
   0     0      0     0
*  RADIN  TH    HOUTL  HOUTV  TOUTL
    .010   .020 0.0    0.0    300.
*  TOUTV  POWIN  POWOFF  RPOWMX  POWSCL
   300.0  0.0    0.0     0.0     0.0
*  *********************************************
* ZA
*DX *  0.45 0.42 0.30 0.20 0.20                 $
* 2D
*DX                           0.20             $
     0.15 0.10 0.08 0.03 .012 0.02             $
     0.08 0.08 0.08 0.077 0.0083               $
*VOL * F    +1.                                $
*FA  * F    +1.                                $
*FRIC* F  0.0                                  $
*GRAV* F  1.0                                  $
* ZA
*HD   * .016 0.08  .0234  .0240  .0273  .0280  $
* 2D
*HD     .012 0.08  .0234  .0240  .0273  .0280  $
              .0322  .0347  .0380  .0446  .0808 $
              0.08 0.08                        $
*********************************************
* ICFLOW=2
* ZA
*ICFLG   .016 0 1 .011 0                       $
* 2D
*ICFLG   .011 0 1 .011 0                       $
*********************************************
*NFF  * F    1    $
*ALPA* F  0.0     $
*VL   * F  0.1    $
*VV   * F  0.1    $
* 403
*TL     F 300.0   $
*TV     F 300.0   $
*P      F 1.04E5  $
* 406
*TL     F 300.0   $



*TV     F 300.0   $
*P      F 1.70E5  $
* 488
*TL *   F 300.1   $
*TV *   F 300.1   $
*P  *   F 2.40E5  $
*
*PA  * F  0.      $
* ()()()()()()()()()()()()()()()()()()()()()()()()()()
*             TIME STEP DATA
*  DTMIN  DTMAX  TEND  RTWFP
   1.E-3  10.    80.   10.0
*  EDINT  GFINT  DMPINT  SEDINT
   10.    1.E-3  80.     1000.0
   -100000.
```

Table 2.1b: MOBY-DICK, typical input data deck for test sections
2 and 3.

```
FREE
*NUMTCR  IEOX  INOPT  NMAT
0        0     1      0
TRAC-PF1/MOD1 14.3 BITS   11/5/88

172
ZA
 TS *172

****************************************************
                    *NAMELIST DATA
 $INOPTS  ICFLOW=0  $END
                    *MAIN CONTROL CARDS
*  DSTEP  TIMET
   0        0.0
*  STDYST  TRANSI  NCOMP  NJUN  IPAK
   1        0       3      2     0
*  EPSO     EPSI     EPSS
   1.0E-3   1.0E-6   1.0E-4
*  OITMAX  IITMAX  SITMAX  ISOLUT
   10       0       10      0
*  NTSV  NTCB  NTCF  NTRP  NTCP
   0      0     0     0     0
*    COMPONENT
     1       5      *  BREAK: INLET
     2       5      *  PIPE
     3       6      *  BREAK : OUTLET
* ()()()()()()()()()()()()()()()()()()()()()()()()()()(
   BREAK    1   1                 INLET
*  JUN1  IBTY  ISAT  IVDV   IOFF
   1      0     0      0     0
*  DXIN    VOLIN      ALPIN  TIN       PIN
*  ZA                        TS
*  0.900  7.70E-6   0.       306.2   0.370E+6
*  ZA                        172
   0.900  7.70E-6   0.       446.6   1.070E+6
*  PAIN  CONCIN   RORB   POFF   BELV
   0.      0.       0.     0.     0.
* ::::::::::::::::::::::::::::::::::::::::::::::::::::
   BREAK   3   3                 OUTLET
*  JUN  IBTY  ISAT  IVDV  IOFF
   2    0      0     0     0
*  DXIN    VOLIN      ALFIN  TIN     PIN
*  TS
    .06     1.27E-4    1.      304.0  0.140E+6
*  172
    .06     1.27E-4    1.      437.4  0.707E+6
*  PAIN  CONCIN  RORB  POFF  BELV
   0.0   0.       0.    0.    0.
* ::::::::::::::::::::::::::::::::::::::::::::::::::::
   PIPE  2   2                   TEST SECTION
*  NCELLS  NODES  JUN1  JUN2  EPST
   25       0      1     2     0
*  ICHF  ICONC  IACC  IPOW
   0      0      0     0
*  RADIN   TH     HOUTL   HOUTV   TOUTL
   .007    .020   0.0     0.0     300.
*  TOUTV  POWIN  POWOFF  RPOWMX  POWSCL
   300.0  0.0    0.0     0.0     0.0
*  ---------------------------------------------------
*DX   * 0.00 0.048 0.26 0.28 0.16                    $
      0.11 0.07 0.04 R12 0.03 0.03                   $
      0.05 0.0030 0.0084 0.00                        $
*VOL  * F    -1.                                     $
*FA   * F    -1.                                     $
*FRIC* 06 1.7E-3   R20 0                             $
*GRAV* F   1.0                                       $
*HD   * R19 0.014  .0184  .0189  .0213  .0230        $
          .0262  .0287  .0323  .0364 R3 0.048        $
* ICFLOW=2
*ICFLG    R14 0 1 R11 0                              $
*NFF * F     1     $
*ALFA* F   0.0     $
*VL  * F   0.1     $
*VV  * F   0.1     $
* TS
*TL     F 306.2    $
*TV     F 306.2    $
*P      F 2.50E5   $
* 172
*TL *   F 446.6    $
*TV *   F 446.6    $
*P  *   F 8.02E5   $
*
*PA  * F   0.      $
```

```
* ()()()()()()()()()()()()()()()()()()()()()()()()()(
*              TIME STEP DATA
*  DTMIN  DTMAX  TEND  RTWFP
   1.E-3  5.     60.   10.0
*  EDINT  GFINT  DMPINT  SEDINT
   2      1.E-2  60.     1200.0
-1000000.
```

Table 2.2: MOBY-DICK, experimental values of the friction factor coefficient.

Test	DP kPa	DZ m	V m/s	10-5*Re	a
403	32.7	2.1	4.36	3.31	0.045
408	90.3	2.1	10.8	8.13	0.047
455	63.9	1.573	10.7	8.62	0.045
79 upper part	7	0.12	10.6	6.03	0.047
79 lower part	119	1.71	10.6	6.03	0.058

Table 2.3: MOBY-DICK, measured and calculated mass flow rate, pressure and void fraction.

Test	403	408	455	79	172
Mass flow rate Mg/m2*s					
Data	4.2	10.3	10.2	10.2	13.3
TRAC	2.6	9.3	8.7	9.2	12.3
Difference %	-39	-10	-15	-10	-7
Throat pressure MPa					
Data	0.151	0.152	0.201	0.204	0.720
TRAC	0.128	0.170	0.229	0.223	0.780
Difference %	-15	+12	+14	+9	+8
Throat void fraction					
Data	0.50	0.05	0.15		
TRAC	0.89	0.07	0.12	0.24	0.60
Difference	+0.39	+0.02	+0.03		

Table 2.4: MOBY-DICK, run statistics.

Test	403	408	455	79	172
Real time s	20.1	60.3	40.0	20.1	20.1
Time step number	428	319	297	237	305
Mean time step s	0.047	0.19	0.13	0.085	0.066
CPU time s	14.2	9.2	9.8	8.4	9.4
CPU time / real time	0.71	0.15	0.24	0.42	0.47
CPU time / (cell*time step)	1.3* 10-3	1.1* 10-3	1.3* 10-3	1.4* 10-3	1.2* 10-3

Table 2.5: MOBY-DICK, comparison of the critical parameters predicted for the test 408 with two different inlet positions.

	Mass flow rate Mg/m2*s	Difference with the data	Throat pressu-rePa	Throat void fraction	Inception boiling pressure MPa
Data	10.3	0 %	0.152	0.05	0.163
Inlet position ZA	9.3	-10 %	0.170	0.07	0.176
Inlet position ZD	6.4	-38 %	0.172	0.09	0.177

Table 2.6: MOBY-DICK, Comparison of the mass flow rates predicted with different throat cells sizes, and discrepancy with the reference.

Cell size m		Test 403	Test 408	Test 455
0.005	Mass flow rate Mg/m2•s Difference %	2.55 -0.4	9.28 0.0	
0.020 (reference)	Mass flow rate Mg/m2•s	2.56	9.28	8.68
0.040	Mass flow rate Mg/m2•s Difference %		9.29 +0.1	
0.080	Mass flow rate Mg/m2•s Difference %	2.77 +8.2	9.41 +1.4	8.86 +2.1

3 SUPER-MOBY-DICK CRITICAL FLOW EXPERIMENTS

3.1 Test Description

The SUPER-MOBY-DICK critical flow steady state tests were conducted in the Service des Transferts Thermiques of the Centre d'Etudes Nucléaires de Grenoble (France), during the year 1980 through 1983 (test section 1: Jeandey et al., 1981, test section 2: Jeandey et al., 1983, test section 3: Jeandey and Gros d'Aillon, 1983).

3.1.1 Test Sections

The SUPER-MOBY-DICK tests were conducted with three different test sections, each for vertical upflow.

Test section 1, named long nozzle with divergent, consists of a vertical straight pipe of 66.7 mm inside diameter and 0.364 m length, followed by a profiled convergent section of 0.100 m length, then by a straight pipe of 20.13 mm inside diameter and 0.363 m length, then by a 7 degrees diverging nozzle 0.437 m long, and finally by a straight pipe of 73.7 mm inside diameter and 0.750 m length.

Test section 2, named long nozzle with sudden expansion, consists of a vertical straight pipe of 87.5 mm inside diameter and 0.300 m length, followed by a profiled convergent section of 0.100 m length, then by a straight pipe of 20.05 mm inside diameter and 0.400 m length, and finally by a straight pipe of 135 mm inside diameter and 1.600 m length (sudden expansion).

Test section 3, named short nozzle, consists of a vertical straight pipe of 87.52 mm inside diameter and 0.300 m length, followed by a profiled convergent section of 0.100 m length, and finally by a straight pipe of 135 mm inside diameter and 2.000 m length (sudden expansion).

3.1.2 Measurements

The **pressure** is measured by pressure taps implemented along the test sections. The upper bound error value, given with 95 % confidence is 0.02 MPa.

The fluid **temperature** at the entrance of the test section is measured by two platinum resistance probes. The upper bound value of the entrance temperature error , given with 95 % confidence, is 0.2 K.

The **mass flow rate** is measured by a turbine flow meter. The upper bound error value is 2 % for flow rates higher than 4 kg/s, and up to

4 % for flow rates of 1 kg/s.

The mean **density** over chords at several locations along the test section is measured using the X-rays attenuation technique, for part of the tests conducted with test section 1 only. The mean error value is about 2 %. The void fraction is calculated from the density measurements, using the following hypotheses: the liquid temperature is the inlet temperature; the vapor temperature is the saturation temperature corresponding to the pressure measured near the density measurement location.

The **power** dissipated in the preheaters is measured in order to calculate the inlet quality through a heat balance, for the tests with positive inlet quality.

For the tests conducted with positive inlet quality, instabilities occured in the loop, and the given values of the measurements errors are not suitable.

3.1.3 Test Matrix

About hundred tests were conducted with test section 1, for mass flux from 10 through 62 Mg/m2.s, pressures from 0.5 through 12 MPa and inlet temperatures from 410 through 600 K. Twelve tests were conducted with test section 2, the conditions of which correspond to twelwe tests of test section 1. Forty tests were conducted with test section 3, the conditions of which correspond to forty tests of test section 1.

The following tests were selected for TRAC simulation in the frame of the ICAP:

Test section 1 (long nozzle with divergent):
Test 1: P = 12 MPa, G = 62 Mg/m2.s, T = 579 K.
Test 2: P = 12 MPa, G = 48 Mg/m2.s, T = 593 K.
Test 3: P = 12 MPa, G = 44 Mg/m2.s, T = 598 K.
Test 4: P = 12 MPa, G = 37 Mg/m2.s, X = 0.05 %.
Test 5: P = 12 MPa, G = 33 Mg/m2.s, X = 2.40 %.
Test 6: P = 4.8 MPa, G = 52 Mg/m2.s, T = 507 K.
Test 7: P = 3.3 MPa, G = 26 Mg/m2.s, T = 507 K.
Test 8: P = 3.1 MPa, G = 22 Mg/m2.s, T = 507 K.
Test 9: P = 3.1 MPa, G = 21 Mg/m2.s, T = 507 K.
Test 10: P = 3.0 MPa, G = 20 Mg/m2.s, T = 507 K.

Density measurements were not included in these tests, but in the following, conducted with similar conditions:
Test 1': P = 12 MPa, T = 579 K.
Test 2': P = 12 MPa, T = 593 K.
Test 3': P = 12 MPa, T = 598 K.
Test 5': P = 12 MPa, X = 3.8 %.
Test 8': P = 3.1 MPa, T = 507 K.

Test section 2 (long nozzle with sudden expansion):
Test 11: P = 12 MPa, G = 62 Mg/m2.s, T = 578 K.
Test 12: P = 12 MPa, G = 47 Mg/m2.s, T = 585 K.
Test 13: P = 12 MPa, G = 42 Mg/m2.s, T = 597 K.

The parameters of test 12, as given in the experiments report, seem to be inconsistent with regard to the values obtained in similar conditions for test 2 in test section 1. As a matter of fact, the conclusions of the experiments report notice that a good agreement is found between the critical mass flow rates measured under the same conditions with divergent and with sudden expansion. After an interview of the experimentators, it seems that the entrance temperature printed in the report has to be suspected. Hence a new test 12' is defined as follows:
Test 12': P = 12 MPa, G = 47 Mg/m2.s, T = 591 K.

Test section 3 (short nozzle with sudden expansion):
Test 14: P = 3.3 MPa, G = 43 Mg/m2.s, T = 507 K.
Test 15: P = 3.0 MPa, G = 21 Mg/m2.s, X = 0.9 %.

3.2 Input Model

Tables 3.1 give typical input data decks used for SUPER-MOBY-DICK simulations.

3.2.1 Components

The test section is modelled with a PIPE component.

Two BREAK components, one at the entrance and the other at the exit of the test section, are used to impose the pressure boundary conditions. The temperature is imposed at the entrance in the BREAK component.

The entrance and exit BREAK lengths are equal respectively to the first and last cell length, in order to impose the entrance and exit pressure at the exact location where they are measured.

3.2.2 Nodalization of the Convergent

3.2.2.1 Definitions

Let us consider the convergent modelled hereafter, where A0 through A3 are the flow areas, V0 through V3 the velocities, and P0 through P3 the pressures. All these values are defined at the cell edges. The pressures P01, P12 and P13 at the cell centers are also defined.

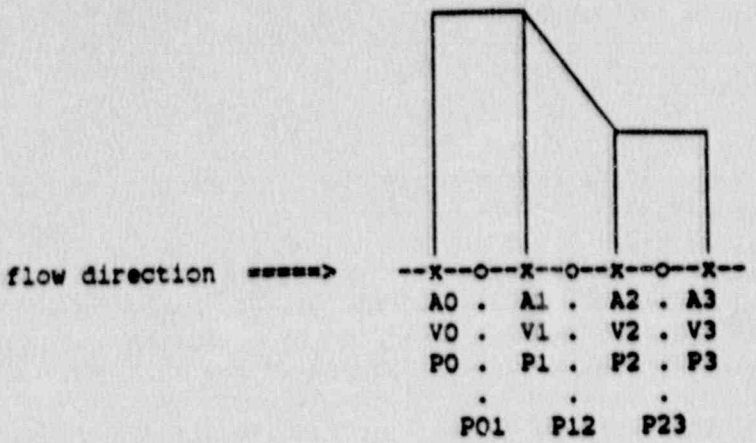

The following hypotheses are made: wall shear stress and gravity pressure drops negligible, liquid single phase flow, constant density. The pressure drop due to the restriction of the flow area is calculated, with the Bernoulli equation on one hand (which corresponds to the data), and like it is predicted by the code on the other hand.

3.2.2.2 Pressure Drop Given by the Bernoulli Equation

The pressure drop P1 - P2, as given by the Bernoulli equation is the following:

$$(P1 - P2) / rho = (V2^2 - V1^2) / 2$$

The mass balance yields:

$$V2 / V1 = A1 / A2$$

x is defined as the flow area ratio; the Bernoulli equation is then written under the following form:

$$(P1 - P2) / rho = V1^2 * (1 - x^2) / 2$$

With our hypotheses, the following equation can also be written, which will be useful for the comparisons:

$$P23 = P2$$

3.2.2.3 Pressure Drop Calculated by TRAC

The staggered mesh scheme used by TRAC yields the following pressure drop (shear stress and gravity terms neglected):

$$(P12 - P23) / rho = V2 * (V2 - V1)$$

Taken into account the mass balance and the definition of x yields:

$$(P12 - P23) / rho = V1^2 * x * (x - 1)$$

The flow areas A0 and A1 are the same, and consequently the velocities V0 et V1 and the pressures P01 and P12, which are equal to P1.

3.2.2.4 Comparison

The difference between the pressure drops calculated by the two methods is the following:
DP(TRAC) - DP(Bernoulli) = rho * Vi**2 * (x - 1)**2 / 2

If the convergent is modelled with several cells in the code, the total pressure drop calculated by TRAC is obtained by addition of the pressure drops calculated between the successive cells.

The comparisons are made for a convergent divided into 1, 2, 5, 10 or 50 cells. The results are given on table 3.2, with values of Vi corresponding to tests 1 and 10 (lower and upper bounds: Vi=8,0 m/s for test 1 and Vi=2,3 m/s for test 10, with rho = 655 kg/m3*s for test 1 and rho = 822 for test 10).

The code TRAC gives a pressure drop corresponding to the Bernoulli pressure drop only with a great number of cells: when the flow area ratio decreases and becomes near 1, the calculated pressure drop becomes near the Bernoulli's one. The use of a great number of cells is then required in order to obtain a realistic simulation of the tests.

Sensitivity studies, presented in paragraph 3.5.2, have led to the choice of a convergent modelled with 25 cells of 0.004 m length. This fine noding allows moreover a fine detection of the predicted boiling inception point, when it is located in the convergent.

3.2.3 Modalisation of the Test Section

In order to compare predictions with data near the throat, where the pressure and void fraction variations are very large, a fine mesh is used at the throat, and natural choking is used. The sensitivity study presented in paragraph 3.5.3 shows that a cell size of 0.004 m is required (same size as in the convergent).

The size of the cells is increasing from the throat and the convergent to the ends of the tube. Fifty-six cells are used to model section 1, fifty-one for section 2, and thirty-six for section 3 (fig. 3.1).

3.2.4 Friction Factor

Experiments were performed in liquid single phase flow in order to evaluate the friction factor. Table 3.3 gives the results obtained for different Reynolds number, where fcode is the code standard friction factor, and fexp the experimental value.

The FRIC parameter is fitted using the following equation:
FRIC = 2 * (fexp - fcode)
The value FRIC = 2.0*10-3 is used for the simulations.

3.2.5 Initial Conditions

The initial values are imposed in each cell of the PIPE component: void fraction is zero, vapor and liquid velocity are 0.1 m/s, vapor and liquid temperature are the inlet temperature, pressure is near the saturation temperature corresponding to the inlet temperature.

The time step is free, with an initial value of 1*10-4 s. The code is run with fixed boundary conditions to reach a steady state for each test, with a steady state convergence criterion of 2*10-2.

3.3 Code Predictions and Comparisons with Data

3.3.1 Steady State

No steady state is reached for tests 10 and 15, with 100 s CPU.

For test 10, the void fraction in the upstream region is weakly oscillating, but the mass flow rate is stable. A run with a steady state convergence criterion of 2.5*10-2 instead of 2.0*10-2 leads to a steady state after 220 time step (real time 4.64 s), with a predicted critical mass flow rate greater of 0.2 % than the predicted one obtained with the reference run.

For test 15, the mass flow rate oscillations are plus or minus 0.1 %, and the void fraction of the upstream cells weakly oscillates. For this test, a modification of the convergence criterion does not alter the results (fig. 3.2).

The better stability of the results obtained for the SUPER-MOBY-DICK simulations compared with the MOBY-DICK simulations (see paragraph 2.3.1), although smaller cell sizes are used for SUPER-MOBY-DICK simulations, is probably due to the high pressure of the SUPER-MOBY-DICK tests (3 MPa and higher) compared to the low pressure of the MOBY-DICK tests (0.7 MPa and lower), for which the constitutive laws are probably less suitable.

3.3.2 Critical Flow

Table 3.4 compares the measured and calculated values of the critical mass flow rates for each test. The predictions are particularly good for the tests with high entrance subcooling, where the two phase flow region is short. They are good for the tests with positive inlet quality, with high inlet void fraction. The worst predictions are obtained for the tests with entrance conditions near saturation, for which the boiling model takes a large part.

The results obtained for tests 12 and 12', compared with the results obtained for tests 1 and 2, confirm the probability of a wrong entrance temperature for test 12.

The simulation of the tests performed in test section 3 (short nozzle with sudden expansion) is in poor agreement with the data. Bidimensional effects are probably significant for these tests.

3.3.3 Pressure Lines

The pressure lines are presented on figures 3.3 through 3.5. The pressure drop in the convergent is overpredicted for the tests with high entrance subcooling, for which the boiling inception point is located downstream the convergent (tests 1, 6 and 11). The fine noding of the convergent is not sufficient to correct the discrepancy with the Bernoulli pressure drop (see paragraph 3.5.2). For tests 1 and 6, the void fraction at the throat is sufficiently low, so that the entrance in the divergent leads to a weak pressure increase, due to the enlargement, which does not appear in the data. For these tests, the pressure increase in the divergent is located more downstream than for the data: the predicted condensation is too slow.

For the tests with entrance conditions near saturation (tests 8, 9 and 10), the large error concerning the critical flow leads to an overpredicted pressure at the convergent outlet. In the divergent, the void fraction is overpredicted and the pressure underpredicted.

A rather good agreement is obtained for the pressure lines relative to the tests with positive entrance quality (tests 4, 5 and 15).

3.3.4 Void Fraction Lines

The void fraction lines are presented on figures 3.3 for the tests with void fraction measurements. The boiling model predicts a boiling inception point located at the saturation conditions, but the data accuracy is not sufficient to track precisely the experimental boiling inception point, which is generally located in the convergent, where the pressure gradient is very large. The predicted void fraction lines indicate a slow initial void fraction increase, and are rather in good agreement with the data in the fully developed boiling region. However, the agreement between a specified test and TRAC may be good for the void fractions but moderate or bad for the pressures and the mass flow rate. It is difficult to draw a conclusion concerning the boiling inception point.

3.4 Run Statistics

The runs are performed on a CRAY-XMP-2200 computer with TRAC-PF1/MOD1 version 14.3. The run statistics are given on table 3.5, and figures 3.6 and 3.7 show typical plots of the time step and CPU time versus real time. A constant value of the time step is rapidly reached for all the tests, including tests 10 and 15 for which no steady state is reached.

3.5 Sensitivity Studies

3.5.1 Entrance Location

The MOBY-DICK simulations made with TRAC (chapter 2) have shown a great sensitivity to the entrance location. For the SUPER-MOBY-DICK tests, the conditions are very different: in the region located upstream the convergent, the pipe diameter is large (0.0667 m), hence the shear stress is low, and the single phase pressure drop in the upstream part of the pipe is weak. Moreover, this pressure drop is very weak with regard to the abolute value of the pressure on one hand (3 MPa for the lower pressure, instead of 0.15 through 0.7 MPa for the MOBY-DICK tests), and to the pressure drop in the convergent on the other hand.

Nevertheless a run was made in simulation of test 1, with the experimental pressure P1 imposed at location Z1 (0.037 m upstream the convergent) on one hand, and with pressure P0 imposed at location Z0 located 1.537 m upstream the convergent on the other hand. P0 is derived from P1 and the experimental value of the wall shear stress (P0 = 12.015 MPa for test 1). The same result is obtained for the two runs. The entrance location sensitivity is negligible for the SUPER-MOBY-DICK tests.

3.5.2 Nodalization of the Convergent

Runs were performed in simulation of test 6 (boiling begins after the convergent), and of test 10 (two phase flow in the convergent), with a convergent modelled with 1, 2, 5, 10, 25 or 50 cells. These runs were performed with throat cells of 0.02 m, before the final choice of the throat cells length, but the conclusions concerning the convergent nodalization do not change. The results are given on table 3.6.

It is found that the more the cells number increases, the more the critical mass flow rate, or the upstream velocity V1, increases. Hence the term V1**2 in the pressure drop formulation increases, and the predicted pressure drop decreases slowly when the cells number increases. Moreover, the pressure drop depending on the squared velocity, a low velocity difference yields a large pressure drop difference: with 50 cells, the difference between TRAC and the data is relatively large in terms of pressure drop. The pressure lines obtained with the different runs are presented on figure 3.8. The pressure being calculated at the cell center, there is a weak difference between the measured and calculated locations of the pressures at the exit of the convergent.

In order to obtain realistic simulations, a fine mesh of the convergent is required. For 50 cells, the CPU time may be long; moreover, the accuracy of the mass flow rates measurements is 2 % for the high flow rates, and 4 % for the low flow rates. Table 3.6 shows that the difference between the models with 25 and with 50 cells are weak. Hence the choice of 25 cells was made for the reference runs.

3.5.3 Throat Cells Nodalization

Runs were performed with a cell size at the throat of 0.002, 0.01 or 0.02 m instead of 0.004 m for the reference runs.

The nodalization sensitivity becomes significant for cells of 0.02 m (table 3.7 and figures 3.9). The choice of the lenghth 0.004 m for the reference runs was made after this sensitivity study, and also in order to obtain precisely the pressure and void fraction profiles at the throat, where their gradient are large. The size 0.004 m corresponds also to the size of the cells in the convergent.

3.5.4 Friction Factor

Runs were performed whitout an adaptation of the code friction factor to the measured one (with FRIC = 0). The critical mass flow rates obtained differ from the reference values from factors that are not higher than the accuracy of the measured mass flow rates (+2.8 % for test 1, +1.4 % for tests 5 and 10), and the pressure and void fraction lines are little modified.

3.5.5 Choked Flow Model

Runs were performed with the use of the choked flow model (option ICFLOW = 2, with choked flow at the throat), and with throat cells of 0.004 m and 0.02 m (table 3.8).

The difference with the reference runs is large for the tests with a large thermal disequilibrium (high inlet subcooling), because the choked flow model is based on the hypothesis of thermally homogeneous flow. The choked flow model is not planned for a fine mesh, and hence the pressure lines are different for the two nodalizations tested (fig 3.10).

3.6 Summary and Conclusions

The simulation of fifteen SUPER-MOBY-DICK steady state critical flow tests, with divergent and with sudden expansion, was performed with the code TRAC-PF1/MOD1 version 14.3. The test sections are modelled with 36, 51 and 56 cells, with throat cells of 0.004 m length, and the natural choking is used.

The staggered scheme used by TRAC does not respect the Bernoulli equation for liquid single phase flow regime. A fine meshing (cells of 0.004 m length) of the convergent located at the entrance of the test sections is then required, in order to obtain realistic simulations.

No steady state is reached for only two tests. However the mass flow rate oscillations are much lower than the data accuracy. The better stability of the SUPER-MOBY-DICK simulations, compared to the MOBY-DICK simulations, is attributed to the higher pressure of the SUPER-MOBY-DICK tests, for which the constitutive laws are probably more suitable.

The predicted critical mass flow rates are in good agreement with the data (discrepancy less than 5 %) for the tests with high entrance subcooling, for which the two phase flow region is short. The discrepancies between predictions and data are larger (up to 10 %) for the tests with high inlet void fraction. The largest discrepancies (up to 23 %) are obtained for the tests with entrance conditions near saturation, for which the boiling model takes a large place.

The boiling model predicts a boiling inception point located at the saturation conditions, but the data accuracy is not sufficient to track precisely the experimental boiling inception point. The predicted void fraction lines indicate a slow initial void fraction increase, and are rather in good agreement with the data, even if the agreement concerning the pressures and mass flow rate is poor.

The sensitivity at the throat cells size becomes significant for a cell length of 0.02 m. The runs performed without an experimentally fitted friction factor lead to critical mass flow rates larger than the reference ones, but with discrepancies not larger than the experimental uncertainties.

The runs performed with the choked flow model give a discrepancy with the data larger than the reference run for the tests with high inlet subcooling, corresponding to a large interphase thermal desequilibrium. For the other tests, the discrepancy is low.

Table 3.1a: SUPER-MOBY-DICK, typical input data deck, test section 1.

```
FREE
*NUMTCT  IEOS  INOPT  NMAT
0        0     1      0

TRAC-PF1/MOD1 14.2 SMD      04/7/88

  TEST 10
1*2*3*4*5*6*7*8*9*10

*****************************************************
                    *NAMELIST DATA
 $INOPTS  ICFLOW=0  $END
                    *MAIN CONTROL CARDS
*  DSTEP  TIMET
   0      0.0
*  STDYST  TRANSI  NCOMP  NJUN  IPAK
   1       0       3      2     0
*  EPSO     EPSI     EPSS
   1.0E-3   1.0E-9   2.00E-2
*  OITMAX  IITMAX  SITMAX  ISOLUT
   10      0       10      0
*  NTSV  NTCB  NTCF  NTSP  NTCP
   0     0     0     0     0
*   COMPONENT
    1      5    *  BREAK: INLET
    2      5    *  PIPE
    3      5    *  BREAK : OUTLET
* ()()()()()()()()()()()()()()()()()()()()()()()()(
   BREAK   1   1                 INLET
*  JUN1  IBTY  ISAT  IVDV   IOFF
   1     0     0     0      0
*            DXIN   VOLIN    ALPIN   TIN    PIN
*TEST    1  0.014  4.00E-9  0.       579.0  11.00000
*TEST    2  0.014  4.80E-9  0.       *92.8  12.00000
*TEST    3  0.014  4.80E-9  0.       587.7  12.00000
*TEST    4  0.014  4.80E-9  .00403   587.9  12.00000
*TEST    5  0.014  4.80E-9  .1007    587.0  11.87400
*TEST    6  0.014  4.00E-9  0.       507.1   4.82000
*TEST    7  0.014  4.80E-9  0.       507.1   3.32000
*TEST    8  0.014  4.80E-9  0.       507.1   3.10000
*TEST    9  0.014  4.80E-9  0.       507.1   3.07000
*TEST   10 *0.014  4.80E-9  0.       507.2   3.02400
*  PAIN  CONCIN  RCON  POFF  BELV
   0.    0.      0.    0.    0.
*  ::::::::::::::::::::::::::::::::::::::::::::::::::
   BREAK   3   3                 OUTLET
*  JUN  IBTY  ISAT  IVDV  IOFF
   2    0     3     0     0
*            DXIN  VOLIN    ALPIN TIN    PIN
*TEST    1   .300  1.04E-9  1.    574.0  6.00200
*P OUT   1   .300  1.04E-9  1.    574.0  8.00000
*TEST    2   .300  1.04E-9  1.    570.8  8.00400
*TEST    3   .300  1.04E-9  1.    570.3  8.39000
*TEST    4   .300  1.04E-9  1.    571.9  8.43000
*TEST    5   .300  1.04E-9  1.    570.3  8.07000
*TEST    6   .300  1.04E-9  1.    480.0  2.61000
*TEST    7   .300  1.04E-9  1.    480.0  2.33000
*TEST    8   .300  1.04E-9  1.    480.8  2.24300
*TEST    9   .300  1.04E-9  1.    480.3  2.21200
*TEST   10 * .300  1.04E-9  1     480.7  2.10150
*  PAIN  CONCIN  RCON  POFF  BELV
   0.0   0.      0.    0.    0.
*  ::::::::::::::::::::::::::::::::::::::::::::::::::
```

```
 PIPE  2   2                  TEST SECTION
*  NCELLS  NODES  JUN1  JUN2  MAT
   99      0      1     2     0
*  ICHF  ICONC  IACC  IPOW
   0     0      0     0
*  RADIN  TH    HOUTL  HOUTV  TOUTL
   .010   .030  0.0    0.0    300.
*  TOUTV  POWIN  POWOFF  RPOWMX  POWSCL
   300.0  0.0    0.0     0.0     0.0
*  -----------------------------------------------------
*DX  *        0.030       R30 0.004                  S
        0.008 0.02  0.03  0.080 0.093                S
        0.05  0.04  0.03  0.023 0.020                S
        0.014 0.01  0.008 R4 0.004                   S
        0.008 0.01  0.014 0.02  0.023                S
        0.03  0.04  0.06  0.08  0.147                S
        0.21  0.38                                   E
*VOL * -1.                                           S
1.382228-8 1.371218-8 1.331088-8 1.272628-8 S
1.104438-8 1.080088-8 0.968438-8 0.880978-8 S
0.721838-8 0.575088-8 0.448428-8 0.308448-8 S
0.301018-8 0.250048-8 0.227388-8 0.203128-8 S
0.184108-8 0.160228-8 0.197388-8 0.140048-8 S
0.160778-8 0.130238-8 0.131308-8 0.126708-8 S
0.127838-8  R30 -1.                          E
*FA  *  F   -1.                              E
*FRIC *F  2.0-5                              E
*FRIC  F  0.0                                E
*GRAV* F  1.0                                E
*HD  * R2 0.0087                             S
0.03843 0.03830 0.03447 0.03279 0.03080      S
0.03760 0.03420 0.03023 0.04840 0.03897      S
0.03080 0.03234 0.03079 0.03779 0.03811      S
0.03477 0.03307 0.03276 0.03202 0.03141      S
0.02824 0.03333 0.03033 0.03010              S
              R17 0.03013                    S
      .03038 .03111 .03180 .03307 .03478     S
      .02734 .03084 .03801 .03803 .04480     S
      .06063 R3 .0737                        E
*ICFLG   R42 0 1 R14 0                       E
*NFF * F   1     E
*ALFA* F  0.0    E
*VL  * F  0.1    E
*VV  * F  0.1    E
*TEST  1
*TL    F  579.0  E
*TV    F  579.0  E
*P     F  9.900  E
*TEST  2
*TL    F  593.0  E
*TV    F  593.0  E
*P     F 11.488  E
*TEST  3
*TL    F  587.7  E
*TV    F  587.7  E
*P     F 12.180  E
*TEST  4
*TL    F  587.9  E
*TV    F  587.9  E
*P     F 12.188  E
*TEST  5
*TL    F  587.0  E
*TV    F  587.0  E
*P     F 11.980  E
*TESTS  6-7-8-9-10
*TL *  F  507.1  E
*TV *  F  507.1  E
*P  *  F  3.280  E
*
*PA  * F  0.     E
* ()()()()()()()()()()()()()()()()()()()()()()()(
*              TIME STEP DATA
*  DTMIN  DTMAX  TEND  RTWFP
   1.E-4  10.    200.  10.0
*  EDINT  GFINT  DMPINT  SEDINT
   20.    0.08   300.    1000.0
 -1000000.
```

Table 3.1b: SUPER-MOBY-DICK, typical input data deck, test section 2.

```
FREE
*NUMTCR  IEOS  INOPT  NMAT
6        0     1      0

TRAC-PF1/MOD1 14.3 SMTC      04/7/88

  TEST 18
14*18

************************************************************
                        *NAMELIST DATA
 $INOPTS  ICFLOW=0  $END
                        *MAIN CONTROL CARDS
*  DSTEP  TIMET
   0      0.0
*  STDYST  TRANSI  NCOMP  NJUN  IPAK
   1       0       3      2     0
*  EPSO    EPSI    EPSS
   1.0E-3  1.0E-5  2.0E-3
*  DITMAX  IITMAX  SITMAX  ISOLUT
   10      0       10      0
*  NTSV  NTCB  NTCF  NTRP  NTCP
   0     0     0     0     0
*   COMPONENT
    1    5     *  BREAK: INLET
    2    5     *  PIPE
    3    6     *  BREAK : OUTLET
* ()()()()()()()()()()()()()()()()()()()()()()()(
   BREAK    1   1                  INLET
*   JUN1  IBTY  ISAT  IVOV   IOFF
          0     0     0      0
*            DXIN   VOLIN    ALPIN   TIN    PIN
*TEST  14  0.018 1.08E-4 0.       507.1  3.31E6
*TEST  15* 0.018 1.08E-4 0.3300 507.3  3.03E6
*  PAIN  CONCIN  RBMX  POFF  BELV
   0.    0.      0.    0.    0.
* ::::::::::::::::::::::::::::::::::::::::::::::::
   BREAK   3   3                  OUTLET
*  JUN  IBTY  ISAT  IVOV  IOFF
   2    0     3     0     0
*             DXIN VOLIN    ALFIN TIN     PIN
*TEST  14     .060 8.50E-4  1.   477.4  1.72E6
*TEST  15 *  .060 8.50E-4  1.   486.4  1.153E6
*  PAIN  CONCIN  RBMX  POFF  BELV
   0.0   0.      0.    0.    0.
* ::::::::::::::::::::::::::::::::::::::::::::::::
  PIPE  2   2                    TEST SECTION
*  NCELLS  NODES  JUN1  JUN2  NAT
   36      0      1     4     0
*  ICHF  ICONC  IACC  IPOW
   0     0      0     0
*  RADIN  TH    HOUTL  HOUTV  TOUTL
   .010   .020  0.0    0.0    300.
*  TOUTV  POWIN  POWOFF  RPOWER  POWSCL
   300.0  0.0    0.0     0.0     0.0
```

```
* -------------------------------------------------------
*DX   *  0.02                  R27 0.704                  S
         0.006 0.01  0.014     0.0. 0.03                  E
         0.03  0.04  0.06                                 E
*VOL  *  -1                                               S
2.395406E-5 2.351606E-5 2.263086E-5 2.1[illegible]E-5 S
1.954546E-5 1.721706E-5 1.461826E-5 1.14[illegible]E-5 S
0.802115E-5 0.556226E-5 0.427006E-5 0.3400[illegible]E-5 S
0.291986E-5 0.252036E-5 0.222006E-5 0.19670[illegible] S
0.180646E-5 0.166206E-5 0.154846E-5 0.145806E-5 S
0.138615E-5 0.133466E-5 0.129466E-5 0.127166E-5 S
0.125996E-5 5.725636-6  R9  -1.                      E
*FA   *  F    -1                                          E
*FRIC*  F   2.0-3                                         E
*GRAV*  F   1.0                                           E
*HD   *  R2 0.0675                                        S
0.06642 0.06560 0.06447 0.06275 0.06050                   S
0.05760 0.05429 0.05025 0.04548 0.03997                   S
0.03590 0.03224 0.02973 0.02773 0.02611                   S
0.02477 0.02367 0.02276 0.02202 0.02141                   S
0.02084 0.02056 0.02033 0.02016                           S
      0.02000   R10 0.135                                 E
*ICFLG    R40 0 1 R12 0                                   E
*NFF  *  F     1     E
*ALFA*  F   0.0     E
*VL   *  F   0.1     E
*VV   *  F   0.1     E
*TEST   14
*TL      F   507.1   E
*TV      F   507.1   E
*P       F   3.2E6   E
*TEST   15
*TL  *   F   507.3   E
*TV  *   F   507.3   E
*P   *   F   3.2E6   E
*
*PA   *  F   0.      E
* ()()()()()()()()()()()()()()()()()()()()()()()(
*                 TIME STEP DATA
*  DTMIN   DTMAX   TEND   RTWFP
   1.E-4   10.     400.   10.0
*  EDINT   GFINT   DMPINT   SEDINT
   20.     0.05    400.     1000.0
 -1000000.
```

Table 3.1c: SUPER-MOBY-DICK, typical input data deck, test section 3.

```
FREE
*NUMTCR  IEOS  INOPT  NMAT
6        0     1      0

TRAC-PF1/MOD1 14.3 SETL      08/7/88

  TEST 12'
11*12*13

****************************************************
                         *NAMELIST DATA
 $INOPTS  ICFLOW=0  $END
                         *MAIN CONTROL CARDS
*  DSTEP   TIMET
   0       0.0
*  STDYST  TRANSI  NCOMP  NJUN  IPAK
   1       0       3      2     0
*  EPSO     EPSI     EPSS
   1.0E-3   1.0E-5   2.0E-3
*  OITMAX  IITMAX  SITMAX  ISOLUT
   10      0       10      0
*  NTSV  NTCB  NTCF  NTRP  NTCP
   0     0     0     0     0
*   COMPONENT
    1    5     *  BREAK: INLET
    2    5     *  PIPE
    3    6     *  BREAK : OUTLET
* ()()()()()()()()()()()()()()()()()()()()()()()()()()(
   BREAK    1   1               INLET
*  JUN1   IBTY   ISAT   IVOV   IOFF
   1      0      0      0      0
*            DXIN   VOLIN    ALPIN   TIN     PIN
*TEST   11   0.058  3.40E-4  0.      577.8   11.66866
*TEST   12   0.058  3.40E-4  0.      588.3   12.01366
*TE     12*  0.058  3.40E-4  0.      593.3   13.01366
*TEST   13   0.058  3.40E-4  0.      590.7   11.90066
*  PAIN   CONCIN   RBMX   POFF   BELV
   0.     0.       0.     0.     0.
* ::::::::::::::::::::::::::::::::::::::::::::::::::::
   BREAK   3   3                  OUTLET
*  JUN   IBTY   ISAT   IVOV   IOFF
   3     0      3      0      0
*               DXIN VOLIN     ALPIN TIN     PIN
*TEST   11      .060 8.50E-4   1.    588.7   6.60686
*TEST   12 *    .060 8.50E-4   1.    590.9   6.67966
*TEST   13      .060 8.50E-4   1.    575.0   6.81066
*  PAIN   CONCIN   RBMX   POFF   BELV
   0.0    0.       0.     0.     0.
* ::::::::::::::::::::::::::::::::::::::::::::::::::::
  PIPE   2   2                  TEST SECTION
*  NCELLS   NODES   JUN1   JUN2   MAT
   51       0       1      3      0
*  ICHF   ICONC   IACC   IPOW
   0      0       0      0
*  RADIN   TH     HOUTL   HOUTV   TOUTL
   .010    .020   0.0     0.0     300.
*  TOUTV   POWIN   POWOFF   RPOWMX   POWSCL
   300.0   0.0     0.0      0.0      0.0

*  ----------------------------------------------------
*DX   *                    R30 0.004                  $
        0.008 0.02  0.LQ  0.08  0.08                  $
        0.062 0.08  0.04  0.08  0.02                  $
        0.014 0.010 0.008 R4 0.004                    $
        0.008 0.010 0.014 0.02  0.03                  $
        0.03  0.08  0.08                              $
*VOL                                                  $
2.399400E-5 2.351900E-5 2.202000E-5 2.131600E-5       $
1.964646E-5 1.731700E-5 1.461836E-5 1.142490E-5       $
0.802111E-5 0.560329E-5 0.437000E-5 0.340946E-5       $
0.291060E-5 0.252039E-5 0.222000E-5 0.198700E-5       $
0.180041E-5 0.160200E-5 0.154640E-5 0.145600E-5       $
0.138016E-5 0.133400E-5 0.129680E-5 0.127150E-5       $
0.129098E-5 R10 -1. 5.72900E-5 R8 -1.                 $
*FA   *   F    -1.                                    $
*FRIC* F   2.0-3                                      $
*GRAV* F   1.0                                        $
*HD   *    0.0078                                     $
0.09842 0.06960 0.05447 0.08279 0.06060               $
0.05700 0.04420 0.05029 0.04846 0.03907               $
0.03590 0.03224 0.02973 0.02772 0.02611               $
0.02477 0.02367 0.02279 0.02202 0.02141               $
0.02094 0.02058 0.02032 0.02016                       $
  R17 0.02000   R10 0.138                             $
*ICFLG   R40 0 1 R12 0                                $
*NFF  * F    1      $
*ALFA* F   0.0      $
*VL   * F   0.1     $
*VV   * F   0.1     $
*TEST   11
*TL      F   577.8  $
*TV      F   577.8  $
*P       F   9.366  $
*TEST   12  12'
*TL      F   600.3  $
*TV      F   600.3  $
*TL  *   F.  601.3  $
*TV  *   F   601.3  $
*P    *  F  10.366  $
*TEST   13
*TL      F   596.7  $
*TV      F   596.7  $
*P       F  12.066  $
*
*FA   * F   0.      $
* ()()()()()()()()()()()()()()()()()()()()()()()()()()(
*               TIME STEP DATA
*  DTMIN   DTMAX   TEND   RTWFP
   1.E-4   10.     600.   10.0
*  EDINT   GFINT   DMPINT   SEDINT
   20.     0.05    400.     1000.0
```

Table 3.2: SUPER-MOBY-DICK, pressure drop in the convergent as given by the Bernoulli equation and by TRAC.

Cell number	1	2	5	10	25	50
DP(TRAC)/(rho*V1**2)	109.3	86.2	73.7	66.9	62.6	61.1
DP(Bernoulli)/(rho*V1**2)	59.6	59.6	59.6	59.6	59.6	59.6
Conditions 1						
DP(TRAC) MPA	4.58	3.61	3.09	2.80	2.62	2.56
DP(Bernoulli) MPa	2.50	2.50	2.50	2.50	2.50	2.50
Difference MPa	2.08	1.11	0.59	0.30	0.12	0.06
Difference %	83.2	44.4	23.6	12.0	4.8	2.4
Conditions 10						
DP(TRAC) MPA	0.48	0.37	0.32	0.29	0.27	0.27
DP(Bernoulli) MPa	0.26	0.26	0.26	0.26	0.26	0.26
Difference MPa	0.22	0.11	0.06	0.03	0.01	0.01
Difference %	85	42	23	11	4	4

Table 3.3: SUPER-MOBY-DICK, experimental values of the friction factor coefficient.

Re*10-6	5.1	5.7	6.2	6.7	7.3	7.9	8.4	11.0	13.6
2*fexp *10+3	6.1	6.0	6.0	6.0	6.0	5.9	6.0	5.6	5.5
2*fcode *10+3	4.2	4.1	4.0	4.0	3.9	3.8	3.8	3.6	3.4
FRIC*10+3	1.9	1.9	2.0	2.0	2.1	2.1	2.2	2.0	2.1

Table 3.4: SUPER-MOBY-DICK, comparison of the measured and predicted critical mass flow rates.

Test	Pressure MPa	Subcooling in K or entrance quality	Measured critical mass flow rate kg/s	Predicted critical mass flow rate kg/s	Discrepancy %
1	12.0	18.8	19.7	20.4	+ 3.6
2	12.0	5.0	15.3	14.7	- 3.9
3	12.0	0.2	14.2	12.4	-12.7
4	12.0	Xe=0.05 %	11.6	12.3	+ 6.0
5	11.8	Xe=2.40 %	10.6	11.1	+ 4.7
6	4.82	27.7	16.6	16.3	- 1.8
7	3.33	5.5	8.4	7.8	- 7.1
8	3.11	1.6	7.1	5.8	-18.3
9	3.07	0.9	6.8	5.4	-20.6
10	3.02	0.0	6.5	5.0	-23.1
11	11.9	19.2	19.5	20.0	+ 2.6
12	12.0	12.6	14.9	17.8	+19.5
12'	12.0	6.6	14.9	15.2	+ 2.0
13	12.0	1.1	13.1	12.6	- 3.8
14	3.32	5.3	13.4	11.0	-17.9
15	3.03	Xe=0.90 %	6.5	5.8	-10.8

Table 3.5: SUPER-MOBY-DICK, run statistics.

Test	Real time s	Time step number	Mean time step s	CPU time s	CPU time / real time	CPU time / (cell*time step)
1	7.0	320	0.022	14.9	2.1	8.3*10-4
2	13.9	590	0.024	24.5	1.8	7.4*10-4
3	17.4	820	0.021	31.9	1.8	6.9*10-4
4	12.1	690	0.018	28.8	2.4	7.5*10-4
5	13.4	770	0.017	29.8	2.2	6.9*10-4
6	24.1	640	0.038	28.3	1.2	7.9*10-4
7	8.9	240	0.037	12.7	1.4	9.4*10-4
8	9.3	320	0.029	15.6	1.7	8.7*10-4
9	6.5	330	0.020	15.7	2.4	8.5*10-4
10	111.8	2897	0.039	99.6	0.9	6.1*10-4
11	4.6	400	0.011	15.0	3.3	7.4*10-4
12	5.7	370	0.015	14.4	2.5	7.6*10-4
12'	8.4	570	0.015	22.1	2.6	7.6*10-4
13	5.7	350	0.016	13.5	2.4	7.6*10-4
14	4.3	250	0.017	8.2	1.9	9.1*10-4
15	42.5	2397	0.018	99.8	2.3	11.6*10-4

Table 3.6: SUPER-MOBY-DICK, simulations of the tests 6 and 10 with a convergent modelled with 1, 2, 5, 10, 25 or 50 cells.

Number of cells	1	2	5	10	25	50
Test 6						
Upstream velocity V1 Measured: 5.74 m/s Predicted by TRAC : Difference %	 4.43 -22.8		 5.28 -8.0	 5.50 -4.2	 5.64 -1.7	 5.72 -0.3
DP convergent Measured: 1.62 MPa Predicted by TRAC: Difference MPa Difference %	 1.81 0.19 +11.7		 1.75 0.13 +8.0	 1.72 0.10 +6.2	 1.70 0.08 +4.9	 1.69 0.07 +4.3
CPU time s	8		12	24	44	240
Test 10						
Upstream velocity V1 Measured: 2.25 m/s Predicted by TRAC: Difference %		 1.71 -24.0	 1.75 -22.0		 1.80 -20.0	 1.81 -19.6
DP convergent Measured: 0.26 MPa Predicted by TRAC: Difference MPa Difference %		 0.21 -0.05 -19	 0.20 -0.06 -23		 0.19 -0.07 -27	 0.18 -0.08 -31
CPU time s		4	8		12	17

Table 3.7: SUPER-MOBY-DICK, critical mass flow rates predicted with different sizes of the throat cells, and discrepancy with the reference run.b

Test	1	3	5	10
Cells of 0.002 m Predicted mass flow rate kg/s Discrepancy with the reference %	20.39 0.0	12.25 -1.2	10.98 -0.9	4.99 -1.2
Cells of 0.004 m Predicted mass flow rate kg/s Reference	20.39	12.40	11.08	5.05
Cells of 0.01 m Predicted mass flow rate kg/s Discrepancy with the reference %	20.42 +0.1	12.49 +0.7	11.16 +0.7	5.12 +1.4
Cells of 0.02 m Predicted mass flow rate kg/s Discrepancy with the reference %	20.41 +0.1	12.76 +2.9		5.19 +2.8

Table 3.8: SUPER-MOBY-DICK, critical mass flow rates predicted with the choked flow model and different throat cells size, and discrepancy with the data.

Test	1	3	5	10
Cells of 0.002 m Predicted mass flow rate kg/s Discrepancy with the data %	18.5 -6	11.9 -16	11.0 +4	5.0 -23
Reference run: discrepancy with the data %	+4	-13	+5	-23
Cells of de 0.02 m Predicted mass flow rate kg/s Discrepancy with the data %	18.9 -4	11.8 -17		5.1 -22

4 CANON BLOWDOWN EXPERIMENTS

4.1 Test Description

The CANON blowdown tests were conducted in the Service des Transferts Thermiques of the Centre d'Etudes Nucléaires de Grenoble (France), during the years 1975 through 1977 (Riegel and Maréchal, 1977).

4.1.1 Test Section

The test section CANON consists of an horizontal straight pipe of 0.1023 m inside diameter and 4.389 m lenght. This pipe is made of stainless steel NS-225 with 6 mm wall thickness. One end of the pipe is closed. A rupture disc assembly is installed at the other end. Interchangeable diaphragms upstream the rupture disc allow the break diameter to be modified.

4.1.2 Measurements

The mean **void fraction** over the entire section is measured at a location 1.502 m from the closed end, by scattering of a neutron beam issued from the Siloette research reactor in the CENG. For void fractions lower than 0.8, measurements show a large dispersion, corresponding to bubble or slug flow regime.

Absolute **pressures** are measured at different locations along the test section. The uncertainty of the pressure measurements is evaluated to 50 kPa.

Temperatures are measured at the same locations as the pressures.

4.1.3 Test Procedure

The test section is heated and pressurized up to the desired initial pressure and temperature. The rupture disc then breaks, and blowdown occurs.

Temperature measurements show that a thermal stratification exists before the blowdown. Radial temperature differences up to 10 K have been observed. After the break opening, the temperature stratification is inverted: it seems that saturated vapor gathers upward, whereas overheated liquid fills the bottom of the pipe.

4.1.4 Test Matrix

The CANON tests have been conducted at an initial pressure of 3.2 MPa, at three different initial temperatures (473, 493 and 503 K), and four different break diameters (30, 50, 70 and 102.3 mm). Some tests were conducted twice or more with the same initial conditions, which yields to several experimental curves for specified conditions.

The following tests were selected for TRAC simulation in the frame of the ICAP:
Test D: Break: 0.1023 m (largest break), T = 473 K.
Test L: Break: 0.1023 m (largest break), T = 503 K.
Test I: Break: 0.0300 m (smallest break), T = 503 K.

4.2 Input Model

Table 4.1 gives a typical input data deck used for the CANON simulations.

4.2.1 Components and Boundary Conditions

The test section is modelled with a PIPE component. A FILL component with FRIC = 1*10+20 simulates the closed end of the test section. A BREAK component is used at the other end, wnere the pressure is imposed.

4.2.2 Nodalization

The cell lengths are chosen to ensure that the pressure and void fraction measurement locations correspond to the center of a cell. Twenty four cells are used, from 0.142 through 0.202 m (bre cell) with a mean length of 0.183 m (fig. 4.1). The wall is modelled with four nodes.

The break diameter is simply imposed as the hydraulic diameter at the outlet edge of the last cell.

4.2.3 Initial Conditions

The initial values imposed at each cell of the PIPE component are staded hereafter: zero void fraction, experimental initial pressure and temperature, velocities of 1*10-5 m/s.

The blowdown is initiated at time zero by setting the break pressure to the value 0.1 MPa. The time step is free, with an initial value of 1 *10-4 s. Base case simulations are made using the choked flow model.

4.3 Code Predictions and Comparison with Data

4.3.1 Largest Break Tests

The blowdowns with a break corresponding to the pipe diameter are very fast (about 1 s from the opening of the break until the atmospheric pressure is reached in the pipe). During the blowdown, the three pressures P1, P2 and P3, measured in the closed end side of the pipe, as well as the predicted ones at the same locations, take values very close each one from the others. Comparisons are then only made for pressures P1, P4 and P5 (locations are shown on figure 4.1) and the void fraction. The complete results are presented on figures 4.2 for test D and L.

The pressure reached at the end of the initial abrupt pressure decrease is overpredicted with a discrepancy of about 0.3 MPa: boiling is beginning in the code as soon as the saturation pressure corresponding to the initial temperature is reached, whereas the experimental pressure decreases under the saturation pressure. The absence of a delayed boiling model is responsible for this discrepancy. Effects of the initial temperature stratification, which canot be taken into account in the code, probably also occur.

During the second stage of the blowdown (slower pressure decrease), the pressure is well predicted, except for the closed end side pressure of test L. The final pressure decrease (corresponding to void fraction higher than 0.9) is anticipated by the code.

The predicted and measured void fractions in the closed end side are consistant with the pressures: the predicted void fraction is first within the data scattering, and is overpredicted at the end of the blowdown.

4.3.2 Smallest Break

The blowdown transient with the smallest break is slower (about 8 s for test I), and some liquid remains in the test section at the end of the transient. All the pressures measured and predicted along the test section have very close values during the blowdown. Hence comparisons are only made for one pressure (P3) and the void fraction. The results are presented on figures 4.3 for test I.

The pressure is predicted within the experimental scattering during the first part of the transient, as is the void fraction. After that, the pressure is overpredicted with a discrepancy up to 0.6 MPa, and the void fraction is underpredicted.

4.4 Run Statistics

The runs were performed on a CRAY-XMP-2200 computer with TRAC-PF1/MOD1 version 14.3. The run statistics are presented on table 4.2, and figures 4.4 and 4.5 show the plot of the time step and CPU time versus real time, for tests D, L and I.

4.5 Sensitivity Studies

4.5.1 Nodalization

In the reference runs, the pipe is divided into 24 cells. Simulations have also been performed with 13 cells (length 0.333 up to 0.342 m), and with 39 cells (length 0.111 up to 0.114 m) for test I. The results show little nodalization sensitivity.

Another simulation is performed, with a fine mesh at the break (44 cells are used, from 0.001 m at the break up to 0.200 m at the closed end). The results are not very different from the base case, but the time step is strongly reduced (fig. 4.6).

It seems that in case of a fine mesh at the break, the Courant stability criterion becomes very limitative. This limitation was not found with our first runs performed with TRAC-PF1/MOD1 version 13.0, but exists for the runs performed with version 14.0.

4.5.2 Natural Choking

The runs performed with natural choking lead to too fast blowdowns: the pressures are underpredicted and the void fraction is overpredicted (fig. 4.7).

The simulations performed with natural choking with a fine mesh noding lead to the same too fast blowdown, and to a time step decrease (fig. 4.8).

The results show a large thermal desequilibrium at the break (about 40 K for test D), and a large slip ratio (larger than 2 for test D). On the opposite, the results obtained with the choked flow model show no thermal desequilibrium (as supposed by the model) and a smaller slip ratio (about 1.5 for test D), and smaller velocities (for test D at time 0.2 s, VL=40 m/s with the choked flow model, and VL=150 m/s without it).

The lack of a virtual mass term for the natural choking (a virtual mass term is included in the choked flow model) probably takes a part in

the bad agreement between the data and the results obtained with natural choking.

4.6 Summary and Conclusion

The simulation of three CANON blowdown tests (initial pressure 3.2 MPa) was performed with TRAC-PF1/MOD1 version 14.3. The pipe is modelled with 24 cells from 0.142 through 0.202 m. A break smaller than the inside pipe diameter is simply modelled with an hydraulic diameter reduction at the outlet edge of the last cell. The choked flow model is used.

For the tests with a break diameter equal to the pipe diameter (fast transients), the pressure at the end of the initial abrupt decrease is somewhat overpredicted: possible explanations are the lack of a delayed boiling model in the code, and the initial experimental temperature stratification. The pressure during the intermediate stage is correctly predicted, but the final pressure decrease is anticipated by the code: voidage of the test section is too fast.

For the test with a break diameter smaller than the pipe diameter, the pressure i predicted within the experimental scattering during the two first stages of the transient. The final pressure decrease is delayed by the code: voidage is too slow.

Void fractions predictions are consistent with the pressure predictions: a void fraction overprediction corresponds to a pressure underprediction.

The predictions are little sensitive to the nodalization. A Courant stability criterion reduces sharply the time step in case of fine mesh at the break. The simulations performed with natural choking lead to very fast blowdowns, far from the data. The lack of a virtual mass term for the runs with natural choking probably takes a part in the bad prediction of fast blowdown transients.

Table 4.1: CANON, typical input data deck.

```
FREE
*NUMTCR  IEOS  INOPT  NMAT
6        0     1      0
TRAC-PF1/MOD1 V 14.3 CANON L 28/1/88

  TEST L
O*L*I

*****************************************************
                        *NAMELIST DATA
 $INOPTS  ICFLOW=1  $END
                        *MAIN CONTROL CARDS
*  DSTEP  TIMET
   0      0.0
*  STDYST  TRANSI  NCOMP  NJUN  IPAK
   0       1       3      2     0
*  EPSO     EPSI     EPSS
   1.0E-3   1.0E-6   1.0E-4
*  OITMAX  IITMAX  SITMAX  ISOLUT
   10      0       10      0
*  NTSV  NTCB  NTCF  NTRP  NTCP
   0     0     0     0     0
*   COMPONENT
    1      5     *  FILL  : BOTTOM
    2      5     *  PIPE  : TEST SECTION
    3      8     *  BREAK : OUTLET
* ()()()()()()()()()()()()()()()()()()()()()()()()(
   FILL    1   1                BOTTOM
*  JUN1   IFTY  IOFF
   1      1     0
*  TWTOLD  RFMX  CONCIN  FELV
   0.      0.    0.      0.
*  DXIN   VOLIN       ALPIN  VLIN  TLIN
   200    1.6438E-3   0.     0.    300.
*  PIN      PAIN  FLOWIN       VVIN  TVIN
   3.2E6    0.    0.           0.    300.
* :::::::::::::::::::::::::::::::::::::::::::::::::
   BREAK   3   3   .            OUTLET
*  JUN  IBTY  ISAT  IVOV  IOFF
   2    0     3     0     0
*  DXIN  VOLIN       ALFIN  TIN    PIN
   202   1.6603E-3   1.     373.2  1.00E+6
*  PAIN  CONCIN  RBMX  POFF  BELV
   0.0   0.      0.    0.    0.
* :::::::::::::::::::::::::::::::::::::::::::::::::
   PIPE  2   2                   TEST SECTION
*  NCELLS  NODES  JUN1  JUN2  MAT
*  38      4      1     3     0
   24      4      1     3     0
*  13      4      1     3     0
*  ICHF  ICONC  IACC  IPOW
   1     0      0     0
*  IQP3TR  IQP3SV  NQP3TB  NQP3SV  NQP3RF
   0       0       0       0       0
*  RADIN   TH     HOUTL  HOUTV  TOUTL
   .06119  .008   0.     0.0    300.
*  TOUTV  POWIN  POWOFF  RPOWMX  POWSCL
   300.   0.0    0.0     0.0     0.0
*  QP3IN  QP3OFF  RQP3MX  QP3SCL
   0.     0.      0.      0.
```

```
*---------------------------------------------------------
*DX     .84  .111 .83  .112 .86  .111   S
      * .82  .112 .84  .113 .812 .114   S
      * .83  .113 .88  .113             E
*DX   *   .200  .200  .200  .180  .180  S
          .170  .153  .146  .146  .142  S
          .190  .170  .200  .200  .170  S
          .170  .200  .200  .206  .203  S
          .200  .200  .202  .202        E
*DX       .333  .334  .334  .334  .334  S
      *   .340  .342  .342  .342  .342  S
      *   .340  .336  .336              E
*VOL * F   -1.                          E
*FA  * F   -1.                          E
*FRIC   1.E+20  .830  .0                E
*FRIC*  1.E+20  .824  .0                E
*FRIC   1.E+20  .813  .0                E
*GRAV* F   0.                           E
*TESTS O L
*HD  * F  .1023                         E
*TEST I
*HD    .824  .1023  .030                E
*NFF * F    1    E
*ALFA* F  0.0    E
*VL  * F 1.E-6   E
*VV  * F 1.E-6   E
*TEST  O
*TL     F 473.1  E
*TV     F 473.1  E
*TESTS L I
*TL  * F 503.1   E
*TV  * F 503.1   S
*P   * F 3.2E+6  E
*PA  * F 0.      E
*QPPP* F 1.      E
*MATID* F 7      E
*TEST  O
*TW      F 473.1 E
*TESTS L I
*TW   * F 503.1 E
* ()()()()()()()()()()()()()()()()()()()()()()()()(
*              TIME STEP DATA
*  DTMIN  DTMAX  TEND  RTWFP
*TESTS O L
   1.E-4  1.00   1.00  10.
*TEST  I
*  1.E-4  1.00   8.00  10.
*  EDINT  GFINT  DMPINT  SEDINT
*TESTS O L
   .2      1.E-3  10.     1000.
*TEST  I
*  1.      1.E-3  10.     1000.
-1000.
```

Table 4.2: CAMON, run statistics.

Test	D	L	I
Real time s	1.0	1.0	8.2
Time step number	133	137	172
Mean time step	7.5•10-3	7.3•10-3	4.8•10-2
CPU time s	7.9	8.2	6.9
CPU time/real time	7.9	8.2	0.84
CPU time/(cell•time step)	2.5•10-3	2.5•10-3	1.7•10-3

5 SUPER-CANON BLOWDOWN EXPERIMENTS

5.1 Test Description

The SUPER-CANON blowdown tests were conducted in the Service des Transferts Thermiques of the Centre d'Etudes Nucléaires de Grenoble (France), during the years 1978 and 1979 (Riegel, 1979).

The SUPER-CANON blowdown tests differ from the CANON blowdown tests by the initial pressure (3.2 MPa for the CANON tests and 15 MPa for the SUPER-CANON tests), and by some features in the test section.

5.1.1 Test Section

The test section SUPER-CANON consists of an horizontal straight pipe of 0.1000 m inside diameter (0.1023 m for CANON) and 4.389 m length (same as for CANON). This pipe is made of stainless steel NS-225 with 12.5 mm wall thickness (6 mm for CANON).

One end of the pipe is closed. A rupture disc assembly is installed at the other end. Interchangeable diaphragms upstream the rupture disc allow the break diameter to be modified.

5.1.2 Measurements

The measurements conducted are the same, and at the same locations, as for the CANON tests.

5.1.3 Test Procedure

The tests procedure is the same as for the CANON tests.

5.1.4 Test Matrix

The SUPER-CANON tests were conducted at an initial pressure of 15 MPa, at three different initial temperatures (553, 573 and 593 K), and four different break diameters (30, 50, 70 and 100 mm).

The following tests were selected for TRAC simulation in the frame of the ICAP:
Test P: Break: 0.100 m (largest break), T = 553 K.
Test X: Break: 0.100 m (largest break), T = 593 K.
Test Q: Break: 0.030 m (smallest break), T = 573 K.

5.2 Input Model

Table 5.1 gives a typical input data deck used for the SUPER-CANON simulations. The same input model is used as for the CANON tests.

5.3 Code Predictions and Comparison with Data

5.3.1 Largest Break Tests

The blowdowns with a break corresponding to the pipe diameter are very fast (about 0.3 s from the opening of the break until the atmospheric pressure is obtained in the pipe). During the blowdown, the three pressures P1, P2 and P3, measured in the closed end side of the pipe, as well as the predicted ones at the same locations, take values very close each one from the others. Comparisons are then only made for pressures P1, P4 and P5 (their locations are shown on figure 4.1) and the void fraction. The results are presented on figures 5.1 for tests P and X.

The pressure reached at the end of the initial abrupt pressure decrease is overpredicted with a discrepancy up to 2 MPa. Boiling is beginning in the code as soon as the saturation pressure corresponding to the initial temperature is reached, whereas the experimental pressure decreases under the saturation pressure. The absence of a delayed boiling model is responsible for this discrepancy. Effects of the initial temperature stratification, which canot be taken into account in the code, probably also occur.

After some time, the predicted pressure takes a value close to the experimental value, until the end of the blowdown. In the bottom side of the pipe, the final pressure decrease is anticipated.

The void fraction is within the data scattering except when the discrepancy between the predicted and measured pressures are high.

5.3.2 Smallest Break

The blowdown transient with the smallest break is slower (about 4 s for test Q), and some liquid remains in the test section at the end of the transient. All the pressures measured and calculated along the test section have very close values during the blowdown. Hence comparisons are only made for one pressure (P3) and the void fraction. The results are presented on figures 5.2 for test Q.

The pressure reached at the end of the initial abrupt pressure decrease is overpredicted, as for the other tests. The calculated pressure rapidly joins the experimental one, and the prediction is good.

The void fraction is well predicted except at the end of the transient, where it is underpredicted: more liquid than measured is predicted to fill the pipe at the end of the transient.

5.4 Run Statistics

The runs were performed on a CRAY-XMP-2200 computer with TRAC-PF1/MOD1 version 14.3. The run statistics are presented on table 5.2, and figures 5.3 and 5.4 show the plots of the time step and CPU time versus real time, for tests P, X and Q.

5.5 Sensitivity Studies

5.5.1 Nodalization

In the reference runs, the pipe is divided into 24 cells. Simulations have also been performed with 13 cells (length 0.333 up to 0.342 m), and with 39 cells (length 0.111 up to 0.114 m) for test P. The results show little nodalization sensitivity (fig. 5.5).

Another simulation is performed, with a fine mesh at the break (44 cells are used, from 0.001 m at the break up to 0.200 m at the closed end). The results are not very different from the base case, but the time step is strongly reduced (fig. 5.5). The observation concerning the time step limitation made for the CANON tests with fine mesh (paragraph 4.5.1) is also valuable here.

5.5.2 Natural Choking

The reference runs use the code choked flow model. The simulations performed with natural choking combined with a fine mesh at the break lead to too fast blowdowns, and a time step decrease (fig. 5.6). The discrepancy between the reference run (choked flow model) and the run with natural choking is not large for test X, for which the break void fraction more rapidly reaches a value close to 1 than for the other tests. For test Q the break slip ratio at time 1 s is about 1.1 with the choked flow model, and is about 4.2 with the natural choking. As for the CANON tests, the lack of a virtual mass term for the runs with natural choking probably takes a part in the bad prediction of fast blowdown transients.

5.6 Summary and Conclusion

The simulation of the SUPER-CANON blowdown tests P, X and Q (initial pressure of 15 MPa) was performed with TRAC-PF1/MOD1 version 14.3. The

pipe is represented by 24 cells from 0.142 through 0.200 m. Break smaller than the inside pipe diameter is simply modelled by a hydraulic diameter reduction at the outlet edge of the last cell. The choked flow model is used.

The pressure at the end of the initial abrupt decrease is somewhat overpredicted: possible explanations are the absence of a delayed boiling model, and the initial experimental temperature stratification.

For the tests with a break diameter equal to the pipe diameter (fast transients), the pressure is close to the experimental pressure, except at the bottom of the pipe, where the final pressure decrease is anticipated.

For the test with a break diameter smaller than the pipe diameter, the boiling inception pressure is overpredicted, and the prediction is good after the boiling inception.

Calculations are few sensitive to the nodalization. A Courant stability criterion reduces sharply the time step in case of fine mesh at the break.

The simulations performed without the choked flow model lead to very fast blowdowns, far from the data. The lack of a virtual mass term for the runs with natural choking probably takes a part in the bad prediction of fast blowdown transients.

Table 5.1: SUPER-CANON, typical input data deck.

```
FREE
*NUMTCR  IEOS  INOPT  NMAT
8        0     1      0
TRAC-PF1/MOD1 V 14.3 SCAN     3/3/88

P*Y*D

****************************************************
                      *NAMELIST DATA
 $INOPTS  ICFLOW=1  $END
                      *MAIN CONTROL CARDS
*  DSTEP  TIMET
   0      0.0
*  STDYST  TRANSI  NCOMP  NJUN  IPAK
   0       1       3      3     0
*  EPSO     EPSI     EPSS
   1.0E-3   1.0E-8   1.0E-4
*  OITMAX  IITMAX  SITMAX  ISOLUT
   10      0       10      0
*  NTSV  NTCB  NTCF  NTRP  NTCP
   0     0     0     0     0
*   COMPONENT
    1      1     *  FILL  : BOTTOM
    2      1     *  PIPE  : TEST SECTION
    3      1     *  BREAK : OUTLET
* ()()()()()()()()()()()()()()()()()()()()()()()()()(
  FILL     1   1                BOTTOM
*  JUN1   IFTY   IOFF
   1      1      0
*  TWTOLD  RFMX  CONCIN  FELV
   0.      0.    0.      0.
*  DXIN   VOLIN      ALPIN  VLIN  TLIN
   .300   1.64E-3    0.     0.    300.
*  PIN      PAIN  FLOWIN      VVIN  TVIN
   15.E6    0.    0.          0.    300.
*  ::::::::::::::::::::::::::::::::::::::::::::::::
  BREAK    3   3                OUTLET
*  JUN  IBTY  ISAT  IVDV  IOFF
   2    0     3     0     0
*  DXIN   VOLIN      ALPIN  TIN     PIN
   .202   1.66E-3    1.     373.3   1.00E+5
*  PAIN  CONCIN  RBMX  POFF  BELV
   0.0   0.      0.    0.    0.
*  ::::::::::::::::::::::::::::::::::::::::::::::::
  PIPE  2   2                   TEST SECTION
*  NCELLS  NODES  JUN1  JUN2  MAT
   24      4      1     2     .0
*  ICHF  ICONC  IACC  IPOW
   1     0      0     0
*  IQPSTB  IQPSSV  NQPSTB  NQPSSV  NQPSRP
   0       0       0       0       0
*  RADIN   TH      HOUTL   HOUTV   TOUTL
   .08     .0125   0.      0.0     300.
*  TOUTV  POWIN  POWOFF  RPOWMX  POWSCL
   300.   0.0    0.0     0.0     0.0
*  QPSIN  QPSOFF  RQPSMX  QPSSCL
   0.     0.      0.      0.
```

```
****************************************************
*DX   *    .200  .200  .200  .180  .180 $
           .170  .155  .145  .146  .145 $
           .190  .170  .200  .200  .170 $
           .170  .200  .200  .200  .200 $
           .200  .200  .202  .202       E
*VOL  * F  -1.                          E
*FA   * F  -1.                          E
*FRIC*  1.E+30  .834  .0                E
*GRAV* F  0.                            E
*TESTS F X
*HD     F  .10                          E
*TEST O
*HD   * .084  .10    .030               E
*NFF  * F    1    E
*ALFA* F  0.0     E
*VL   * F  1.E-5  E
*VV   * F  1.E-5  E
*TEST  P
*TL     F 583.1   E
*TV     F 593.1   E
*TEST X
*TL     F 583.1   E
*TV     F 583.1   E
*TEST O
*TL   * F 573.1   E
*TV   * F 573.1   E
*P    * F 15.E+6  E
*PA   * F 0.      E
*QPPP* F 1.       E
*MATID* F 7       E
*TEST  P
*TW      F 583.1 E
*TEST  X
*TW      F 583.1 E
*TEST  O
*TW  *   F 573.1 E
* ()()()()()()()()()()()()()()()()()()()()()()()()()(
*              TIME STEP DATA
*  DTMIN  DTMAX  TEND  RTWFP
*TEST  P
*  1.E-4  1.00   0.40  10.
*TEST  X
*  1.E-4  1.00   0.30  10.
*TEST  O
   1.E-4  1.00   4.00  10.
*  EDINT  GFINT  DMPINT  SEDINT
*TESTS P X
*  .1     1.E-5  10.     1000.
*TEST  O
   1.     1.E-5  10.     1000.
  -1000.
```

Table 5.2: SUPER-CANON, run statistics.

Test	P	X	Q
Real time s	0.4	0.3	4.0
Time step number	113	103	158
Mean time step	3.3•10-3	2.9•10-3	2.3•10-2
CPU time s	7.6	7.4	6.8
CPU time/real time	19	25	1.7
CPU time/(c\ll•time step)	2.8•10-3	3.0•10-3	1.7•10-3

6 VERTICAL-CANON BLOWDOWN EXPERIMENTS

6.1 Test Description

The VERTICAL-CANON blowdown tests were conducted in the Service des Transferts Thermiques of the Centre d'Etudes Nucléaires de Grenoble (France), during the year 1982 (Gully et Blanc, 1982).

6.1.1 Test Section

The test section VERTICAL-CANON consists of a succession of five vertical straight pipes, successively of 0.6288, 0.6063, 1.8183, 0.6063 and 0.8278 m length, and of 0.100, 0.103, 0.100, 0.103 and 0.100 m inside diameter. The total length is 4.4830 m. The pipes with 0.103 m inside diameter are the void fraction spool pieces. The pipes are made of stainless steel 316L of 12.5 mm thickness. The test section is insulated, except the void fraction spool pieces.

The bottom end of the test section is closed. The upper head is followed by a converging nozzle of 7 degrees and 0.098 m length. The junction of the pipe with the nozzle is a toric piece with a radius depending on the break diameter. The nozzle is followed by a straight pipe of 4 mm length and the desired break inside diameter, and by the rupture disc.

6.1.2 Measurements

Absolute **pressures** are measured at the bottom and at the break, with an accuracy of 1 %. Seven pressure taps along the test section give **pressure differences**. The measurement error is evaluated to 2 %.

The fluid **temperature** is measured at the bottom and at the top of the test section by chromel-alumel thermocouples, with an uncertainty evaluated to 1 K.

The diametral mean **void fraction** is measured at two locations, by a gamma ray attenuation technique.

6.1.3 Test Procedure

The test section is heated and pressurized up to the desired initial pressure and temperature. The rupture disc then breaks, and blowdown occurs.

6.1.4 Test Matrix

Eighteen CANON VERTICAL tests have been performed, with initial pressures from 5.5 up to 15 MPa, initial temperatures from 500 up to 590 K and break diameters of 3, 5, 7 and 15 mm.

The following tests were selected for TRAC simulation in the frame of the ICAP:
Test 9: break: 10 mm, P = 13 MPa, T = 574 K.
Test 22: break: 5 mm, P = 6 MPa, T = 505 K.
Test 24: break: 5 mm, P = 13 MPa, T = 573 K.

6.2 Input Model

Table 7.1 gives a typical input data deck used for the VERTICAL-CANON simulations.

6.2.1 Components and Boundary Conditions

The test section is modelled with a PIPE component. A FILL component with FRIC = 1*10+20 simulates the closed end of the test section. A BREAK component is used at the other end, where the pressure is imposed.

6.2.2 Nodalization

The cell lengths are chosen to ensure that the pressure and void fraction measurement locations correspond to the center of a cell. Forty two cells are used, with a minimum length of 0.061 m and a maximum length of 0.170 m (fig. 6.1). The converging nozzle is modelled with one cell (0.098 m length).

The wall is modelled with four nodes.

6.2.3 Initial Conditions

The initial conditions imposed at each cell of the PIPE component are staded hereafter: zero void fraction, experimental initial temperature, initial pressures (the hydrostatic pressure distribution is evaluated in order to obtain a correct initialization of the pressure differences), velocities of 1.10-5 m/s.

The blowdown is initiated at time zero by setting the break pressure to 0.1 MPa. The time step is free, with an initial value of 1*10-3 s. The reference runs are performed with the choked flow model.

6.3 Code Predictions and Comparison with Data

Pressure P0 at the bottom of the pipe is calculated through extrapolation from the predicted pressures of the two first cells. The complete results are presented on figures 6.2.

6.3.1 Pressure

The pressure decrease at the bottom of the test section is well predicted by the code for the three tests. At the end of the initial abrupt pressure decrease, the pressure is slightly overpredicted (from 0.1 through 0.4 MPa). During the slow pressure decrease, the discrepancy between the predicted and measured pressures is less than 0.4 Mpa.

6.3.2 Void Fraction

The void fractions predicted by the code show two types of oscillations: little amplitude oscillations (lower than 0.1) when the void fraction is within the interval 0.3-0.4 (tests 22 and 24, with 5 mm break diameter), and large amplitude oscillations (0.5-0.9) beginning at a void fraction of about 0.65 (test 9, with 10 mm break diameter).

6.3.2.1 Large oscillations

For tests 22 and 24, the void fraction in the bottom part of the test section (under the liquid level) is always lower than 0.5, whereas the cells located above the liquid level have a void fraction close to 1. For these two tests, no cell has a void fraction between 0.6 and 0.7 more than a few time steps, and that is why large oscillations do not appear.

On the other hand, the void fraction of the bottom cells for test 9 rapidly increases to values of about 0.6-0.7. For these values of the void fraction, the interfacial shear stress coefficient decreases sharply when the pressure is low. It corresponds to the transition between bubbly-slug flow and annular flow. Figure 6.3 shows the interfacial shear stress coefficient versus the void fraction, for conditions corresponding to test 9 when oscillations exist.

The mechanism of the oscillations is the following: a high void fraction beeing reached, the interfacial shear stress decreases sharply; then the liquid is no more entrained by the vapor; then the void fraction is reduced and the interfacial shear stress consequently increases. Liquid is then entrained again, and the void fraction becomes high again. The cycle goes on, until all the liquid is evaporated (due to the wall heating). The explicit calculation of the interfacial shear

stress coefficient also takes a part in the existence of the oscillations.

Figures 6.2a and 6.2b show that the large oscillations appear when the pressure is sufficiently low (about 0.3 MPa). The interfacial shear stress coefficient variation, between void fractions 0.50 and 0.75, increases when pressure decreases (fig. 6.4). The large oscillations noding sensitivity is studied in paragraph 6.5.1.

6.3.2.2 Low Oscillations

For tests 22 and 24, the oscillations are much more low and correspond to void fractions between 0.3 and 0.4. In this region the interfacial shear stress sharply decreases, for sufficiently large liquid and vapor velocity differences (more slugs than bubbles in the flow). Figure 6.5 shows the interfacial shear stress coefficient versus the void fraction, for conditions corresponding to tests 22 and 24 when oscillations exist.

6.3.2.3 Comparison with Data

Disregarding the oscillations, the void fractions predictions are very good for tests 9 and 22. For test 24 the void fraction is underpredicted at the end of the transient: the simulation does not predict the passage of the liquid level at the bottom void fraction measurement location, whereas data do.

6.3.3 Pressure Differences

The pressure differences predictions are consistent with the void fractions predictions: disregarding the oscillations, the pressure differences are correctly predicted for tests 9 and 24. The pressure differences are first high (mainly liquid), and at the end of the transient, the differences are very low (mainly vapor). For test 24 the pressure differences in the bottom of the pipe are overpredicted at the end of the transient.

6.4 Run Statistics

The runs were performed on a CRAY-XMP-2200 computer with TRAC-PF1/MOD1 version 14.3. The run statistics are shown on table 6.2, and figures 6.6 and 6.7 show the plots of the time step and CPU time versus real time, for tests 9, 22 and 24.

6.5 Sensitivity Studies

6.5.1 Nodalization

In the reference runs, the pipe is divided into 42 cells. Simulations have also been performed with 27 and 15 cells, the last cell being larger than the converging nozzle (respectively 0.171 and 0.260 m). The results show little nodalization sensitivity concerning the global results. However, the reduction of the cell number leads to a reduction of the low and particularly of the large oscillations (fig. 6.8).

Another simulation is performed, with a fine mesh at the break (59 cells are used, with the break cell of 0.004 m length). Results are not very different from the base case, but the time step is sharply reduced (fig. 6.9). Pressure P8 at the break is calculated in this run: it is overpredicted when boiling beginns, and underpredicted since about time 60 s.

It seems that in case of a fine mesh at the break, the Courant stability criterion becomes very limitative. This limitation was not found with our first runs performed with TRAC-PF1/MOD1 version 13.0, but exists for the runs performed with version 14.0. This time limit criterion is calculated in subroutine TF1DS1, line TF1DS1.790. Version 13.0 gives typically for the time step limit DELVMX 5.85 s (test 22, t = 50 s), and version 14.3 gives 5.75*10-3 s. The value of parameter CSF1D is 1*10+6 in version 13.0, and is 1*10+3 in version 14.0 and 14.3, hence the value of DELVMX is reduced by a factor 1*10+3.

6.5.2 Natural Choking

The simulations performed with natural choking lead to too fast blowdowns: pressures are underpredicted, and void fractions overpredicted (fig. 6.10).

The simulations performed with natural choking and a fine noding at the break yield a too fast blowdown, however less fast than in the previous simulation, with a reduced time step (figures 6.10). The discrepancy between the results obtained with natural choking and with the choked flow model is less large than for the CANON or SUPER-CANON tests, probably because a single phase vapor flow regime is rapidly obtained at the break for the VERTICAL-CANON tests.

6.6 Summary and Conclusion

The simulation of three VERTICAL-CANON blowdown tests was performed with TRAC-PF1/MOD1 version 14.3. The test section is modelled with 42 cells with a length from 0.061 through 0.170 m. The converging nozzle is modelled by one cell. The choked flow model is used.

The pressure at the boiling inception are sligthly overpredicted.

The predictions (pressure, void fraction, pressure drops) for the test with a 10 mm break diameter are in good agreement with the data, despite large void fraction oscillations, imputed to the sharp decrease of the interfacial shear stress in the transition zone between the bubble-slug flow regime and the annular flow regime at low pressure, associated with the explicit calculation of the interfacial shear stress coefficient.

The predictions for the tests with a 5 mm break diameter are in good agreement with the data, except a too slow decrease of the liquid level for the test at 13 MPa. For these tests, low amplitude oscillations exist, corresponding to the sharp interfacial shear stress decrease in the transition zone between bubble and slug flow.

Predictions are few sensitive to the nodalization. The use of large cells reduces the void fraction oscillations. A Courant stability criterion reduces sharply the time step in case of fine mesh at the break. This limitation is not found when the version 13.0 of TRAC is used, where the parameter CSF1D in subroutine TF1DS1 had a value 1*10+6 instead of 1*10+3 in version 14.3.

The blowdowns predicted with natural choking are too fast, however with discrepancies less large than for the CANON and SUPER-CANON tests, for which a two phase flow regime exists at the break during a large part of the transient, unlike the VERTICAL-CANON tests.

Table 6.1: VERTICAL-CANON, typical input data deck.

```
FREE
*NUMTCO  IEOS  INOPT  NMAT
6        0     1      0
TRAC-PF1/MOD1 V 14.3 CAMV    13/6/88

9*22*24


*****************************************************
*NAMELIST DATA
 $INOPTS  ICFLOW=1  $END
*MAIN CONTROL CARDS
*  DSTEP  TIMET
   0      0.0
*  STDYST  TRANSI  NCOMP  NJUN  IPAK
   0       1       3      2     0
*  EPSO     EPSI     EPSS
   1.0E-3   1.0E-5   1.0E-4
*  OITMAX  IITMAX  SITMAX  ISOLUT
   10      0       10      0
*  NTSV  NTCB  NTCF  NTRP  NTCP
   0     0     0     0     0
*   COMPONENT
    1     5     * FILL : INLET
    2     5     * PIPE
    3     6     * BREAK : OUTLET
* ()()()()()()()()()()()()()()()()()()()()()()()()()()
  FILL     1   1                  INLET
*  JUN1  IFTY  IOFF
   1     1     0
*  TWTOLD  RFMX  CONCIN  FELV
   0.      0.    0.      0.
*  DXIN    VOLIN     ALPIN  VLIN  TLIN
   0.060   4.71E-4   0.     0.    300.
*  PIN       PAIN  FLOWIN      VVIN  TVIN
*TEST 9
   13.28E+6  0.    0.          0.    300.
*TEST 22
*  5.00E+6   0.    0.          0.    300.
*TEST 24
*  13.42E+6  0.    0.          0.    300.
*  ::::::::::::::::::::::::::::::::::::::::::::::::::::
  BREAK    3   3                 OUTLET
*  JUN  IBTY  ISAT  IVOV  IOFF
   2    0     0     0     0
*  DXIN  VOLIN     ALFIN  TIN    PIN
*TEST 9
   .060  2.10E-6   0.     300.   0.1E+6
*TESTS 22 24
*  .060  1.33E-6   0.     300.   0.1E+6
*  PAIN  CONCIN  RBMX  POFF  BELV
   0.0   0.      0.    0.    0.
```

```
*  ::::::::::::::::::::::::::::::::::::::::::::::::::::
   PIPE  2   2                     TEST SECTION
*  NCELLS  NODES  JUN1  JUN2  ICT
   42      4      1     2     0
*  ICHF  ICONC  IACC  IPOW
   1     0      0     0
*  IQP3TR  IQP3SV  NQP3TS  NQP3SV  NQP3RF
   0       0       0       0       0
*  RADIN  TH     HOUTL  HOUTV  TOUTL
   .090   .0128  0.0    0.0    300.
*  TOUTV  POWIN  POWOFF  RPOWER  POWSCL
   300.0  0.0    0.0     0.0     0.0
*  QP3IN    QP3OFF  RQP3MX  QP3SCL
   0.       0.      0.      0.
*  *****************************************************
*DX  * 0.0610 0.0600 0.0700 0.0630 0.0640        $
       0.0663 0.0710 0.0600 0.0630 0.0610        $
       0.0610 0.0610 0.0600 0.0644 0.0608        $
       0.0604 0.0660 0.1100 0.1300 0.1330        $
       0.1490 0.1900 0.1900 0.1902 0.1990        $
       0.1980 0.1900 0.1330 0.1390 0.1600        $
       0.1700 0.1402 0.1301 0.1300 0.1160        $
       0.1100 0.1000 0.0600 0.0630 0.0640        $
       0.0640 0.0600                             E
*TEST 9
*VOL  * R41 =1.  2.1014E-5                       E
*FA   * R41 =1.  1.5608-3  7.604E-6              E
*TESTS 22 24
*VOL    R41 =1.  1.23300-5                       E
*FA     R41 =1.  1.9608-3  1.96306-6             E
*FRIC* 1.E+30 R42 0.                             E
*GRAV* F  1.0                                    E
*HD  * R10 .100  R6 .103  R16 .100  R3 .103      $
*TEST 9
*    * R6  .00   0.04407   0.0100                E
*TESTS 22 24
     * R6  .100  0.04409   0.0060                E
*NFF * F   1    E
*ALFA* F  0.0   E
*VL  * F  1.E-5 E
*VV  * F  1.E-5 E
*TEST  9
*TL  * F  574.1  E
*TV  * F  574.1  E
*P   * R10 13.304660 R7 13.300860 R6 13.301200 $
       R4 13.287060 R4 13.287060 R8 13.266460  $
       R7 13.263560                            E
*TEST  22
*TL    F  500.1  E
*TV    F  500.1  E
*P     R10 5.714306 R7 5.703060 R6 5.704460    $
     * R4 5.6000300 R4 5.6940060 R6 5.6606750  $
     * R7 5.6020060                            E
*TEST  24
*TL    F  572.1  E
*TV    F  573.1  E
*P     R10 13.446660 R7 13.446200 R6 13.441300 $
     * R4 13.437026 R4 13.632080 R6 13.426564  $
     * R7 13.423606                            E
*PA  * F  0.     E
*QPPP* F  1.     E
*MATID* F  7     E
*TEST  9
*TW  * F  574.1  E
*TEST  22
*TW    F  506.1  E
*TEST  24
*TW    F  573.1  E
* ()()()()()()()()()()()()()()()()()()()()()()()()()()
*             TIME STEP DATA
*  DTMIN  DTMAX  TEND  RTWFP
*TEST 9
   1.E-3  10.    120.  10.0
*TESTS 22 24
*  1.E-3  10.    400.  10.0
*  EDINT  GFINT  DMPINT  SEDINT
   40.    1.E-3  40.     1000.0
   -111111.
```

Table 6.2: VERTICAL-CANON, run statistics.

Test	9	22	24
Real time s	120	400	400
Time step number	3939	4360	4901
Mean time step	0.030	0.092	0.082
CPU time s	186	225	239
CPU time/real time	1.55	0.56	0.60
CPU time/(cell.time step)	1.1•10-3	1.2•10-3	1.2•10-3

7 MARVIKEN BLOWDOWN EXPERIMENTS

7.1 Test Description

The MARVIKEN critical flow tests were conducted between mid-1977 and december 1979 as a multinational project at the Marviken Power Sation in Sweden (Marviken, 1982a).

7.1.1 Test Facility

The four major components of the facility are a vessel, originally designed to be the nuclear power plant vessel, a discharge pipe, connected at the bottom of the vessel, a test nozzle with the minimum flow area in the system, and a rupture disk assembly (Marviken, 1982b).

The total height of the vessel is 24.55 m. The vessel diameter is 5.22 m, and the diameter of the top cupola is 1.5 m. The total volume of the vessel is 421.147 m3. Some initial components of the vessel are included in the vessel (core superstructure, moderator tank), and three gratings were installed to eliminate vortex formation. A schematic of the vessel is shown on figure 7.1a.

The discharge pipe is made up of a streamlined inlet, a connection piece, instrumentation ring 1, the upstream pipe spool, instrumentation ring 2, the ball valve and the downstream pipe spool. The total length of the discharge pipe is 6.308 m, with 0.740 m inside the vessel. The diameter is 0.752 m throughout most of the pipe.

The nozzle consists of a rounded inlet, with a radius of curvature equal to the nozzle radius, followed tangentially by a cylindrical section. The dimensions of the nozzle depend on the test. The nozzle outlet is equipped with an assembly containing two rupture discs. A schematic of the discharge pipe, the nozzle and the rupture discs is shown on figure 7.1b.

7.1.2 Measurements

The Marviken reports give detailed informations concerning the measurements and the data accuracy (Marviken, 1982a and 1982c).

The **pressure** is measured with pressure transducers of the strain gauge type, located at the top and at the bottom of the vessel, at the instrumentation rings of the discharge pipe, and at the inlet and outlet of the nozzle. The maximum error (evaluated from the accuracy specifications released by the manufacturers of the apparatuses) is 90 kPa, and the probable error (obtained by a statistical analysis of the spread of

data from groups of data channels which measured the same quantity) is 9 kPa.

The mean **density** over a diameter and two chords is measured by a gamma densitometer, upstream the second instrumentation ring of the discharge pipe. The probable error is 50 kg/m3.

The **temperature** is measured by chromel-alumel thermocouples, at different locations along the vessel and the discharge pipe. The maximum error is 2 K, and the probable error is 0.6 K.

The pressure differences measured between the wall and Pitot tubes located in the discharge pipe are used to obtain the mass flux profile in the pipe. This profile, together with the measured density, gives the **mass flow rate** throughout the tests. The error concerning the mass flow rate depends on the flow conditions (subcooling or saturation) and on the nozzle diameter. For subcooling conditions and a diameter of 0.300 m, the error is 5 %. For a diameter of 0.500 m, the error is 3 %. The mass flow rate is also evaluated from the axial differential pressures, but the accuracy is less good.

7.1.3 Test Procedure

The first step in the test preparation is to fill the vessel with deionized water until the specified elevation. The water is heated by circulating from the bottom of the vessel through an external electric heater and re-introducing it into the vessel steam dome. A water circulation in the discharge pipe is also organized.

The transient beginns at time zero at the rupture of the discs, and is achieved when the ball valve is closed, or if there is no more liquid in the vessel.

7.1.4 Test Matrix

Twenty-seven tests were conducted, with nozzle diameters of 0.200, 0.300 and 0.500 m, nozzle length to diameter ratios of 0.3 through 3.6, and initial subcooling up to 50 K.

The following tests were selected for TRAC simulation in the frame of the ICAP (D is the nozzle diameter, L is the nozzle cylindrical length, and DT is the initial subcooling):

Test 6: D = 0.3 m, L/D = 1.0, DT = 30 K.
Test 17: D = 0.3 m, L/D = 3.7, DT = 30 K.
Test 24: D = 0.5 m, L/D = 0.3, DT = 30 K.

7.2 Input Model

Tables 7.1 give typical input data decks used for the MARVIKEN simulations.

7.2.1 Components and Boundary Conditions

The vessel is modelled with a PIPE component, and the discharge pipe together with the nozzle by a second PIPE component. The closed end of the vessel is modelled with a FILL component with zero velocities. The break is modelled with a BREAK component, where the pressure is imposed.

7.2.2 Nodalization

The PIPE component modelling the vessel is divided into 15 cells, with a minimum length of 0.7 m, and a maximum of 2.3 m. The discharge pipe is modelled with 10 cells (length 0.38 through 0.74 m). The nozzle (including the rounded inlet) is modelled with 2 or 3 cells depending on the test (test 6: cell length of 0.15 and 0.29 m, test 17: 0.42, 0.43 and 0.43 m, test 24: 0.22 and 0.17 m).

7.2.3 Initial Conditions

The initial conditions imposed in each cell of the PIPE components are stated hereafter. The pressure is the hydrostatic pressure calculated from the pressure at the top of the vessel. The liquid temperature profile is the experimental profile. The vapor temperature is the saturation temperature corresponding to the pressure at the top of the vessel. The void fraction is 1 for the cells located above the initial level, and 0 for the cells located under. For the cell including the level, the void fraction is calculated from the level position. The initial velocities are 1*10-5 m/s.

The blowdown is initiated at time zero by setting the break pressure to the value 0.1 MPa. The time step is free, with an initial value of 1 *10-2 s. Base case simulations are performed with the choked flow model.

7.3 Code Predictions and Comparisons with Data

7.3.1 Tests 17 and 24

The initial pressure trough is not predicted by the code, due to the absence of a delayed boiling model. The pressure is then underpredicted, with a maximum difference with data of about 0.2 MPa, and is overpredicted at the end of the transient.

The mass flow rate is underpredicted with a difference with the data of about 20 % for test 17, and about 30 % for test 24. The simulation with the choked flow model (homogeneous model) is more convenient for test 17 with a long nozzle, than for test 24 with probably a more large thermal desequilibrium.

The predicted temperature in the discharge pipe is in good agreement with the data at the beginning of the transient. From 50 s for test 17, and from 30 s for test 24, the temperature becomes slightly overpre-

dicted, when it has reached the saturation value, and corresponds to the overestimation of the pressure.

The results of tests 17 and 24 are presented on figures 7.2.

7.3.2 Test 6

Test 6 is analysed apart from the other, because it was performed in experimental conditions less good than the other tests: changes were made after test 14 in the internal devices of the vessel, the rupture discs geometry, and the test procedures. The initial temperature profile is questionable, and radial temperature differences as high as 8 K are measured in the discharge pipe during the transient, whereas temperatures differences lower than the data accuracy are measured for tests 17 and 24.

The density used for the evaluation of the experimental mass flow rate is the liquid density until time 39 s, and after this time it is a two phase density deduced from pressure difference measurements in the discharge pipe. The discrepancy at time 39 s is caused by the use of these two methods, and is probably not a real mass flow rate discrepancy.

The pressure predictions are similar to the other tests. The mass flow rate is underpredicted with a difference with the data of about 25 % in the period of single phase flow in the discharge pipe. The temperature in the discharge pipe is underpredicted from the beginning of the blowdown, whereas it was in good agreement with the data for the other tests. This confirms the dubious test conditions of test 6, especially concerning the initial temperature profile.

The results of test 6 are presented on figures 7.3.

7.4 Run Statistics

The runs were performed on a CRAY-XMP-2200 computer with TRAC-PF1/MOD1 version 14.3. The run statistics are shown on table 7.2, and figures 7.4 and 7.5 show the plots of the time step and CPU time versus real time for tests 6, 17 and 24.

7.5 Sensitivity Studies

7.5.1 Nozzle Alone

As the pressure and temperature conditions are measured during the transient at the nozzle entrance, it is possible to simulate the MARVIKEN tests without the vessel. The measured pressure and temperature conditions at 0.675 m upstream the nozzle inlet are imposed in a BREAK com-

ponent, and also the void fraction. During the period of two phase flow in the nozzle, the experimental void fraction at this location is not known, nence only the initial period of the transient, with single phase in the discharge pipe is simulated with nozzle alone.

For test 17, the perdicted mass flow rate discrepancy with the data is about -10 %, whereas it was about -20 % for the reference run. For test 24, the two runs differ only from the time where the pressure is underpredicted in the reference run. For test 6, the discrepancy is -35 % whereas the reference was -25 %, and this difference comes from the underprediction of the discharge pipe temperature for the reference run.

The results of the runs with nozzle alone, and the comparison with the reference runs are presented on figures 7.6.

7.5.2 Modalization

The simulation of test 24 was performed with a fine mesh at the break. The nozzle was modelled with 6 cells (0.125, 0.100, 0.066, 0.050, 0.030 and 0.020 m) instead of 2. The results show little variations with regard to the reference run, but the time steps are divided into 3 or 4 (fig. 7.7).

7.5.3 Natural Choking

7.5.3.1 Reference Meshing

The simulation of test 24 was performed with natural choking. The predicted blowdown is somewhat faster than for the reference run, and the mass flow rate is underpredicted by only about 14 % instead of 30 % (fig. 7.8).

7.5.3.2 Fine Mesh

The simulation of tests 17 and 24 was performed with natural choking and with a fine mesh at the break. The results are the same as the reference for test 17, whereas the mass flow rate discrepancy is -24 % instead of -30 % for test 24 (fig. 7.9).

These differences are attributed to the predominance of interphase desequilibrium effects caused by the short nozzle length for test 24. The choked flow model does not take into account the thermal desequilibrium phenomena.

7.6 Summary and Conclusions

The simulation of three MARVIKEN blowdown tests was performed with the code TRAC-PF1/MOD1 version 14.3. The vessel is modelled with 15 cells, the discharge pipe with 10 cells, and the nozzle with 2 or 3 cells.

The initial pressure undershoot is not predicted, due to the absence of a delayed boiling model. The mass flow rates are underpredicted with discrepancies of 20 % for test 17 with long nozzle, and of 25 % (test 17) and 30 % (test 6, initial temperature profile questionable) for the tests with short nozzles, where the interphase thermal desequilibrium phenomena are probably more considerable.

The runs performed with a simulation of the nozzle alone differ from the reference runs when the conditions predicted by the reference runs upstream the nozzle are in desagreement with the data. The mass flow rates with the nozzle alone are underpredicted with a discrepancy of 10 % for test 17 with long nozzle, and of 30 and 35 % for the tests with short nozzles.

The run performed with a fine mesh at the break gives similar results as the reference run, with a reduced time step (test 24).

The runs performed with a fine mesh at the break and natural choking give similar results as the reference for test 17 with a long nozzle, and a mass flow rate larger than the reference run (discrepancy of -24 % instead of -30 %) for test 24 with a short nozzle. The absence of thermal desequilibrium for test 17 leads to equivalent results with and without the choked flow model. For test 24, a better agreement is found when the thermal desequilibrium is taken into account.

Table 7.1a: HARVIKEN, typical input data deck, reference run.

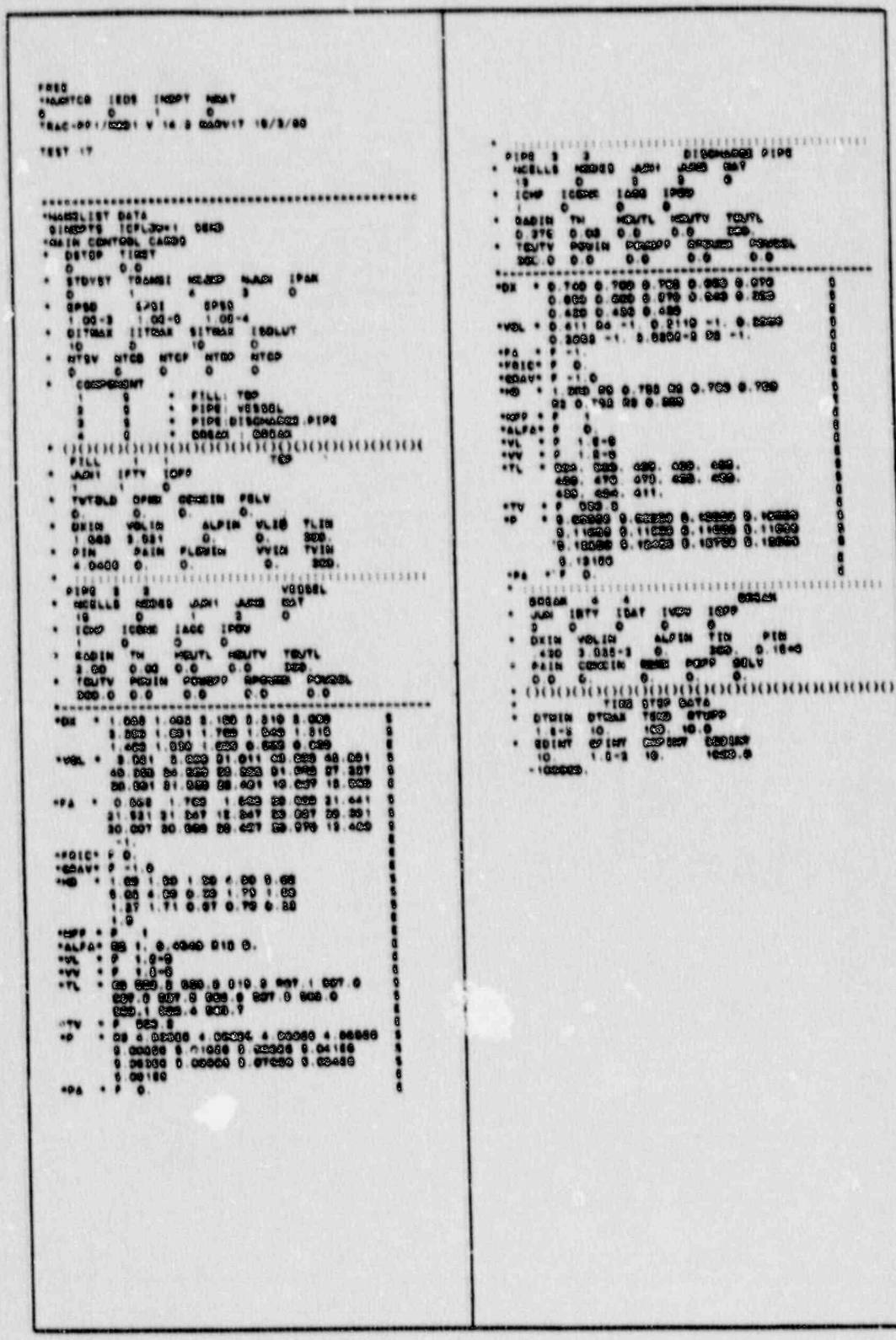

Table 7.1b: HARVIKEN, typical input data deck, nozzle alone run.

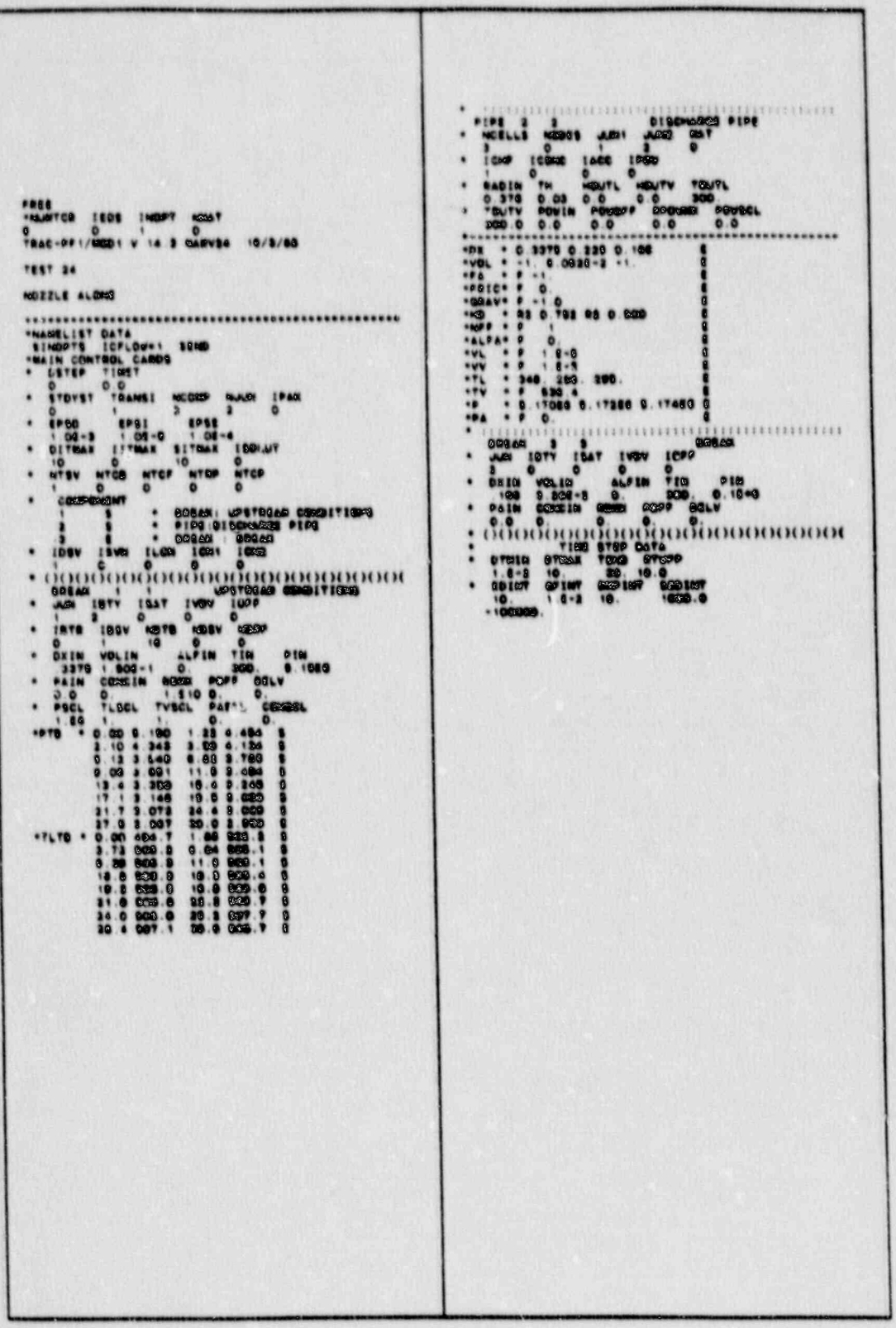

Table 7.2: MARVIKEN, run statistics.

Test	6	17	24
Real time s	101	100	80
Time step number	160	143	211
Mean time step	0.63	0.70	0.38
CPU time s	7.1	7.8	10.2
CPU time/real time	0.07	0.08	0.13
CPU time/(cell.time step)	1.6•10-3	1.9•10-3	1.8•10-3

8 OMEGA-TUBE BLOWDOWN EXPERIMENTS

8.1 Test Description

The OMEGA-TUBE blowdown tests were conducted in the Service des Transferts Thermiques of the Centre d'Etudes Nucléaires de Grenoble (France), during the year 1978 (Juhel, 1980).

8.1.1 Test Section

The test section OMEGA-TUBE consists of a straight vertical electrically heated pipe, connected upwstream and downstream to capacities (fig. 8.1). The connection pipes support spool pieces.

The heated tube simulates a reactor core subchannel. It consists of an insulated tube made of inconel 600, with 12 mm inside diameter, 2.14 mm thicknoss and 3.657 m length. The capacities simulate the primary circuit volumes. They are cylindrical, with a converging nozzle at one end, leading to the break. The capacities are connected to the main circuit of the loop through flexible pipes and quick closing valves.

8.1.2 Measurements

The procedure of the measurements is complex, and many corrections are added to the primary measurements. Few indications concerning the uncertainties are given in the experiment report.

The **pressure** is measured at different locations along the test section. The uncertainty is 2 %.

The **fluid temperature** is measured at different locations along the test section, by chromel-alumel thermocouples. The temperature error is 2 K. The indications given by the fluid temperature thermocouples may be erroneous: if droplets are traped by the thermocouples, a single phase vapor flow may not be detected.

The **wall temperature** is measured at different locations along the heated tube by 50 chromel-alumel thermocouples brazed on the outer wall of the heated tube.

The mean **void fraction**, along a diameter and along a chord is measured upstream and downstream the heated pipe, by a gamma rays attenuation technique.

The **mass flow rates** are measured by symetrical venturis and by flowmeters located upstream and downstream the heated pipe. The measure-

ments by the flowmeters are more accurate than the venturi measurements, but probably overpredicted at the end of the slow transients. The mass flow rates in the connection pipes are measured by venturis located near the quick closing valves.

The power dissipated in the heated pipe is calculated from amperage and voltage measurements.

8.1.3 Test Procedure

The test procedure beginns with the establishment of a steady state vertical upflow. When the nominal conditions are reached, the system is vented to the atmospheric pressure by bursting the break(s) rupture discs. Valves insulating the test section from the loop are closed after the opening of the break(s). The closure of the two valves is not simultaneous. The electric power decay is programed versus time. In addition, the power is cut off when one wall thermocouple reaches a chosen threshold.

8.1.4 Test Matrix

Twenty-six OMEGA-TUBE tests were performed, with the initial flow conditions stated hereafter: the pressure is 16 MPa (except one test with 11 and one test with 13 MPA), the inlet temperature is 558 K and the mass flow rates is 0.4 through 0.6 kg/s. Three wall heat flux (0.0, 0.6 and 1.25 Mw/m2), three break area (7.5, 15, 30 and 50 mm2) and three break positions (bottom break, top break and double break) are used.

The following tests were selected for TRAC simulation in the frame of the ICAP:

Test 3: bottom break(50 mm2), Fi=0.0 Mw/m2, P=13 MPa, Q=0.5 kg/s.
Test 6: top break(50 mm2), Fi=1.25 Mw/m2, P=16 MPa, Q=0.5 kg/s.
Test 8: double break(30 mm2), Fi=1.25 Mw/m2, P=16 MPa, Q=0.5 kg/s.
Test 9: double break(30 mm2), Fi=0.0 Mw/m2, P=16 MPa, Q=0.6 kg/s.
Test 29: bottom break(7.5 mm2), Fi=0.60 Mw/m2, P=16 MPa, Q=0.4 kg/s.
Test 30: double break(7.5 mm2), Fi=0.60 Mw/m2, P=16 MPa, Q=0.4 kg/s.

8.2 Input Model

Table 8.2 gives typical input data decks used for OMEGA-TUBE simulations with TRAC.

8.2.1 Components and Boundary Conditions

The test section is modelled with a combination of eleven components (fig. 8.2). The capacities and connections are modelled with a TEE. The spool pieces, expansion joint, transition pieces and heated tube are modelled with five successive PIPE components, each with a different wall thickness.

The entrance and exit of the initial steady state flow are modelled with a FILL component, where the mass flow rate is imposed. The breaks are modelled with a BREAK component when the break opens, and with a FILL component when the break remains closed.

8.2.2 Nodalization

The measurement locations correspond to the center of a cell (pressure, temperature, void fraction), or to the edge of a cell (mass flow rate). Exception is made for the pressure and temperature measurements at the entrance and exit of the heated pipe (the difference between the measurement location and the cell center is about 3 cm). The nodalization of the heated tube used for tests 29 and 30 slightly differs from the nodalization used for the other tests, because the significant wall temperatures are not located at the same positions. The area variations along the test section (spool pieces) are taken into account in the cell volume evaluation.

The heated length is modelled with 20 cells, and the whole test section with 63 or 67 cells, depending on the test. Two nodalizations of the capacities are used: a coarse mesh with 3 cells, and a fine mesh with 7 cells (fig. 8.3). The better nodalization is used for each test to ensure a realistic blowdown of the capacities. The sensitivity to the nodalization of the capacities is studied in paragraph 8.5.1.

The wall of each PIPE and TEE is modelled with 4 nodes.

8.2.3 Friction Factor

The standard option is used for all components, except for the expansion joint, where the experimental value is used (NFF=0 and FRIC=0.05).

8.2.4 Steady State Flow

The simulation of each test is performed with two successive runs. A first run gives the initial steady state regime (option STDYST=1). The experimental mass flow rate is imposed at the two connections, bottom inflow, and top outflow. The inlet temperature is imposed at the bottom junction. The pressure is imposed at the break location for single break tests. For double break tests, a slight overpressure (0.2 MPa) is imposed at the bottom break, in order to avoid liquid losses through the bottom break. The experimental pressure is imposed at the top break.

The initial values imposed at each cell are the following: velocities of 3 m/s, experimental pressure, inlet temperature for the heated tube and the bottom components, outlet temperature for the top components. The time step is free, with an initial value of 1*10-2 s.

When the steady state is reached, the results are dumped to be used as the initial state for the blowdown simulation. The steady state is reached within about 100 time steps (about 9 s CPU) for the tests with heated wall.

8.2.5 Blowdown

The second run simulates the blowdown. The simulation begins at the experimental time zero. Breaks are opening at time 2.55 or 2.60 s, not always simultaneously in case of double break. In the model, the imposed pressure decreases from the initial value to 0.1 Mpa within 0.003 s. The experimental mass flux at the connections and the experimental power dissipated in the heated tube are imposed versus time.

The initial time step is 1*10-3 s. The time step is bounded upwards within specified periods, in order that the breaks opening, valves closure and power cut off correspond to the experimental times. The choked flow model is used.

8.3 Code Predictions and Comparison with Data

The comparisons between the predictions and the data are made for the following parameters: pressure P9 at the bottom of the heated tube, mass flow rates and void fractions at the top and bottom of the heated tube, fluid temperatures TF4 and TF5 at the top and bottom of the heated tube and wall temperatures at different locations along the heated tube.

8.3.1 Tests with Bottom Break

The tests with bottom break are characterized by a mass flow rate which reverses towards the break as soon as the break opens.

8.3.1.1 Test 3

Test 3 is performed without heat flux. The fine mesh is used to model the top capacity, and the coarse mesh for the bottom one. The results are presented on figures 8.4.

The pressure at the beginning of the boiling is overpredicted with a discrepancy of 0.2 MPa, and the final pressure decrease is anticipated. The oscillations after the sharp decrease of the pressure correspond to the period between the opening of the break and the closure of the valves. The beginning of boiling is predicted too early, and hence the short period of zero mass flow rate (3.5 - 4 s) is not predicted. The blowdown of the top capacity is well predicted. The bottom temperature oscillations correspond to oscillations of the heat transfert coefficient between transition and vapor single phase flow regime.

8.3.1.2 Test 29

Test 29 is performed with the smallest break area and a heat flux cut off at time 31.5 s. The coarse mesh is used to model the two capacities. The results are presented on figures 8.5.

The boiling inception pressure is overpredicted and the final pressure decrease anticipated. During the first stage of the blowdown, the mass flow rates and void fractions are well predicted. From time 12 s, the mass flow rates and the top void fraction are overpredicted: the predicted blowdown of the top capacity is too fast. The final transition to vapor single phase is anticipated.

The boiling crisis is well predicted in the bottom part of the heated tube. The final wall temperature increase is anticipated, due to the too fast voidage of the top capacity, and the boiling crisis is predicted in the top region, whereas the measurements show little wall temperature increases. After the power cut off, the predicted wall temperatures decrease very slowly because the blowdown is quite ended, and the velocities are low. The predicted maximum wall temperature is 1150 K, compared to 940 K for the data.

8.3.2 Test 6 with Top Break

Test 6 with top break is characterized by a mass flow rate which remains upwards. The power is cut off at time 9 s. The bottom capacity is modelled with the fine mesh, and the top one with the coarse mesh.

The boiling inception pressure is overpredicted and the final pressure decrease anticipated. The two slope ruptures correspond to the inception of boiling in the hot top capacity first, and in the cold bottom capacity secondly. During the first period of the blowdown, the mass flow rates and void fractions are well predicted. After time 6 s, the predicted bottom flow rate increase is too late, and the void fraction is underpredicted. The voidage of the bottom capacity is somewhat too fast.

The wall temperatures are well predicted in the top region of the heated tube, with a too fast decrease after the power cut off, which corresponds to an overprediction of the mass flow rate. The maximum wall temperature is 840 K for the code, and 835 K for the data. In the bottom region , a boiling crisis is predicted at time 5.5 s, whereas the data indicate no temperature increase. The Biasi critical heat flux correlation used by TRAC is not suitable for the low qualities that exist in the bottom part of the tube.

8.3.3 Tests with Double Break

The tests with double break are characterized by a mass flow rate which reverses during the transient, depending on the position of the stagnation point. The two capacities are modelled with the coarse mesh.

8.3.3.1 Test 9

Test 9 is performed without heat flux, with the same area for the two breaks. The results are presented on figures 8.7.

The pressure is slightly overpredicted. The position of the stagnation point compares poorly with the data. It is predicted in the middle part of the test section at the beginning of boiling, whereas data indicate its location in the bottom capacity. Later at time 9 s, the downwards flow of liquid from the top capacity is not predicted by the code. The predicted bottom void fraction evolution is much more regular than indicated by the data. For this test, the model used for the capacities is not satisfactory.

8.3.3.2 Test 8

Test 8 differs from test 9 only by the existence of a heat flux, which is cut off between 6 and 7 s. The results are presented on figures 8.8.

The boiling inception pressure is overpredicted with a discrepancy of 0.5 MPa. The pressure is then underpredicted, and overpredicted at the end of the transient. The mass flow rates and void fractions are well predicted, as is the blowdown of the two capacities. The fluid temperature increases are anticipated by the code. The oscillations at the end of the blowdown correspond to intermittent liquid flow from the top capacity.

The boiling crisis is predicted since boiling beginns, and the wall temperatures are overpredicted. The maximum wall temperature as seen by the code is 810 K, and is 780 K in the data. The anticipation of the boiling crisis is caused by the use of the Biasi CHF correlation, the mass flow rate range of which beeing limited to 6*10+3 kg/m2*s, whereas the predicted mass flow rate is 10*10+3 kg/m2*s. The critical heat flux given by the correlation decreases for increasing mass flow rates, hence for large mass flow rates too low heat flux are obtained, and a too early boiling crisis.

8.3.3.3 Test 30

Test 30 is performed with two breaks with the smallest area, and a heat flux cut off at time 13.5 s. The results are presented on figures 8.9.

The boiling inception pressure is overpredicted with a discrepancy of 0.6 MPa. The pressure is underpredicted at the end of the transient. The increase of the bottom void fraction is anticipated, hence the bottom mass flow rate vanishes to early. The downwards voidage of the top capacity is too fast: it is achieved at time 11 s for the code, and 13 s for the data. The model used for the capacities, and particularly the top one is not satisfactory. Fluid temperature increases are predicted which do not exist in the data. At the bottom of the heated tube, successive vapor single phase flow are indicated by both the code and the data.

The boiling crisis is slightly anticipated at the two ends of the tube. The maximum wall temperature is overpredicted: 1000 K for the code, and 960 K for the data. The quenching of the top region is not predicted, due to the too early voidage of the top capacity.

8.4 Run Statistics

The runs were performed on a CRAY-XMP-2200 computer with TRAC-PF1/MOD1 version 14.3. The run statistics are presented on table 8.2, and figures 8.10 and 8.11 show the plots of the time step and CPU time versus real time, for each test.

8.5 Sensitivity Studies

8.5.1 Capacity Meshing

The agreement between test and TRAC results is strongly dependent on a good prediction of the capacities voidage. For tests 3 (no power, bottom break), 6 (top break), and 8 (double break) only, the models used are satisfactory. Before the obtention of the reference models, several meshing of the capacities were tested. Examples of the sensitivity to the meshing of the capacities are presented on figures 8.12. Depending on the number of cells modelling the capacities, the liquid is retained a more or less long time in the capacity, before to be voided into the tube or through the break.

For tests 9 (no power, double break), 29 (small bottom break) and 30 (small double break), several meshing were also tested, with no better results than those obtained with a coarse mesh modelling the two capacities. Examples are presented on figures 8.13.

No correspondance is found between a specified geometry (break area or break position) and a specified meshing; nothing systematic appears.

8.5.2 Use of PLENUM Components

The simulation of tests 8 and 30 was made with the two capacities modelled with a PLENUM component. As no wall exists for the PLENUM components, the comparison was made with runs performed with the capacities modelled with TEE components without wall.

The results obtained are very different from the reference runs, and the agreement with the data is bad (fig. 8.14). The PLENUM component is not convenient to model the cylindrical capacities of the test section OMEGA-TUBE.

8.5.3 Nodalization

Test 8 was simulated with 37 cells modelling the whole test section instead of 63 (10 cells are used instead of 20 for the heated tube), and with the same capacity meshing. The results show little nodalization sensitivity. The coarse mesh leads to a maximum wall temperature higher from about 10 K (fig. 8.15).

8.5.4 Natural Choking

The simulation of test 30 was made with natural choking, and with a fine mesh at the break: the converging nozzle is modelled with 3 cells of length 0.04, 0.02 and 0.01 m. The predicted blowdown is too fast and the time step is divided into about a decade (fig. 8.16).

8.6 Summary and Conclusion

The simulation of six OMEGA-TUBE blowdown tests was performed with TRAC-PF1/MOD1 version 14.3. The test section is modelled with 63 or 67 cells. The bottom and top capacities are modelled with a TEE component, the vertical part of which being divided into 3 or 7 cells.

The general agreement between data and TRAC is moderate: the major trends are correctly predicted, but the predicted parameters are frequently outside the data uncertainties. During the period between the opening of the breaks and the closure of the valves, which insulate the test section, large pressure oscillations occur. The absence of a delayed boiling model leads to a boiling inception pressure overpredicted with discrepancies up to 0.6 Mpa. The voidage of the capacities towards the test section or the break, which governs the blowdown, is not correctly predicted for some tests. The Biasi CHF correlation used in TRAC is not suitable for low qualities on one hand, and for large mass flow rates on the other hand and leads to anticipated boiling crisis.

The sensitivity of the results to the meshing of the capacities is significant. Whether a capacity is modelled with more or less cells, the voidage of the capacity into the test section is more or less fast. Nevertheless, a satisfactory meshing for all the tests was not found. Furthermore, the use of a PLENUM component is not adapted to model the cylindrical capacities of the test section.

The sensitivity to the nodalization of the test section (except capacities) is weak. The run performed with natural choking and with a fine mesh at the breaks leads to a too fast blowdown. The use of a fine mesh induces a sharply reduced time step.

Table 8.1a: OMEGA-TUBE, typical input data deck, single break test, steady state run.

```
FREE
*NUMTCB  IEOS  INOPT  NMAT
2        0     1      0
TRAC MOD1 V 14.3 OMT20  11/3/88

TEST 20

STEADY STATE

**************************************************
*   NAMELIST DATA
 $INOPTS  ICFLOW=1  $END
*  DSTEP  TIMET
    0      0.0
*  STDYST  TRANSI  NCOMP  NJUN  IPAK
   1       0       11     10    0
*  EPSO     EPSI     EPSS
   1.0E-3   1.0E-5   1.0E-4
*  OITMAX  IITMAX  SITMAX  ISOLUT
   10      0       10      0
*  NTSV  NTCB  NTCF  NTRP  NTCP
   1     0     0     0     0
*   COMPONENT
    1     5    * BREAK  : UPSTREAM BREAK
    2     5    * TEE    : UPSTREAM VOLUME
    3     5    * PIPE   : UPSTREAM SPOOL PIECE
    4     5    * PIPE   : EXPANSION JOINT
    5     5    * PIPE   : UPSTREAM CONNEXION
    6     5    * PIPE   : HEATED TUBE
    7     5    * PIPE   : DOWNSTREAM CONNEXION
    8     5    * TEE    : DOWNSTREAM VOLUME
    9     5    * FILL   : DOWNSTREAM BREAK
    10    5    * FILL   : INLET
    11    5    * FILL   : OUTLET
* IDSV  ISVN  ILCN  ICN1  ICN2
  1     0     0     0     0
* ()()()()()()()()()()()()()()()()()()()()()()()()(
  BREAK   1   1        UPSTREAM BREAK
*  JUN  IBTY  ISAT  IVOV  IOFF
   1    1     0     1     0
*  IBTR  IBSV  NBTB  NBSV  NBRF
   0     1     4     0     0
*  DXIN  VOLIN     ALPIN  TIN     PIN
   .120  2.046E-4  0.     560.2   15.61866
*  PAIN  CONCIN  RBMX   POFF  BELV
   0.0   0.      1.E16  0.    0.
*  PSCL *        1.E6
* PTB * 0.000  15.616  2.600  15.616  S
        2.603  0.10    50.0   0.10    E
* ::::::::::::::::::::::::::::::::::::::::::::::::
  TEE   2   2            UPSTREAM VOLUME
*  JCELL   NODES  MAT  COST  ICHF
   2       4      0    0.    1
*  ICONC1  NCELL1  JUN1  JUN2  IPOW1
   0       3       1     2     0
*  IOPTR1  IOPSV1  NOPTB1  NOPSV1  NOPRF1
   0       0       0       0       0
*  RADIN1  TH1     HOUTL1  HOUTV1  TOUTL1
   .0043   0.012   0.      0.      300.
*  TOUTV1  PWIN1   PWOFF1  RPWMX1  PWSCL1
   300.0   0.      0.      0.      0.
*  QPIN1     QPOFF1  RQPMX1  QPSCL1
   0.        0.      0.      0.
*  ICONC2  NCELL2  JUN3  IPOW2
   0       4       3     0
*  IOPTR2  IOPSV2  NOPTB2  NOPSV2  NOPRF2
   0       0       0       0       0
*  RADIN2  TH2     HOUTL2  HOUTV2  TOUTL2
   .008    0.002   0.      0.      300.
*  TOUTV2  PWIN2   PWOFF2  RPWMX2  PWSCL2
   300.0   0.      0.      0.      0.
*  QPIN2     QPOFF2  RQPMX2  QPSCL2
   0.        0.      0.      0.
*  PRIMARY SIDE ----------------------------------
*DX    * 0.120 0.124 0.270                 E
*VOL   * 2.0277E-4    -1.  1.9604E-3       E
*FA    * F -1.                             E
*FRIC* * F 0.                              E
*GRAV* * F  1.0                            E
*HD    * 0.00310 R2 0.006  0.030           E
*NFF   * F     1           E
*ALPA* * F  0.0            E
*VL    * F  3.0            E
*VV    * F  3.0            E
*TL    * F  560.2          E
*TV    * F  560.2          E
*P     * F  15.666         E
*PA    * F  0.             E
*QPPP* * F  0.             E
*MATI* * F  7              E
*TW    * F  560.2          E
*   SECONDARY SIDE --------------------------------
*DX    * 0.110 0.100 0.120 0.300 E
*VOL   * F   -1.     E
*FA    * F  -1.      E
*FRIC* * F  0.       E
*GRAV* * F  0.0      E
*HD    * F  0.016    E
*NFF   * F    1      E
*ALPA* * F  0.0      E
*VL    * F  3.0      E
*VV    * F  3.0      E
*TL    * F  560.2    E
*TV    * F  560.2    E
*P     * F 15.666    E
*PA    * F  0.       E
*QPPP* * F  0.       E
*MATI* * F 7         E
*TW    * F  560.2    E
* ::::::::::::::::::::::::::::::::::::::::::::::::
  PIPE   3   3           UPSTREAM SPOOL PIECE
*  NCELLS  NODES  JUN1  JUN2  MAT
   10      4      2     3     0
*  ICHF  ICONC  IACC  IPOW
   1     0      0     0
*  IQP3TR  IQP3SV  NQP3TB  NQP3SV  NQP3RF
   0       0       0       0       0
*  RADIN   TH      HOUTL  HOUTV  TOUTL
   .0118   .010    0.0    0.     300.
*  TOUTV   POWIN   POWOFF  RPOWMX  POWSCL
   300.0   0.0     0.0     0.0     0.0
*  QP3IN     QP3OFF  RQP3MX  QP3SCL
   0.        0.      0.      0.
* ------------------------------------------------
*DX  * 0.140 0.180 0.175 0.170 0.170             S
       0.175 0.180 0.170 0.147 0.130             E
*VOL * 9.0051E-6 R2 -1. 8.7310E-6 -1. 8.[illegible]E-6 S
       6.1602E-6 7.0360E-6 -1. 3.[illegible]E-6  E
*FA  * R10 -1.   3.6363E-4                       E
*FRIC* R10 0. 0.08                               E
*GRAV* R8  1.0 0.88 0.0                          E
*HD  * 0.020 R3 0.0200 R2 0.0277 0.0288 0.0364   S
       R2 0.080 0.0086                           E
*NFF * R10  1 0        E
*ALPA* F  0.0          E
*VL  * F  3.0          E
*VV  * F  3.0          E
*TL  * F  560.2        E
*TV  * F  560.2        E
*P   * F  15.666       E
*PA  * F  0.           E
*QPPP* F  0.           E
*MATI* F  7            E
*TW  * F  560.2        E
* ::::::::::::::::::::::::::::::::::::::::::::::::
  PIPE   4   4           EXPANSION JOINT
*  NCELLS  NODES  JUN1  JUN2  MAT
   8       4      3     4     0
*  ICHF  ICONC  IACC  IPOW
   1     0      0     0
*  IQP3TR  IQP3SV  NQP3TB  NQP3SV  NQP3RF
   0       0       0       0       0
*  RADIN   TH      HOUTL  HOUTV  TOUTL
   .00475  .008    0.0    0.     300.
*  TOUTV   POWIN   POWOFF  RPOWMX  POWSCL
   300.0   0.0     0.0     0.0     0.0
*  QP3IN     QP3OFF  RQP3MX  QP3SCL
   0.        0.      0.      0.
* ------------------------------------------------
*DX  * R2 0.175 R2 0.120 R2 0.175                       E
*VOL * R2 4.0010E-6 R2 3.0041E-6 R2 4.0010E-6           E
*FA  * F   2.0000E-4                                    E
*FRIC* F  0.08                                          E
*GRAV* R2 0.0 0.200 0.004 0.200 R7 0.0                  E
*HD  * F 0.0080      E
*NFF * F  0          E
*ALPA* F  0.0        E
*VL  * F  3.0        E
*VV  * F  3.0        E
*TL  * F  560.2      E
*TV  * F  560.2      E
*P   * F  15.666     E
*PA  * F  0.         E
*QPPP* F  0.         E
*MATI* F  7          E
*TW  * F  560.2      E
* ::::::::::::::::::::::::::::::::::::::::::::::::
  PIPE   5   5           UPSTREAM CONNEXION
*  NCELLS  NODES  JUN1  JUN2  MAT
   2       4      4     5     0
*  ICHF  ICONC  IACC  IPOW
   1     0      0     0
*  IQP3TR  IQP3SV  NQP3TB  NQP3SV  NQP3RF
   0       0       0       0       0
*  RADIN   TH      HOUTL  HOUTV  TOUTL
   .00664  .010    0.0    0.     300.
*  TOUTV   POWIN   POWOFF  RPOWMX  POWSCL
   300.0   0.0     0.0     0.0     0.0
*  QP3IN     QP3OFF  RQP3MX  QP3SCL
   0.        0.      0.      0.
```

Table 8.1a (continued)

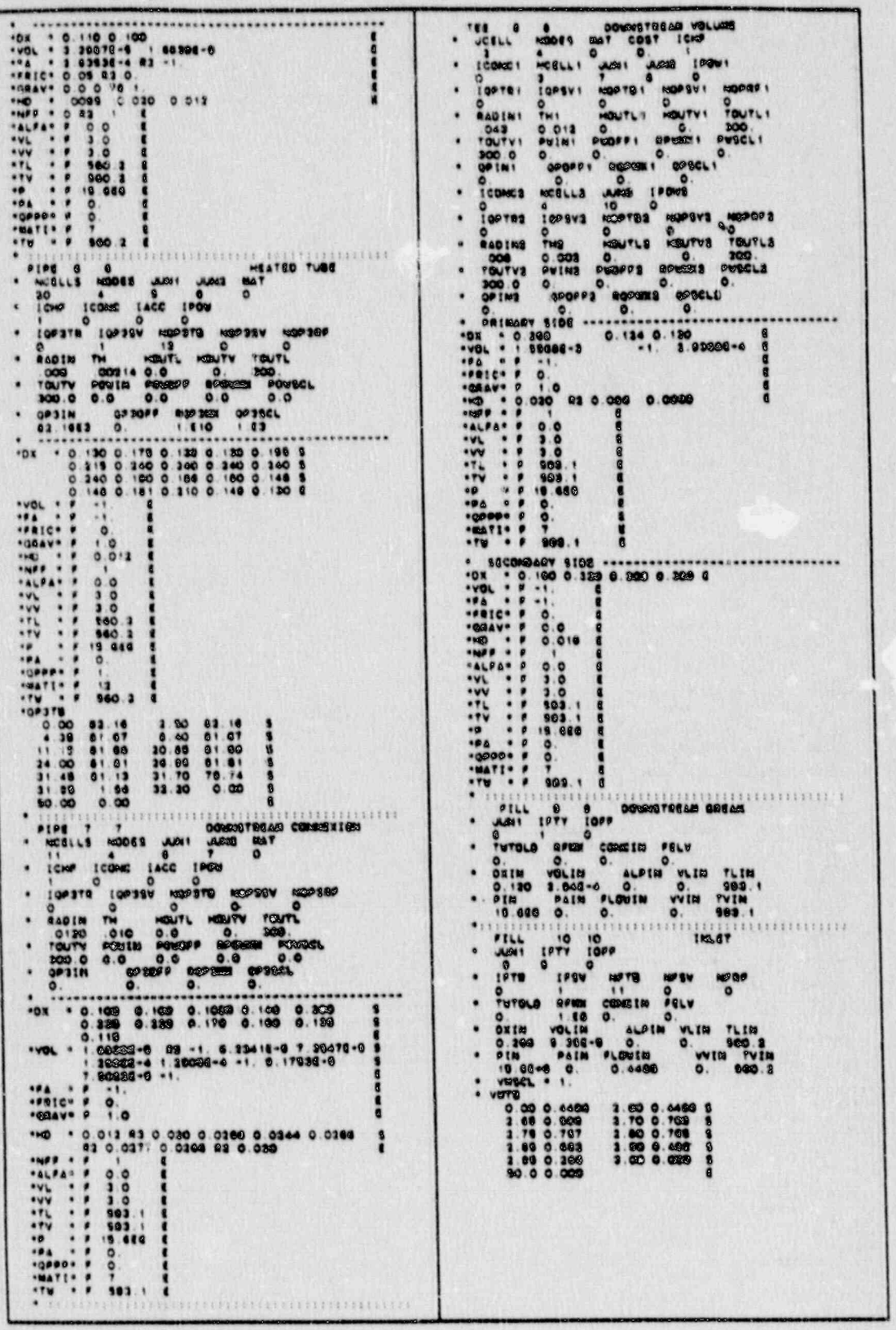

Table 8.1a (continued)

```
* ::::::::::::::::::::::::::::::::::::::::::::::::::::
  FILL      11   11              OUTLET
* JUN1   IFTY   IOFF
  10     6      0
* IFTR     IFSV    NFTB    NFSV    NFRF
  0        1       11      0       0
* TWTOLD   DPEN   CONCIN   FELV
  0.       1.54   0.       0.
* DXIN    VOLIN       ALPIN   VLIN   TLIN
  0.240   7.038-3     0.      0.     543.1
* PIN       PAIN   FLOWIN       VVIN   TVIN
  15.5E+6   0.     -0.4400      0.     553.1
* VMSCL   =  1.
* VFTB
    0.00  -0.4400      2.00  -0.4400   S
    2.60   0.117       2.70   0.246    S
    2.75   0.230       2.80   0.273    S
    2.85   0.253       2.90   0.195    S
    2.95   0.144       3.00   0.000    S
    50.    0.000                       E
* ()()()()()()()()()()()()()()()()()()()()()()()()()(
*              TIME STEP DATA
* DTMIN   DTMAX   TEND   RTWFP
  1.E-3   50.      50.   10.0
* EDINT   GFINT    DMPINT   SEDINT
   5.     1.E-2   10.       1000.0
  -100000.
```

Table 8.1b: OMEGA-TUBE, typical input data deck, transient run.

```
FREE
*NUMTCR  IEOS  INOPT  NMAT
6        0     1      0
TRAC MOD1 V 14.3 OMT20R  1/4/88

TEST 20

RESTART

*********************************************
*   NAMELIST DATA
 $INOPTS  ICFLOW=1  $END
*  DSTEP  TIMET
   -1     0.00
*  STDYST  TRANSI  NCOMP  NJUN  IPAK
   0       1       11     10    0
*  EPSO     EPSI     EPSS
   1.0E-3   1.0E-6   1.0E-4
*  OITMAX  IITMAX  SITMAX  ISOLUT
   10      0       10      0
*  NTSV  NTCB  NTCF  NTRP  NTCP
   1     0     0     0     0
*   COMPONENT
  1  2  3  4  5  5
  6  7  8  9  10 5
 11              6
* IOSV  ISVN  ILCN  ICN1  ICN2
  1     0     0     0     0
* ()()()()()()()()()()()()()()()()()()()()()()(
END
* ()()()()()()()()()()()()()()()()()()()()()()(
*           TIME STEP DATA
*----------------------------------------------
*  DTMIN  DTMAX  TEND   RTWFP
   1.     1.      2.0    10.0
*  EDINT  GFINT  DMPINT  SEDINT
   2.            10.     1000.0
*----------------------------------------------
*  DTMIN  DTMAX  TEND   RTWFP
   1.E-1  1.E-1   2.40   10.0
*  EDINT  GFINT  DMPINT  SEDINT
   2.     1.E-1  10.     1000.0
*----------------------------------------------
*  DTMIN  DTMAX  TEND   RTWFP
   1.E-2  1.E-2   2.50   10.0
*  EDINT  GFINT  DMPINT  SEDINT
   2.     1.E-2  10.     1000.0
*----------------------------------------------
*  DTMIN  DTMAX  TEND   RTWFP
   1.E-3  1.E-3   2.60   10.0
*  EDINT  GFINT  DMPINT  SEDINT
   2.     1.E-3  10.     1000.0
*----------------------------------------------
*  DTMIN  DTMAX  TEND   RTWFP
   1.E-3  5.E-2   3.10   10.0
*  EDINT  GFINT  DMPINT  SEDINT
   3.     1.E-3  10.     1000.0
*----------------------------------------------
*  DTMIN  DTMAX  TEND   RTWFP
   1.E-3   1.E-1 4.20    10.0
*  EDINT  GFINT  DMPINT  SEDINT
   0.5    1.E-3  10.     1000.0
*----------------------------------------------
*  DTMIN  DTMAX  TEND   RTWFP
   1.E-3  5.E-2  4.30    10.0
*  EDINT  GFINT  DMPINT  SEDINT
   4.     1.E-3  10.     1000.0
*----------------------------------------------
*  DTMIN  DTMAX  TEND   RTWFP
   1.E-3  1.      7.30   10.0
*  EDINT  GFINT  DMPINT  SEDINT
   2.     1.E-3  10.     1000.0
*----------------------------------------------
*  DTMIN  DTMAX  TEND   RTWFP
   1.E-3  1.E-1  8.20    10.0
*  EDINT  GFINT  DMPINT  SEDINT
   4.     1.E-3  10.     1000.0
*----------------------------------------------
*  DTMIN  DTMAX  TEND   RTWFP
   1.E-3  5.E-3   8.40   10.0
*  EDINT  GFINT  DMPINT  SEDINT
   4.     1.E-3  10.     1000.0
*----------------------------------------------
*  DTMIN  DTMAX  TEND   RTWFP
   1.E-3  1.     10.00   10.0
*  EDINT  GFINT  DMPINT  SEDINT
   4.     1.E-3  10.     1000.0
*----------------------------------------------
*  DTMIN  DTMAX  TEND   RTWFP
   1.E-3  1.E-1  11.00   10.0
*  EDINT  GFINT  DMPINT  SEDINT
   1.     1.E-3  10.     1000.0
*----------------------------------------------
*  DTMIN  DTMAX  TEND   RTWFP
   1.E-3  5.E-2  11.10   10.0
*  EDINT  GFINT  DMPINT  SEDINT
   5.     1.E-3  10.     1000.0
*----------------------------------------------
*  DTMIN  DTMAX  TEND   RTWFP
   1.E-3  1.     19.70   10.0
*  EDINT  GFINT  DMPINT  SEDINT
   4.     1.E-3  10.     1000.0
*----------------------------------------------
*  DTMIN  DTMAX  TEND   RTWFP
   1.E-3  1.E-1  20.70   10.0
*  EDINT  GFINT  DMPINT  SEDINT
   4.     1.E-3  10.     1000.0
*----------------------------------------------
*  DTMIN  DTMAX  TEND   RTWFP
   1.E-3  5.E-2  20.80   10.0
*  EDINT  GFINT  DMPINT  SEDINT
   4.     1.E-3  10.     1000.0
*----------------------------------------------
*  DTMIN  DTMAX  TEND   RTWFP
   1.E-3  1.     22.00   10.0
*  EDINT  GFINT  DMPINT  SEDINT
   4.     1.E-3  10.     1000.0
*----------------------------------------------
*  DTMIN  DTMAX  TEND   RTWFP
   1.E-3  1.E-1  23.00   10.0
*  EDINT  GFINT  DMPINT  SEDINT
   4.     1.E-3  10.     1000.0
*----------------------------------------------
*  DTMIN  DTMAX  TEND   RTWFP
   1.E-3  5.E-2  24.00   10.0
*  EDINT  GFINT  DMPINT  SEDINT
   4.     1.E-3  10.     1000.0
*----------------------------------------------
*  DTMIN  DTMAX  TEND   RTWFP
   1.E-3  1.     25.00   10.0
*  EDINT  GFINT  DMPINT  SEDINT
   4.     1.E-3  10.     1000.0
*----------------------------------------------
*  DTMIN  DTMAX  TEND   RTWFP
   1.E-3  1.E-1  26.00   10.0
*  EDINT  GFINT  DMPINT  SEDINT
   4.     1.E-3  10.     1000.0
*----------------------------------------------
*  DTMIN  DTMAX  TEND   RTWFP
   1.E-3  5.E-2  28.00   10.0
*  EDINT  GFINT  DMPINT  SEDINT
   4.     1.E-3  10.     1000.0
*----------------------------------------------
*  DTMIN  DTMAX  TEND   RTWFP
   1.E-3  1.     30.20   10.0
*  EDINT  GFINT  DMPINT  SEDINT
   3.     1.E-3  10.     1000.0
*----------------------------------------------
*  DTMIN  DTMAX  TEND   RTWFP
   1.E-3  1.E-1  31.20   10.0
*  EDINT  GFINT  DMPINT  SEDINT
   4.     1.E-3  10.     1000.0
*----------------------------------------------
*  DTMIN  DTMAX  TEND   RTWFP
   1.E-3  5.E-2  32.20   10.0
*  EDINT  GFINT  DMPINT  SEDINT
   4.     1.E-3  10.     1000.0
*----------------------------------------------
*  DTMIN  DTMAX  TEND   RTWFP
   1.E-3  1.      90.0   10.0
*  EDINT  GFINT  DMPINT  SEDINT
   10.    1.E-3  10.     1000.0
   -1000000.
```

Table 8.1c: OMEGA-TUBE, typical input data deck, double break test, steady state run.

```
FREE
*NAMLCP  IEOS  INOPT  NDAT
0        0     1      0
TRAC MOD1 V 14.3 CNTS  23/5/88

TEST 8

STEADY STATE

*-***********************************************
*    NAMELIST DATA
 $INOPTS  ICFLOW=1  $END
*  DSTEP   TIMET
    0       0.0
*  STDYST  TRANSI  NCOMP  NJUN  IPAK
   1        0       11     10    0
*  EPSO     EPSI     EPSS
   1.0E-3   1.0E-5   1.0E-4
*  OITMAX  IITMAX  SITMAX  ISOLUT
   10       0       10      0
*  NTSV  NTCB  NTCF  NTRP  NTCO
   1      0     0     0     0
*    COMPONENT
     1    $   *  BREAK  : UPSTREAM BREAK
     2    $   *  TEE    : UPSTREAM VOLUME
     3    $   *  PIPE   : UPSTREAM SPOOL PIECE
     4    $   *  PIPE   : EXPANSION JOINT
     5    $   *  PIPE   : UPSTREAM CONNEXION
     6    $   *  PIPE   : HEATED TUBE
     7    $   *  PIPE   : DOWNSTREAM CONNEXION
     8    $   *  TEE    : DOWNSTREAM VOLUME
     9    $   *  BREAK  : DOWNSTREAM BREAK
    10    $   *  FILL   : INLET
    11    $   *  FILL   : OUTLET
* IDSV  ISVN  ILCN  ICN1  ICN2
   1     0     0     0     0
*()()()()()()()()()()()()()()()()()()()()()()()()()(
  BREAK   1    1        UPSTREAM BREAK
*  JUN   IBTY  ISAT  IVOV  IOFF
    1     1     0     1     0
*  ISTR  IBSV  NBTB  NBSV  NBRF
   0      1     0     0     0
*  DXIN   VOLIN     ALPIN  TIN     PIN
   .120   7.058-4   0.     960.2   16.080
*  PAIN   CONCIN  RBMX   POFF  BELV
   0.0    0.       1.810  0.     0.
*  PSCL *           1.88
*  PTB  * 0.000 16.0    2.650 16.0   $
          2.603 0.1     34.0  0.1    $
*  ::::::::::::::::::::::::::::::::::::::::::::::::::
  TEE    2    2          UPSTREAM VOLUME
*  JCELL   NODES  MAT  COST  ICHF
    2       4      0    0.    1
*  ICONC1  NCELL1  JUN1  JUN2  IPOW1
    0       3       1     2     0
*  IQPTR1  IQPSV1  NQPTB1  NQPSV1  NQPRF1
    0       0       0       0       0
*  RADIN1  TH1    HOUTL1  HOUTV1  TOUTL1
   .08675  0.030  0.       0.      300.
*  TOUTV1  POWIN1  POWOFF1  RPOWMX1  POWSCL1
   300.0   0.      0.       0.       0.
*  QPIN1    QPOFF1  RQPMX1  QPSCL1
   0.       0.      0.      0.
*  ICONC2  NCELL2  JUN3  IPOW2
    0       4       0     0
*  IQPTR2  IQPSV2  NQPTB2  NQPSV2  NQPRF2
    0       0       0       0       0
*  RADIN2  TH2    HOUTL2  HOUTV2  TOUTL2
   .008    0.008  0.       0.      300.
*  TOUTV2  POWIN2  POWOFF2  RPOWMX2  POWSCL2
   300.0   0.      0.       0.       0.
*  QPIN2    QPOFF12  RQPMX2  QPSCL2
   0.       0.       0.      0.
*   PRIMARY SIDE ------------------------------------
*DX   * 0.120 0.134 0.270           E
*VOL  * 7.0628-4 R1 -1. 3.7703E-3   E
*FA   * F -1.                       E
*FRIC* F 0.                         E
*GRAV* F  1.0                       E
*HD   * 0.00610 R2 0.1338 0.020     E
*NFF  * F    1          E
*ALFA* F  0.0           E
*VL   * F  3.0          E
*VV   * F  [illegible]  E
*TL   * F  [illegible].2 E
*TV   * [illegible].2   E
*P    * F 1[illegible]  E
*PA   * F  0.           E
*QPPP* F  0.            E
*MATI* F  7             E
*TW   * F  960.2        E
*   SECONDARY SIDE ---------------------------------
*DX   * 0.110 0.180 0.120 0.300 E
*VOL  * F  -1.      E
*FA   * F  -1.      E
*FRIC* F  0.        E
*GRAV* F  0.0       E
*HD   * F  0.016    E
*NFF  * F    1      E
*ALFA* F  0.0       E
*VL   * F  3.0      E
*VV   * F  3.0      E
*TL   * F  960.2    E
*TV   * F  960.2    E
*P    * F  10.780   E
*PA   * F  0.       E
*QPPP* F  0.        E
*MATI* F  7         E
*TW   * F  960.2    E
*  ::::::::::::::::::::::::::::::::::::::::::::::::::
  PIPE   3    3          UPSTREAM SPOOL PIECE
*  NCELLS  NODES  JUN1  JUN2  MAT
   10       4      2     3     0
*  ICHF  ICONC  IACC  IPOW
   1      0      0     0
*  IQPSTR  IQPSSV  NQPSTB  NQPSSV  NQPSRF
   0        0       0       0       0
*  RADIN   TH     HOUTL  HOUTV  TOUTL
   .0110   .010   0.0    0.     300.
*  TOUTV   POWIN  POWOFF  RPOWMX  POWSCL
   300.0   0.0    0.0     0.0     0.0
*  QPSIN    QPSOFF  RQPSMX  QPSSCL
   0.       0.      0.      0.
*  ------------------------------------------------
*DX   * 0.160 0.160 0.175 0.170 0.170           E
        0.175 0.160 0.170 0.147 0.120           E
*VOL  * 0.00813-3 R3 -1. 0.7316E-3 -1. 0.9030E-3 E
        6.1083E-3 7.0388E-3 -1. 3.0270E-3       E
*FA   * R10 -1.   2.0352E-4                     E
*FRIC* R10 0. 0.05                              E
*GRAV* R8  1.0 0.00 0.0                         E
*HD   * 0.020 R8 0.0308 R2 0.0277 0.0280 0.0304 E
        R2 0.020 0.0227                         E
*NFF  * R10  1 0        E
*ALFA* F  0.0           E
*VL   * F  3.0          E
*VV   * F  3.0          E
*TL   * F  960.2        E
*TV   * F  960.2        E
*P    * F  10.780       E
*PA   * F  0.           E
*QPPP* F  0.            E
*MATI* F  7             E
*TW   * F  960.2        E
*  ::::::::::::::::::::::::::::::::::::::::::::::::::
  PIPE   4    4          EXPANSION JOINT
*  NCELLS  NODES  JUN1  JUN2  MAT
   8        4      3     4     0
*  ICHF  ICONC  IACC  IPOW
   1      0      0     0
*  IQPSTR  IQPSSV  NQPSTB  NQPSSV  NQPSRF
   0        0       0       0       0
*  RADIN   TH     HOUTL  HOUTV  TOUTL
   .07476  .008   0.0    0.     300.
*  TOUTV   POWIN  POWOFF  RPOWMX  POWSCL
   300.0   0.0    0.0     0.0     0.0
*  QPSIN    QPSOFF  RQPSMX  QPSSCL
   0.       0.      0.      0.
*  ------------------------------------------------
*DX   * R3 0.175 R2 0.180 R3 0.170                E
*VOL  * R3 4.8910E-3 R2 5.0241E-3 R3 4.8410E-3    E
*FA   * F   2.0352E-4                             E
*FRIC* F  0.05                                    E
*GRAV* R3 0.0 0.320 0.000 0.240 R2 0.0            E
*HD   * F 0.0320            E
*NFF  * F   0               E
*ALFA* F  0.0               E
*VL   * F  3.0              E
*VV   * F  3.0              E
*TL   * F  960.2            E
*TV   * F  960.2            E
*P    * F  19.780           E
*PA   * F  0.               E
*QPPP* F  0.                E
*MATI* F  7                 E
*TW   * F  960.2            E
*  ::::::::::::::::::::::::::::::::::::::::::::::::::
  PIPE   5    5          UPSTREAM CONNEXION
*  NCELLS  NODES  JUN1  JUN2  MAT
   2        4      4     5     0
*  ICHF  ICONC  IACC  IPOW
   1      0      0     0
*  IQPSTR  IQPSSV  NQPSTB  NQPSSV  NQPSRF
   0        0       0       0       0
*  RADIN   TH     HOUTL  HOUTV  TOUTL
   .03864  .010   0.0    0.     300.
*  TOUTV   POWIN  POWOFF  RPOWMX  POWSCL
   300.0   0.0    0.0     0.0     0.0
*  QPSIN    QPSOFF  RQPSMX  QPSSCL
   0.       0.      0.      0.
```

Table 8.1c (continued)

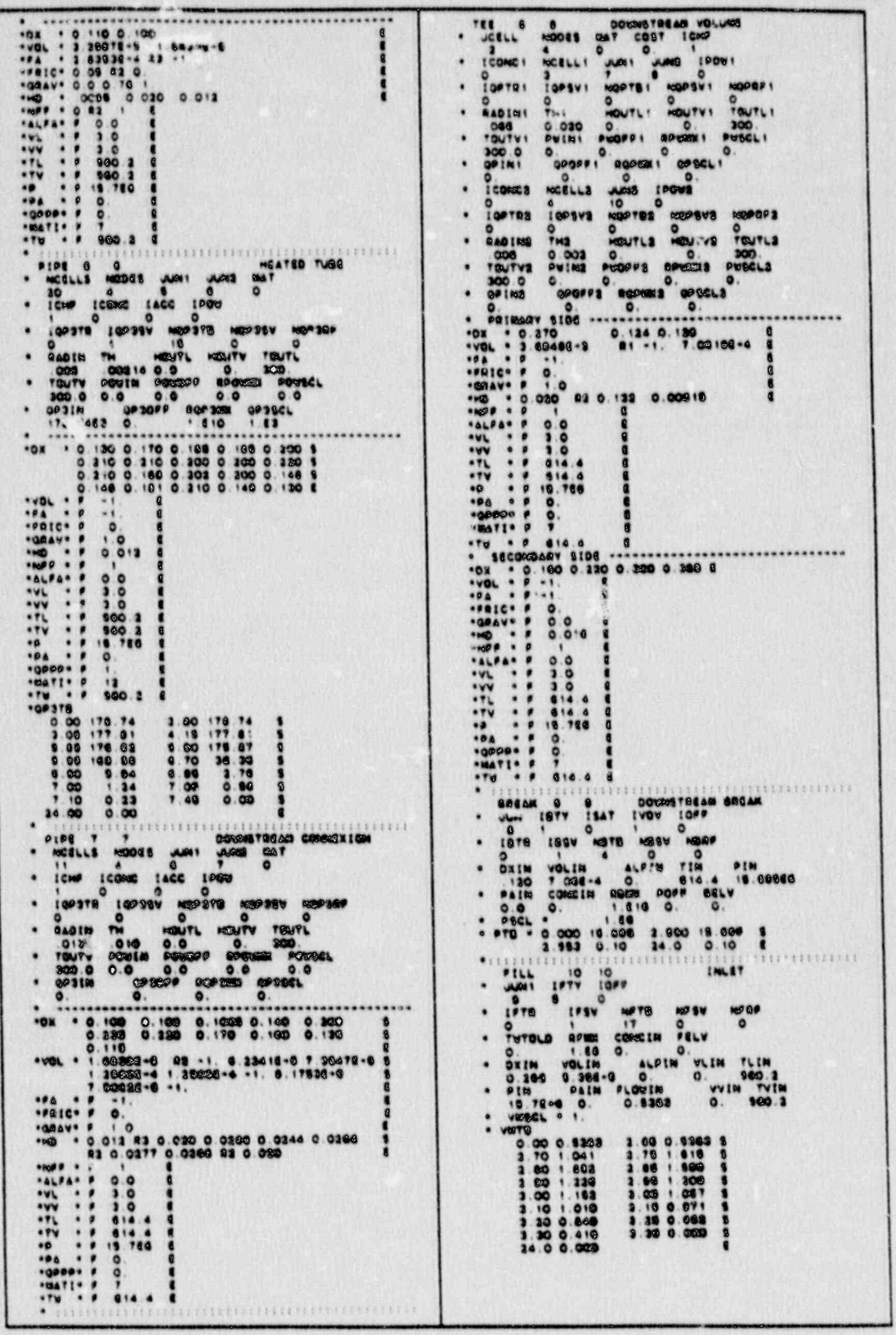

Table 8.1c (continued)

```
* ::::::::::::::::::::::::::::::::::::::::::::::::
  FILL    11  11           OUTLET
* JUN1  IFTY  IOFF
  10    9     0
* IFTR    IPSV   NFTB   NFSV   NFRF
  0       1      16     0      0
* TWTOLD  GFVN  CONCIN  FELV
  0.      1.84  0.      0.
* DXIN   VOLIN     ALPIN  VLIN  TLIN
  0.240  7.630-6   0.     0.    614.4
* PIN      PAIN  FLOWIN      VVIN  TVIN
  15.7E+6  0.    -0.9363     0.    614.4
* VMSCL = 1.
* VMTB
    0.00  -0.9363    2.96  -0.3302   5
    2.60   0.187     2.66   0.573    5
    2.70   1.044     2.75   1.820    5
    2.80   1.804     2.88   1.640    5
    2.90   1.953     2.98   1.667    5
    3.00   1.624     3.08   1.606    5
    3.10   1.817     3.15   1.038    5
    3.20   0.000    24.     0.000    5
* ()()()()()()()()()()()()()()()()()()()()()()()(
*             TIME STEP DATA
* DTMIN  DTMAX  TEND  RTUPD
  1.E-3  60.    90.   10.0
* EDINT  GPINT  DMPINT  SEDINT
  5      1.E-3  10.     1000.0
  -100000.
```

Table 8.2: OMEGA-TUBE, run statistics.

Test	3	6	8	9	29	30
Real time s	30.5	30.1	24.1	40.1	50.1	60.6
Time step number	508	539	735	582	688	563
Mean time step s	6.0 *10-2	5.6 *10-2	3.3 *10-2	6.9 *10-2	7.3 *10-2	1.1 *10-1
CPU time s	49.7	48.4	69.8	57.4	58.2	52.2
CPU time/real time	1.6	1.6	2.9	1.4	1.2	0.9
CPU time/cell *time step	1.5 *10-3	1.3 *10-3	1.5 *10-3	1.6 *10-3	1.3 *10-3	1.5 *10-3

9 OMEGA-BUNDLE BLOWDOWN EXPERIMENTS

9.1 Test Description

The OMEGA-BUNDLE blowdown tests were conducted in the Service des Transferts Thermiques of the Centre d'Etudes Nucléaires de Grenoble (France), during the years 1981 and 1982 (Chauliac, 1982).

9.1.1 Test Section

The test section OMEGA-BUNDLE consists of a rod bundle, connected upstream and downstream to capacities (fig. 9.1). The connection pipes support spool pieces.

The rod bundle simulates a reactor core. It consists of 36 rods, arranged in a 6 x 6 array on a 12.6 mm square pitch, with a 3,656 m heated legnth. The outer wall of the cluster is formed by ceramic shrouds, which delimit a 78.7 mm side square. The rods are made of inconel 600 and are electrically heated. Their external diameter is 9.5 mm. The thickness of the rod is continuously varying, from 0.5 mm in the middle of the rod, up to 2.25 mm at each end, in order to obtain a cosine axial heat flux. The thickness variation is given by the following expression:
2*e = D-(D*D-4/(a*cos(k*z)))**0.5,
where e is the rod thickness, D the external rod diameter, z the elevation measured from the middle of the rod, k = 0.70640 radian/m, and
a = 0.222*10+6 m-2.
The heat flux Fi is then given by the following expression:
Fi = 1.[illegible]*Fim*cos(k*z),
where Fim is the mean heat flux.

The capacities simulate the primary circuit water volumes. They are spheres of 0.5 m internal diameter, made of stainless steel 45 mm thick. They are connected upwards to the main part of the loop, from which they can be insulated by quick closing valves. They are connected downwards to the spool pieces.

A converging nozzle is connected laterally to the spheres, leading to the breaks. The convergent is 7 degrees angle, and 0.198 m length. Several break diameters are used.

9.1.2 Measurements

The measurements performed during the OMEGA-BUNDLE tests are very similar to those performed during the OMEGA-TUBE tests (see paragraph 8.1.2).

The **pressure** is measured at different locations along the test section. The uncertainty is 2 %. **Pressure differences** are measured between the top and the bottom of the rod bundle, and between the poles and equator of the capacities.

The **fluid temperature** is measured at different locations along the test section by chromel-alumel thermocouples.

The **wall temperature** of the rods is measured by 120 thermocouples brazed on the inner wall of the rods. There is 5 thermocouples per rod, distributed on 14 levels.

The mean **void fraction**, along a diameter and along a chord, is measured upstream and downstream the rod bundle, by a gamma ray attenuation technique.

The **mass flow rates** are measured by symetrical venturis, and by flowmeters located upstream and downstream the rod bundle. The mass flow rate in the upstream connection pipe is measured by a venturi located near the quick closing valve. The downstream connection mass flow rate is obtained by the difference between the mass flowing out of the loop pressurizer and the upstream connection mass flow.

The **power** dissipated in the rod bundle is obtained from amperage and voltage measurements.

9.1.3 Test Procedure

The test procedure beginns with the establishment of a steady state vertical upflow in the rod bundle. When the nominal conditions are reached, the system is vented to the atmospheric pressure by bursting the break(s) rupture discs. Valves insulating the test section from the loop are closed after the opening of the break(s). The closure of the two valves is not simultaneous. The electric power decay is programed versus time. In addition, the power is cut off when one wall thermocouple reaches a chosen threshold.

9.1.4 Test Matrix

Thirty-seven tests were performed, with initial flow conditions stated hereafter: the pressure is 13 MPa (except four tests with 15 MPa), the inlet temperature is 558 K, and the mass flow rate is 10 through 19 kg/s. Three wall heat flux (0.0, 0.6 and 1.0 Mw/m2), ten break diameters and three break positions (lower, upper and double breaks) are used.

The following tests were selected for TRAC simulation in the frame of the ICAP:

Test 2: 25 mm upper break, Fi=0.0 Mw/m2, Q=10 kg/s.
Test 3: 25 mm upper break, Fi=0.6 Mw/m2, Q=11 kg/s.
Test 9: 11 mm lower, 23 mm upper breaks, Fi=0.6 Mw/m2, Q=12 kg/s.
Test 11: 23 mm lower, 11 mm upper breaks, Fi=0.6 Mw/m2, Q=12 kg/s.
Test 13: 14 mm lower, 7 mm upper breaks, Fi=0.6 Mw/m2, Q=12 kg/s.
Test 16: 23 mm lower, 11 mm upper breaks, Fi=0.0 Mw/m2, Q=12 kg/s.
Test 19: 23 mm lower, 11 mm upper breaks, Fi=0.9 Mw/m2, Q=17 kg/s.

9.2 Input Model

Tables 9.2 give typical input data decks used for OMEGA-BUNDLE simulations.

9.2.1 Components and Boundary Conditions

The test section is modelled with a combination of 13 components (fig. 9.2). The capacities are modelled with a TEE component. The junctions, spool pieces and connection pipes are modelled by successive PIPE components. The rod bundle is modelled with a CORE component with one rod.

The entrance and exit of the initial steady state flow are modelled with a FILL component, where the mass flow rate is imposed versus time. The breaks are modelled with a BREAK component when the break opens, and with a FILL component when the break remains closed.

9.2.2 Hydraulic Modalization

The choice of the meshing is imposed by the geometry of the test section elements, and by the position of the measurements devices. The measurement locations correspond to a cell center (pressure, temperature and void fraction), or to a cell edge (mass flow rate). The area variations along the test section are taken into account in the evaluation of the cell volumes.

The rod bundle is modelled with 14 cells. The capacities are modelled with 3 cells (fig. 9.3), the flow areas of which are the areas of the sphere at the cell edges. The cell volumes are the volumes of the sphere slices defined by the cell edges.

9.2.3 Wall Modalization

The walls of all the components are modelled with 4 nodes, and the thermal losses are not taken into account.

The square wall of the cluster is modelled with a cylinder of 0.172 m inner diameter and 0.065 m thickness. The axially variable thickness of the rods cannot be modelled by TRAC. The rod thickness used is then the mean rod thickness (0.80 mm), in order to simulate globally the total thermal inertia of the rods. The experimental axial heat flux profile is imposed.

9.2.4 Singular Pressure Drops

The experimental singular pressure drop coefficient of a mixing grid is 1.0, and the one corresponding to the power lead plaits is 11.0. In the code the FRIC parameter is used to model these singular pressure drops.

9.2.5 Steady State Flow

The simulation of each test is performed with two successive runs. A first run gives the initial steady state regime. The experimental mass flow rate is imposed at the two connections, lower inflow, upper outflow. The inlet temperature is imposed at the lower junction. The pressure is imposed at the break location for single break tests. For double break tests, the pressures at the breaks are fitted in order to make the flow losses at the breaks during the steady state run very low (less than 1 % of the total mass flow rate).

The initial values imposed at each cell are the following: velocities of 4 m/s, experimental pressure, inlet temperatures for the rod bundle, and the lower components, outlet temperatures for the upper components. The time step is free, with an initial value of 1*10-2 s.

When the steady state is reached, the results are dumped to be used as the initial regime for the blowdown simulation. The steady state is reached within about 100 time steps (about 9 s CPU) for the tests with heated rods.

9.2.6 Blowdown

The second run simulates the blowdown. It beginns at the experimental time zero. The breaks open at a time between 2.70 and 2.85 s, not always simultaneously. In the model, the imposed pressure decreases from the initial value to 0.1 MPa within 0.003 s. The mass flow rates versus time at the connections are evaluated from the experimental total mass flow rate between the breaks opening and the valves closure, assuming a linear variation versus time. The experimental power is imposed versus time.

The initial time step is 1*10-3 s. The time step is bounded upwards during specified periods, in order that the breaks opening, valves closure and power cut off correspond to the experimental times. The choked flow model is used.

9.3 Code Predictions and Comparisons with Data

9.3.1 Parameters

The comparisons between the predictions and the data are made for the following parameters: pressure P9 at the bottom of the rod bundle, mass flow rates, void fractions and fluid temperatures in the upper and lower spool pieces, wall temperatures along the rod bundle, and pressure differences between the top and middle and between the middle and the bottom of the spheres.

These pressure differences are measured between very different flow area: 0.006, 0.013, 0.045 or 0.057 m2 on one hand (top or bottom, upper or lower sphere), and 0.20 m2 on the other hand (middle). For flow area

variations like that, the pressure drop predicted by TRAC is different from the pressure drop given by the Bernoulli equation, for liquid single phase flow regime (see paragraph 3.2.2). Furthermore, the meshing used for the spheres does not allow a correct evaluation of the pressure drop in the lower part of the spheres. As a matter of fact the code gives the pressure differences between the cells center Z=0.094 and 0.250 m (with Z=0 at the bottom of the sphere), whereas the measured pressure drop corresponds to Z=0.040 m (lower sphere), and Z=0.030 m (upper sphere), and Z=0.250 m. A liquid level passage cannot then be detected at the same time by the code and the data.

The predicted rod wall temperatures are only indicative, because the actual rod thickness is not modelled in the code. The mean value used in the code is 0.80 mm, whereas it is changing from 0.50 mm in the middle of the rod, up to 2.25 mm at the two ends. Furthermore, the inertia of the thermocouples brazing is not negligible, and a correction of the predicted wall temperatures should be made.

9.3.2 Tests with Upper Break

The tests with upper break are characterized by a mass flow rate which remains upwards in the bundle.

9.3.2.1 Test 2

Test 2 is performed with zero power, with a 25 mm break diameter. The results are presented on figures 9.4.

The pressure at the boiling inception is overpredicted, and the final pressure decrease is anticipated. The oscillations at the break opening correspond to the period before the closure of the valves. The beginning of boiling is predicted too early, just after the valves closure. The mass flow rate trough at this time is then not predicted. Furthermore, a short period of upper mass flow increase at time 11 s is predicted, together with an underprediction of the upper void fraction. In the lower part of the test section, the void fraction and mass flow rate are in good agreement with the data. The liquid entrainment in the lower part is probably too low; liquid accumulates and is then carried over towards the break.

9.3.2.2 Test 3

Test 3 is performed with a 25 mm break diameter, and a power cut off at time 7.9 s. The results are presented on figures 9.5.

The pressure at the boiling inception is overpredicted, and the final pressure decrease is anticipated. The mass flow rates and void fractions are well predicted, however with a vanishing of the liquid phase predicted too early, which corresponds to a too fast voidage of the lower sphere. The pressure drops in the lower sphere are well predicted (with an initial discrepancy corresponding to the violation of the Bernoulli

equation). In the top of the upper sphere, the predicted void fraction rapidly reaches the value 1.0, the vapor is practically stagnant, and the predicted pressure drop is weak. In the bottom part, the pressure drop trough corresponds to the void fraction trough in the test section (beginning of boiling in the cold lower sphere). The predicted fluid temperatures follow the pressure decrease. The single phase vapor regime is anticipated in the upper part, but it may have not been detected by the thermocouples.

The boiling crisis is predicted too early, and the wall temperatures are overpredicted. The Biasi critical heat flux correlation used by TRAC is not suitable for the low qualities which exist in the bottom part of the rod bundle. The maximum predicted temperature is 1150 K, whereas the data give 980 K. These comparisons are made notwithstanding the simplified rod wall model used.

9.3.3 Tests with Preponderant Lower Break

The tests with preponderant lower break are characterized by a mass flow rate which reverses as soon as the breaks open.

9.3.3.1 Test 18

Test 18 is performed with zero power, with a 23 mm lower break diameter and a 11 mm upper break diameter. The results are presented on figures 9.6.

The pressure at the boiling inception is sligthly overpredicted, and the final pressure decrease is anticipated. The void factions are underpredicted, with a trough in the upper part that is not observed in the data. The mass flow rates are well predicted.

9.3.3.2 Test 11

Test 11 is performed in conditions which differ from test 18 only by the power, cut off at time 9 s. The results are presented on figures 9.7.

The pressure at the boiling inception is overpredicted, and the final pressure decrease is anticipated. The void fractions and mass flow rates are well predicted. However, the single phase vapor flow is anticipated in the upper part. The pressure drops evolutions are correctly predicted, with an initial discrepancy corresponding to the violation of the Bernoulli equation. The predicted fluid temperatures follow the pressure decrease. The predicted single phase vapor flow is anticipated.

The boiling crisis is predicted with about 1 s delay. The wall temperatures are underpredicted. The predicted maximum wall temperature is 800 K whereas data indicate 950 K.

9.3.3.3 Test 19

Test 19 is performed in conditions which differ from test 19 only by the power (0.9 instead of 0.6 Mw/m2), cut off at time 7 s, and the mass flow rate (17 instead of 12 kg/s). The results are presented on figures 9.8.

The agreement between TRAC results and data is comparable for tests 11 and 19. The predicted maximum wall temperature for test 19 is 800 K whereas data indicate 1050 K.

9.3.3.4 Test 13

Test 13 is performed with a 14 mm lower break diameter and a 7 mm upper break diameter, with power cut off at time 7 s. The results are presented on figures 9.9.

The pressure at the boiling inception is overpredicted, with a discrepancy of 0.8 MPa, and the final pressure decrease is somewhat anticipated. The void fractions and mass flow rates are well predicted. However the single phase vapor flow is anticipated in the upper part. The pressure drops evolutions are correctly predicted, with an initial discrepancy corresponding to the violation of the Bernoulli equation. The predicted fluid temperatures follow the pressure decrease.

The boiling crisis is somewhat anticipated, and the wall temperatures are underpredicted. The predicted maximum wall temperature is 860 K whereas data indicate 980 K.

9.3.4 Test 9 with Preponderant Upper Break

Test 9 is performed with a 11 mm lower break diameter and a 23 mm upper break diameter, with a power cut off at time 6.1 s. The stagnation point is located at the bottom of the rod bundle at the beginning of the transient, and then in the lower sphere. The results are presented on figures 9.10.

The pressure at the boiling inception is sligthly overpredicted, and the final pressure decrease is anticipated. The void fractions and mass flow rates are well predicted. However, the single phase vapor flow is anticipated. The pressure drops evolutions are correctly predicted, with an initial discrepancy corresponding to the violation of the Bernoulli equation. In the bottom of the lower sphere, the predicted pressure drop is evaluated between two points nearer than for the data, and the level passage is detected too early. The predicted fluid temperatures follow the pressure decrease. Single phase vapor flows are predicted by the code but not by the thermocouples.

The boiling crisis is somewhat anticipated, and the wall temperatures are rather well predicted, despite the simplified model used. The predicted maximum wall temperature is 1000 K whereas data indicate 1050 K.

9.3.5 Summary

Two discrepancies appear between the predicted and measured pressures: the boiling inception pressure is overpredicted, and the pressure at the end of the transient is underpredicted. The voidage of the capacities towards the break or into the test section are well predicted, as indicated by the mass flow rates and void fractions in the test section, and the pressures drops in the spheres. The wall temperatures are overpredicted, underpredicted, or well predicted, depending on the test. However the use of a wall model with constant thickness, and with no model of the thermocouples brazing, is not very satisfactory.

9.4 Run Statistics

The runs were performed on a CRAY-XMP-2200 computer with TRAC-PF1/MOD1 version 14.3. The run statistics are presented on table 9.2, and figures 9.11 and 9.12 show the plots of the time step and CPU time versus real time, for each test.

9.5 Sensitivity Studies

9.5.1 Capacity Meshing

Runs were performed with the capacities modelled with 5 vertical cells instead of 3, in order that the center of the bottom cell correspond to the bottom pressure tap of the spheres. The results obtained are sligthly different from the reference runs, except for the bottom pressure drop of the spheres. With 5 cells, the void fraction in the bottom cell rapidly increases up to 1.0, and falls down before the end of the transient, whereas the void fraction of the second cell remains to about 0.4. The pressure drop is then irrealistic (fig. 9.13).

9.5.2 Use of PLENUM Components

The simulation ot test 9 was made with the two spheres modelled with a PLENUM component. As no wall exists for the PLENUM components, the comparison was made with a run performed with the spheres modelled with TEE components without wall. The results obtained are slightly different for the two runs (fig 9.14).

9.5.3 Nodalization

Test 9 was simulated with 47 cells modelling the whole test section instead of 67 (7 cells are used instead of 14 for the rod bundle). The results show little differences with the reference run (fig. 9.15).

9.5.4 Natural Choking

The simulation of test 9 was made with natural choking and a fine mesh at the breaks, where the converging nozzle is modelled with 4 cells of length 0.098, 0.050, 0.030 and 0.020 m, instead of one cell. The predicted blowdown is too fast, and the time step is divided into about a decade (fig. 9.16).

9.6 Summary and Conclusion

The simulation of seven OMEGA-BUNDLE blowdown tests was performed with TRAC-PF1/MOD1 version 14.3. The test section is modelled with 67 cells. The upper and lower spheres are modelled with a TEE component, with 3 vertical cells each. The rod bundle is modelled with a CORE component, with one equivalent rod. The rod wall thickness used is the mean thickness, in order to model the global rod inertia. The experimental axial heat flux is used.

The general agreement between data and TRAC is moderate: the major trends are correctly predicted, but the predicted parameters are frequently outside the data uncertainties. The voidage of the spheres towards the break and into the test section is well predicted. The violation of the Bernoulli equation in case of a flow area variation leads to a systematic initial discrepancy between the initial predicted and measured pressure drops in the spheres. However, the correct trends are predicted. During the period between the opening of the breaks and the closure of the valves, which insulate the test section, large pressure oscillations occur. The absence of a delayed boiling model leads to boiling inception pressures overpredicted with discrepancies up to 0.8 Mpa. The blowdown end is generally predicted too early. The use of a rod wall model with constant thickness does not allow a draw of conclusions concerning the wall temperatures. A complete model should have a thermocouple brazing model.

The runs are little sensitive to the meshing of the capacities, which can also be modelled with a PLENUM component instead of a TEE.

The sensitivity to the nodalization of the test section is weak. The runs performed with natural choking and a fine mesh at the breaks lead to too fast blowdowns and to sharply reduced time steps.

Table 9.1a: OMEGA-BUNDLE, typical input data deck, single break test, steady state run.

```
FREE
*NUMTCR  IEOS  INOPT  NMAT
6        0     1      0
TRAC MOD1 V 14.3 OMEG 30/3/88

TEST 3

STEADY STATE

***************************************************
*   NAMELIST DATA
 $INOPTS  ICFLOW=1  $END
*  DSTEP  TIMET
    0     0.0
*  STDYST  TRANSI  NCOMP  NJUN  IPAK
   1       0       13     13    0
*  EPSO    EPSI    EPSS
   1.0E-3  1.0E-6  1.0E-4
*  OITMAX  IITMAX  SITMAX  ISOLUT
   10      0       10      0
*  NTSV  NTCB  NTCF  NTRP  NTCP
   1     0     0     0     0
*   COMPONENT
      1    5    *  FILL   : INLET
      2    5    *  PIPE   : UPSTREAM JUNCTION
      3    5    *  TEE    : UPSTREAM VOLUME
      4    5    *  PIPE   : UPSTREAM SPOOL PIECE
      5    5    *  PIPE   : UPSTREAM CONNEXION
      6    5    *  CORE   : ROD BUNDLE
      7    5    *  PIPE   : DOWNSTREAM CONNEXION
      8    5    *  PIPE   : DOWNSTREAM SPOOL PIECE
      9    5    *  TEE    : DOWNSTREAM VOLUME
     10    5    *  PIPE   : DOWNSTREAM JUNCTION
     11    5    *  FILL   : OUTLET
     12    5    *  FILL   : UPSTREAM BREAK
     13    5    *  BREAK  : DOWNSTREAM BREAK
* IDSV  ISVN  ILCN  ICN1  ICN2
  1     0     0     0     0
* ()()()()()()()()()()()()()()()()()()()()()()()()()(
  FILL    1   1                  INLET
*  JUN1  IFTY  IOFF
   1     5     0
*  IFTR   IFSV   NFTB   NFSV   NFRF
   0      1      8      0      0
*  TWTOLD  RFMX  CONCIN  FELV
   0.      1.E0  0.      0.
*  DXIN   VOLIN     ALPIN  VLIN  TLIN
   0.230  1.30E-3   0.     0.    550.2
*  PIN       PAIN  FLOWIN      VVIN  TVIN
   13.0E+6   0.    11.24       0.    550.2
*  VMSCL * 1.
*  VMTB
    0.00 11.34     3.00 11.34 S
    3.00 17.36     3.05 0.00  S
    40.0 0.00                 E
* ::::::::::::::::::::::::::::::::::::::::::::::::
  PIPE  2   2             UPSTREAM JUNCTION
*  NCELLS  NODES  JUN1  JUN2  EAT
   3       4      1     2     0
*  ICHF  ICONC  IACC  IPOW
   1     0      0     0
*  IQP3TR  IQP3SV  NQP3TB  NQP3SV  NQP3RF
   0       0       0       0       0
*  RADIN   TH     HOUTL  HOUTV  TOUTL
   .00438  .018   0.0    0.     300.
*  TOUTV  POWIN  POWOFF  RPOWMX  POWSCL
   300.0  0.0    0.0     0.0     0.0
*  QP3IN    QP3OFF  RQP3MX  QP3SCL
   0.       0.      0.      0.
*  ------------------------------------------------
*DX   * 0.230 0.210 0.165          E
*VOL  * F -1.                      E
*FA   * F -1.                      E
*FRIC* F  0.                       E
*GRAV* 0.  -0.06 -0.72 -0.84       E
*HD   * F 0.0373 E
*NFF  * F    1   E
*ALFA* F  0.0    E
*VL   * F  4.0   E
*VV   * F  4.0   E
*TL   * F  550.2 E
*TV   * F  550.2 E
*P    * F 13.0E6 E
*PA   * F  0.    E
*QPPP* F  0.     E
*MATI* F  7      E
*TW   * F  550.2 E
* ::::::::::::::::::::::::::::::::::::::::::::::::
```

```
  TEE   3   3            UPSTREAM VOLUME
*  JCELL  NODES  EAT  COST  ICHF
   3      4      0    0.    1
*  ICONC1  NCELL1  JUN1  JUN2  IPOW1
   0       5       2     3     0
*  IQPTR1  IQPSV1  NQPTB1  NQPSV1  NQPRF1
   0       0       0       0       0
*  RADIN1  TH1    HOUTL1  HOUTV1  TOUTL1
   0.230   0.048  0.      0.      300.
*  TOUTV1  POWIN1  POWOFF1  RPOWMX1  POWSCL1
   300.0   0.      0.       0.       0.
*  QPIN1    QPOFF1  RQPMX1  QPSCL1
   0.       0.      0.      0.
*  ICONC2  NCELL2  JUN3  IPOW2
   0       1       11    0
*  IQPTR2  IQPSV2  NQPTB2  NQPSV2  NQPRF2
   0       0       0       0       0
*  RADIN2  TH2    HOUTL2  HOUTV2  TOUTL2
   0.330   0.048  0.      0.      300.
*  TOUTV2  POWIN2  POWOFF2  RPOWMX2  POWSCL2
   300.0   0.      0.       0.       0.
*  QPIN2    QPOFF2  RQPMX2  QPSCL2
   0.       0.      0.      0.
*  PRIMARY SIDE -----------------------------------
*DX   * 0.24 0.1070  0.125 0.1575 0.150           S
*VOL  * -1. 2.07028E-3              2.40324E-3    S
           2.07028E-3         -1.                 S
*FA   * R2 -1.  R3 0.164070 R2 -1.                S
*FRIC* F 0.                                       S
*GRAV* -0.06 R5 -1.                               S
*HD   * R2 0.0373  R3 0.484 R2 0.0373             E
*NFF  * F    1     E
*ALFA* F  0.0      E
*VL   * F  4.0     E
*VV   * F  4.0     E
*TL   * F  550.2   E
*TV   * F  550.2   E
*P    * F 13.0E6   E
*PA   * F  0.      E
*QPPP* F  0.       E
*MATI* F  7        E
*TW   * F  550.2   E
*  SECONDARY SIDE ---------------------------------
*DX   * 0.150              E
*VOL  * 2.3830E-4          E
*FA   * F -1.              E
*FRIC* 0.  1.530           E
*GRAV* F  0.               E
*HD   * 0.0503 0.03504     E
*NFF  * F    1   E
*ALFA* F  0.0    E
*VL   * F  4.0   E
*VV   * F  4.0   E
*TL   * F  550.2 E
*TV   * F  550.2 E
*P    * F 13.0E6 E
*PA   * F  0.    E
*QPPP* F  0.     E
*MATI* F  7      E
*TW   * F  550.2 E
* ::::::::::::::::::::::::::::::::::::::::::::::::
  PIPE  4   4            UPSTREAM SPOOL PIECE
*  NCELLS  NODES  JUN1  JUN2  EAT
   17      4      3     4     0
*  ICHF  ICONC  IACC  IPOW
   1     0      0     0
*  IQP3TR  IQP3SV  NQP3TB  NQP3SV  NQP3RF
   0       0       0       0       0
*  RADIN  TH     HOUTL  HOUTV  TOUTL
   .0438  .018   0.0    0.     300.
*  TOUTV  POWIN  POWOFF  RPOWMX  POWSCL
   300.0  0.0    0.0     0.0     0.0
*  QP3IN    QP3OFF  RQP3MX  QP3SCL
   0.       0.      0.      0.
*.-------------------------------------------------
*DX   *        0.300 0.332 0.400 0.400            S
        0.440 0.300 0.400 0.410 0.410             S
        0.400 0.440 0.430 0.430 0.430             S
        0.410 0.410 0.407                         E
*VOL  * R7 -1. 2.34700E-3 1.33178E-3 3.23648E-3   S
        2.54178E-3 R6 -1. 2.07450E-3              E
*FA   * F -1.                                     E
*FRIC* F  0.                                      E
*GRAV* R13 -1. -0.07 -0.18 -0.10 0.06             S
        0.90                                      E
*HD   * R8 0.0373 0.0726 0.0768 0.080 R4 0.0373   S
         0.064                                    E
*NFF  * F    1   E
*ALFA* F  0.0    E
*VL   * F  4.0   E
*VV   * F  4.0   E
*TL   * F  550.2 E
*TV   * F  550.2 E
*P    * F 13.0E6 E
*PA   * F  0.    E
*QPPP* F  0.     E
*MATI* F  7      E
*TW   * F  550.2 E
```

Table 9.1a (continued)

```
*  :::::::::::::::::::::::::::::::::::::::::::::::::::::::::::::::
   PIPE  8   8          UPSTREAM CONNECTION
*  NCELLS  NODES  JUN1  JUN2  EPSW
   3       4      6     8     0
*  ICHF   ICONC  IACC  IPOW
   1       0      0     0
*  IQP3TB  IQP3SV  NQP3TB  NQP3SV  NQP3RF
   0       0       0       0       0
*  RADIN   TH      HOUTL   HOUTV   TOUTL
   0.087   0.10    0.0     0.      300.
*  TOUTV   POWIN   POWOFF  RPOWMX  POWSCL
   300.0   0.0     0.0     0.0     0.0
*  QP3IN       QP3OFF  RQP3MX  QP3SCL
   0.          0.      0.      0.
*  -----------------------------------------------------------
*DX    * 0.418 0.488 0.330                      $
*VOL   * 4.4498E-3 8.7082E-3 0.1720E-4          $
*FA    * R2 -1. 8.8708E-3 3.0428-3              $
*FRIC* 0. 0. 0.444 0.021                        $
*GRAV* 0.00 R3  1.                              $
*HD    * 0.084 0.160  0.0237 0.0109             $
*NFF   * F    1          $
*ALPA* F   0.0          $
*VL    * F   4.0          $
*VV    * F   4.0          $
*TL    * F   588.2        $
*TV    * F   588.3        $
*P     * F   13.080       $
*PA    * F   0.           $
*QPPP* F   0.           $
*MATI* F   7            $
*TW    * F   588.8        $
*  :::::::::::::::::::::::::::::::::::::::::::::::::::::::::::::::
   CORE  6   6                ROD BUNDLE
*  NCELLS  JUN1   JUN2  MAT  ICHF
   14      6      6     0    1
*  ICONC  ICRU  ICRL
   0      14    0
*  IRPWTY  NDGX  NDTS  NHIST
   7       0     300   0
*  IRPWTB  IRPWSV  NRPWTB  NRPWSV
   0       1       10      0
*  IZPWTB  IZPWSV  NZPWTB  NZPWSV  NZPWRF
   0       1       1       0       0
*  IRFTB  NODX  NFCI  NFCIL  NZMAX
   0       0     0     0      14
*  NRODS  NDRDS  NODES  NSLBS  NFBPWT
   1       4      4      0      0
*  REACT  TNEUT  RPWOFF  RRPWMX  RPWSCL
   0.     0.     0.      1.E20   1.00
*  RPOWRI  ZPWIN  ZPWOFF  RZPWMX  QP3IN
   2.21300 0.     0.      0.      0.
*  RADIN   TH      HOUTL   HOUTV   TOUTL
   0.044   0.088   0.      0.      300.
*  TOUTV   PLDR   PDRAT  FUCRAC  NSARD
   300.    0.     1.33   1.      0.
*  DTXHT1  DTXHT2  DZNHT
   3.      10.     0.00
*  -----------------------------------------------------------
*DX    * R2 0.304 R10 0.380 0.304 0.380           $
*VOL   * R2 8.8180E-4 R10 8.4800E-4 8.8180E-4     $
         0.8818E-4                                $
*FA    * F 3.0428-3                               $
*FRIC* 0.021 0. 0.020 0. 0.080                    $
               0. 0.020 0. 0.020                  $
               0. 0.020 0. 0.020                  $
               0. 0.010                           $
*GRAV* F   1.0   $
*HD    * F 0.0109 $
*NFF   * F   1   $
*ALPA* F   0.0   $
*VL    * F   4.0   $
*VV    * F   4.0   $
*TL    * F   [illegible].8 $
*TV    * F   [illegible].8 $
*P     * F   13.080 $
*PA    * F   0.    $
*QPPP* F   1.    $
*MATI* F   7     $
*TW    * F   [illegible].8 $
*-------------------------------------------------------------
*Z     * 0.304 0.830 0.760 1.040 1.320            $
         1.066 1.020 2.026 2.348 2.620            $
         2.866 3.126 3.382 3.657                  $
*RDPWR* F 1.                                      $
*CPOWR*    1.                                     $
*ZPWTB* 0.                                        $
         0.4208 0.8018 0.0158 0.0849 1.1414       $
         1.2004 1.3174 1.3428 1.3178 1.2000       $
         1.1410 0.9047 0.8160 0.0020 0.4201       $
*RDX   * 3K.                                      $
*RADRD*    3.008-3 4.2178-3 4.4808-3 4.788-3      $
*MATRD* F    12                                   $
*RPWTB*  0.00  2.213        3.88  2.213           $
         4.38  2.232        4.70  2.221           $
         7.38  2.221        7.60  2.193           $
         7.69  2.030        7.80  1.030           $
         7.90  0.0          40.   0.0             $
```

```
*NFAX  * F  0     $
*FPUQ3*  0.       $
*FTD   *  1.      $
*GMIX  * F  0.    $
*GMLES*  0.       $
*PGAPT*  0.       $
*PLVOL*  0.       $
*PSLEN*  0.       $
*CLEN*   0.       $
*BURN  *   0.     $
*RFTN  * F [illegible]8.2 $
*  :::::::::::::::::::::::::::::::::::::::::::::::::::::::::::::::
   PIPE  7   7          DOWNSTREAM CONNECTION
*  NCELLS  NODES  JUN1  JUN2  EPSW
   3       4      6     7     0
*  ICHF   ICONC  IACC  IPOW
   1       0      0     0
*  IQP3TB  IQP3SV  NQP3TB  NQP3SV  NQP3RF
   0       0       0       0       0
*  RADIN   TH      HOUTL   HOUTV   TOUTL
   0.088   0.10    0.0     0.      300.
*  TOUTV   POWIN   POWOFF  RPOWMX  POWSCL
   300.0   0.0     0.0     0.0     0.0
*  QP3IN       QP3OFF  RQP3MX  QP3SCL
   0.          0.      0.      0.
*  -----------------------------------------------------------
*DX    * 0.378 0.199 0.380                                 $
*VOL   * 3.3427E-3 3.2788E-3 3.0807E-3                     $
*FA    * 3.0428E-3 3.0863E-3 1.3782E-2 1.1071E-2           $
*FRIC* 0.010 R2 0.0                                        $
*GRAV* 1.0  0.77 0.0 0.00                                  $
*HD    * 0.0109 0.0212 0.080 0.0873                        $
*NFF   * F    1         $
*ALPA* F   0.0          $
*VL    * F   4.0          $
*VV    * F   4.0          $
*TL    * F   593.0        $
*TV    * F   593.0        $
*P     * F   13.080       $
*PA    * F   0.           $
*QPPP* F   0.           $
*MATI* F   7            $
*TW    * F   593.0        $
*  :::::::::::::::::::::::::::::::::::::::::::::::::::::::::::::::
   PIPE  8   8          DOWNSTREAM SPOOL PIECE
*  NCELLS  NODES  JUN1  JUN2  EPSW
   13      4      7     8     0
*  ICHF   ICONC  IACC  IPOW
   1       0      0     0
*  IQP3TB  IQP3SV  NQP3TB  NQP3SV  NQP3RF
   0       0       0       0       0
*  RADIN   TH      HOUTL   HOUTV   TOUTL
   .00436  .019    0.0     0.      300.
*  TOUTV   POWIN   POWOFF  RPOWMX  POWSCL
   300.0   0.0     0.0     0.0     0.0
*  QP3IN       QP3OFF  RQP3MX  QP3SCL
   0.          0.      0.      0.
*  -----------------------------------------------------------
*DX    * 0.380 0.476 0.900 0.460 0.308                     $
         0.360 0.482 0.400 0.338 0.330                     $
         0.320 0.360 0.210                                 $
*VOL   * 1.8804E-3 3.1028E-3 2.7087E-3 3.0083E-3           $
         -1. 3.3010E-3 3.9001E-3 1.9408E-3 R3 -1.          $
*FA    * 1.1071E-2 R2 4.8204E-3 4.0800E-3 R10 -1.          $
*FRIC* F  0.                                               $
*GRAV* 0.03 0.03 1.00 0.38 0.74                            $
         R6 1.0                                            $
*HD    * 0.0873 R2 0.024 0.080 R8 0.0873 0.080             $
         0.0884 R5 0.0873                                  $
*NFF   * F    1         $
*ALPA* F   0.0          $
*VL    * F   4.0          $
*VV    * F   4.0          $
*TL    * F   593.0        $
*TV    * F   593.0        $
*P     * F   13.080       $
*PA    * F   0.           $
*QPPP* F   0.           $
*MATI* F   7            $
*TW    * F   593.0        $
*  :::::::::::::::::::::::::::::::::::::::::::::::::::::::::::::::
```

Table 9.1a (continued)

```
  TEE    9   9        DOWNSTREAM VOLUME
*  JCELL   NODES  MAT  COST  ICHF
    3       4      0    0.    1
*  ICONC1  NCELL1  JUN1  JUN2  IPOW1
   0       5       8     9     0
*  IQPTR1  IQPSV1  NQPTR1  NQPSV1  NQPRF1
   0       0       0       0       0
*  RADIN1  TH1     HOUTL1  HOUTV1  TOUTL1
   0.280   0.048   0.      0       300.
*  TOUTV1  PWIN1   PWOFF1  RPWMX1  PWSCL1
   300.0   0.      0.      0.      0.
*  QPIN1    QPOFF1  RQPMX1  QPSCL1
   0.        0.      0.      0
*  ICONC2  NCELL2  JUN3  IPOW2
   0       1       12    0
*  IQPTR2  IQPSV2  NQPTR2  NQPSV2  NQPRF2
   0       0       0       0       0
*  RADIN2  TH2     HOUTL2  HOUTV2  TOUTL2
   0.280   0.048   0.      0.      300.
*  TOUTV2  PWIN2   PWOFF2  RPWMX2  PWSCL2
   300.0   0.      0.      0.      0.
*  QPIN2    QPOFF12 RQPMX2  QPSCL2
   0.        0.      0.      0.
*  PRIMARY SIDE ------------------------------------
*DX   * 0.15 0.1875 0.125 0.1875 0.220          E
*VOL  * -1. 2.07068E-2 2.40325E-2 2.07068E-2   S
         -1.                                    E
*FA   * R2 -1.    R2 0.184078 R2 -1.            E
*FRIC* F 0.                                     E
*GRAV* F  1.                                    E
*HD   * R2 0.0873 R2 0.484 R2 0.131             E
*NFF  * F    1        E
*ALFA* F   0.0        E
*VL   * F   4.0       E
*VV   * F   4.0       E
*TL   * F   5[illegible].0     E
*TV   * F   5[illegible].0     E
*P    * F  13.0E6     E
*PA   * F   0.        E
*QPPP* F   0.         E
*MATI* F   7          E
*TW   * F   582.0     E
*  SECONDARY SIDE ---------------------------------
*DX   * 0.196              E
*VOL  * 2.2828E-4          E
*FA   * F -1.              E
*FRIC* F  0.               E
*GRAV* F  0.               E
*HD   * 0.0663 0.02994     E
*NFF  * F    1          E
*ALFA* F   0.0          E
*VL   * F   4.0         E
*VV   * F   4.0         E
*TL   * F   582.0       E
*TV   * F   582.0       E
*P    * F  13.0E6       E
*PA   * F   0.          E
*QPPP* F   0.           E
*MATI* F   7            E
*TW   * F   582.0       E
* ::::::::::::::::::::::::::::::::::::::::::::::::::
  PIPE  10  10        DOWNSTREAM JUNCTION
*  NCELLS  NODES  JUN1  JUN2  MAT
   2       4      9     10    0
*  ICHF  ICONC  IACC  IPOW
   1     0      0     0
*  IQPSTR  IQPSSV  NQPSTR  NQPSSV  NQPSRF
   0       0       0       0       0
*  RADIN   TH      HOUTL   HOUTV   TOUTL
   .0875   .016    0.0     0.      300.
*  TOUTV   POWIN   POWOFF  RPOWMX  POWSCL
   300.0   0.0     0.0     0.0     0.0
*  QPSIN     QPSOFF  RQPSMX  QPSSCL
   0.        0.      0.      0.
*  ------------------------------------------------
*DX   * 0.130 0.280        E
*VOL  * -1. 4.1833E-3      E
*FA   * F -1.              E
*FRIC* F  0.               E
*GRAV* F  1.0              E
*HD   * 0.131 0.1319 0.15  E
*NFF  * F    1      E
*ALFA* F   0.0      E
*VL   * F   4.0     E
*VV   * F   4.0     E
*TL   * F   582.0   E
*TV   * F   582.0   E
*P    * F  13.0E6   E
*PA   * F   0.      E
*QPPP* F   0.       E
*MATI* F   7        E
*TW   * F   582.0   E
* ::::::::::::::::::::  ::::::::::::::::::::::::::::

  FILL    11  11             OUTLET
*  JUN1  IFTY  IOFF
   10    5     0
*  IFTR    IFSV   NFTB   NFSV   NFRF
   0       1      6      0      0
*  TWTOLD  RFMX  CONCIN  FELV
   0.      1.E4  0.      0.
*  DXIN    VOLIN     ALPIN  VLIN  TLIN
   0.283   4.18E-3   0.     0.    582.0
*  PIN     PAIN  FLOWIN      VVIN  TVIN
   13.0E+6 0.    -11.24      0.    582.0
*  VMSCL * 1.
* VMTB
    0.00 -11.24      2.00 -11.24 S
    2.06  67.8       3.40  67.8  S
    3.80  0.00      40.0   0.00  E
* ::::::::::::::::::::::::::::::::::::::::::::::::::
  FILL    12  12      UPSTREAM BREAK
*  JUN11  IFTY  IOFF
   11     1     0
*  TWTOLD  RFMX  CONCIN  FELV
   0.      0.    0.      0.
*  DXIN    VOLIN     ALPIN  VLIN  TLIN
   0.196   2.28E-4   0.     0.    580.3
*  PIN     PAIN  FLOWIN  VVIN  TVIN
   13.0E6  0.    0.      0.    580.3
* ::::::::::::::::::::::::::::::::::::::::::::::::::
  BREAK   13  13      DOWNSTREAM BREAK
*  JUN  IBTY  ISAT  IVOV  IOFF
   12   1     0     1     0
*  IBTR  IBSV  NBTB  NBSV  NBRF
   0     1     4     0     0
*  DXIN  VOLIN     ALPIN  TIN     PIN
   .196  2.28E-4   0.     580.0   13.0E6
*  PAIN  CONCIN  RBMX  POFF  BELV
   0.0   0.      1.E10  0.    0.
*  PSCL *       1.00
* PTB * 0.000 13.0  2.00 13.0  S
        2.053 0.10  40.0 0.10  E
* ()()()()()()()()()()()()()()()()()()()()()()()()()(
*            TIME STEP DATA
*  DTMIN  DTMAX  TEND  RTWFP
   1.E-3  40.    40.   10.0
*  EDINT  GFINT  DMPINT  SEDINT
   10.    1.E-3  10.     1000.0
   -100000.
```

Table 9.1b: OMEGA-BUNDLE, typical input data deck, transient run.

```
FREE
*NUMTCR  IEOS  INOPT  NMAT
6        0     1      0
TRAC MOD1 V 14.3 CMD30 30/3/88

TEST 3

TRANSIENT

*************************************************
*   NAMELIST DATA
 $INOPTS  ICFLOW=1  $END
*  DSTEP  TIMET
    -1     0.0
*  STDYST  TRANSI  NCOMP  NJUN  IPAK
   0       1       13     12    0
*  EPSO     EPSI     EPSS
   1.0E-3   1.0E-6   1.0E-4
*  OITMAX  IITMAX  SITMAX  ISOLUT
   10      0       10      0
*  NTSV  NTCB  NTCF  NTRP  NTCP
   1     0     0     0     0
*    COMPONENT
  1  2  3  4  5  0
  6  7  8  9 10  0
 11 12 13        0
* IDSV  ISVN  ILCN  ICN1  ICN2
  1     0     0     0     0
* ()()()()()()()()()()()()()()()()()()()()()()()(
END
* ()()()()()()()()()()()()()()()()()()()()()()()(
*             TIME STEP DATA
*------------------------------------
*  DTMIN   DTMAX   TEND   RTWFP
   1.      1.      3.     10.0
*  EDINT   GFINT   DMPINT   SEDINT
   3.      1.      10.      1000.0
*------------------------------------
*  DTMIN   DTMAX   TEND   RTWFP
   1.E-1   1.E-1   3.6    10.0
*  EDINT   GFINT   DMPINT   SEDINT
   3.      1.E-1   10.      1000.0
*------------------------------------
*  DTMIN   DTMAX   TEND   RTWFP
   1.E-2   1.E-2   3.64   10.0
*  EDINT   GFINT   DMPINT   SEDINT
   3.      1.E-2   10.      1000.0
*------------------------------------
*  DTMIN   DTMAX   TEND   RTWFP
   1.E-3   1.E-3   3.66   10.0
*  EDINT   GFINT   DMPINT   SEDINT
   3.      1.E-3   10.      1000.0
*------------------------------------
*  DTMIN   DTMAX   TEND   RTWFP
   1.E-3   5.E-2   4.75   10.0
*  EDINT   GFINT   DMPINT   SEDINT
   3.      1.E-3   10.      1000.0
*------------------------------------
*  DTMIN   DTMAX   TEND   RTWFP
   1.E-3   5.E-1   5.80   10.0
*  EDINT   GFINT   DMPINT   SEDINT
   1.5     1.E-3   10.      1000.0
*------------------------------------
*  DTMIN   DTMAX   TEND   RTWFP
   1.E-3   1.E-1   7.40   10.0
*  EDINT   GFINT   DMPINT   SEDINT
   4.      1.E-3   10.      1000.0
*------------------------------------
*  DTMIN   DTMAX   TEND   RTWFP
   1.E-3   5.E-2   7.60   10.0
*  EDINT   GFINT   DMPINT   SEDINT
   4.      1.E-3   10.      1000.0
*------------------------------------
*  DTMIN   DTMAX   TEND   RTWFP
   1.E-3   1.      40.    10.0
*  EDINT   GFINT   DMPINT   SEDINT
   5.      1.E-3   10.      1000.0
*------------------------------------
  -100000.
```

1

IMAGE EVALUATION TEST TARGET (MT-3)

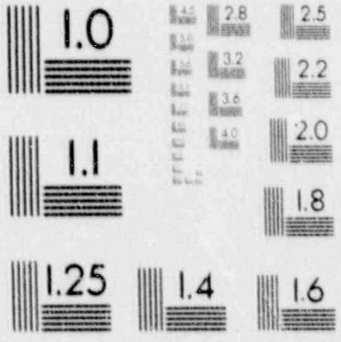

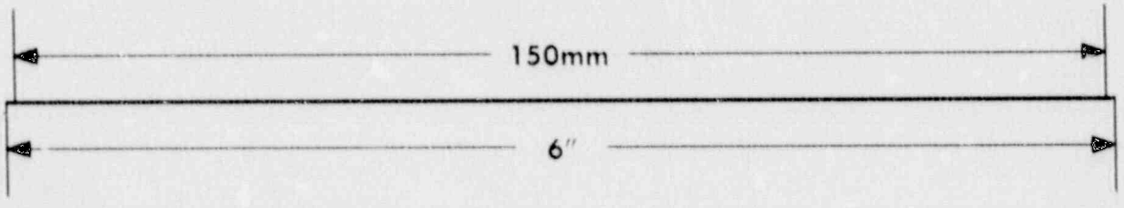

1

IMAGE EVALUATION TEST TARGET (MT-3)

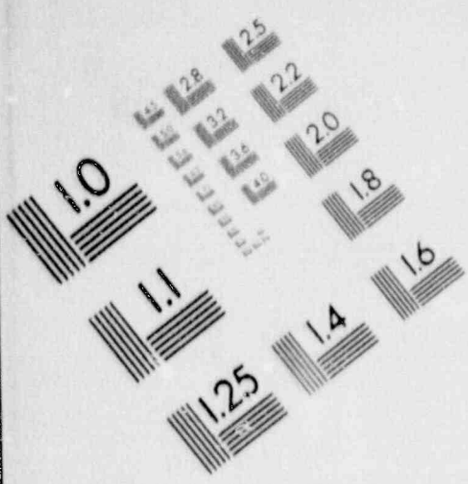

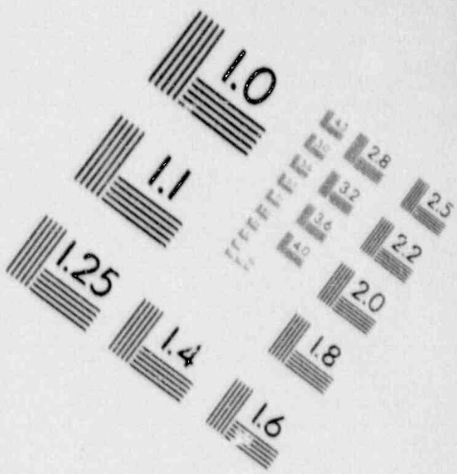

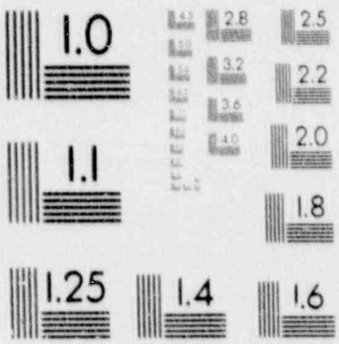

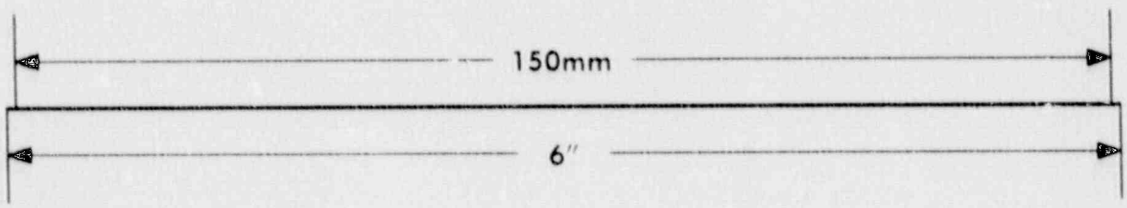

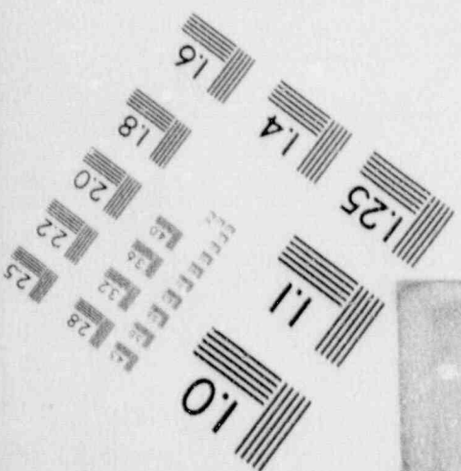

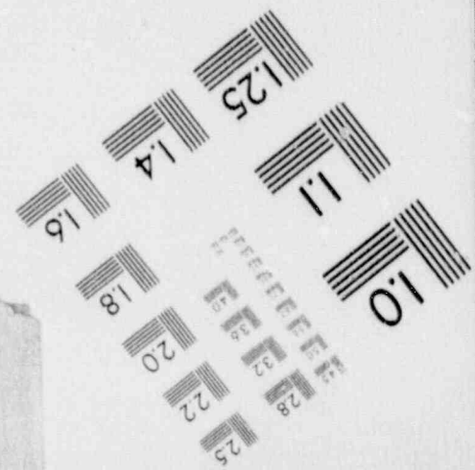

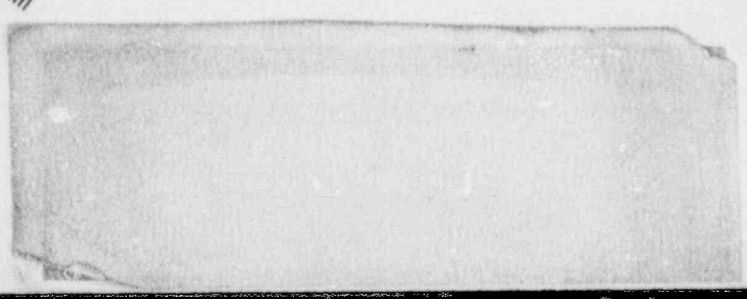

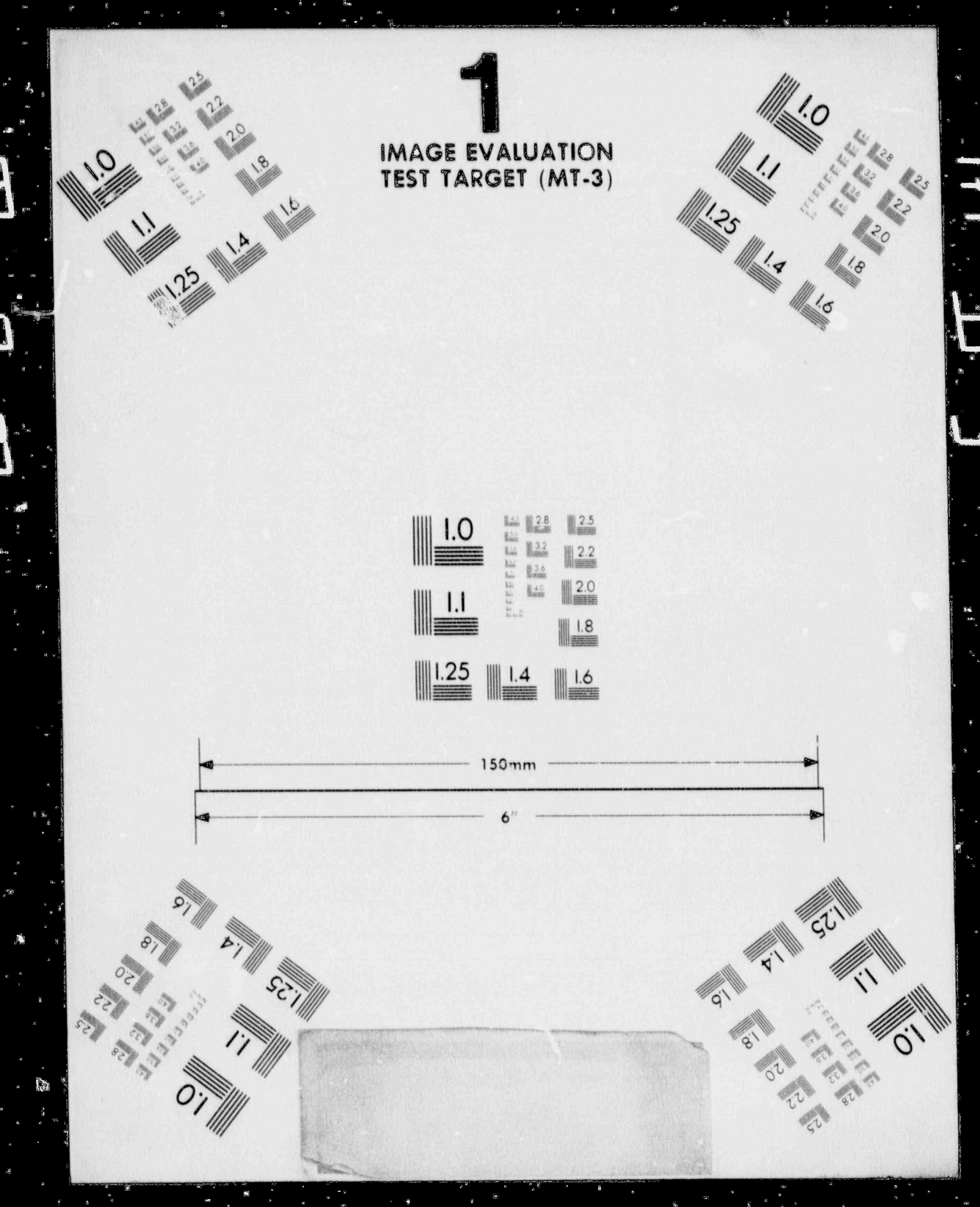
1
IMAGE EVALUATION
TEST TARGET (MT-3)
1.0
1.1
1.25
1.4
1.6
1.8
2.0
2.2
2.5
2.8
3.2
3.6
4.0
150mm
6"

1

IMAGE EVALUATION TEST TARGET (MT-3)

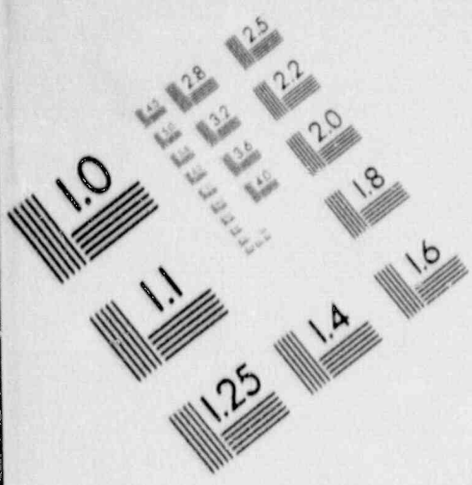

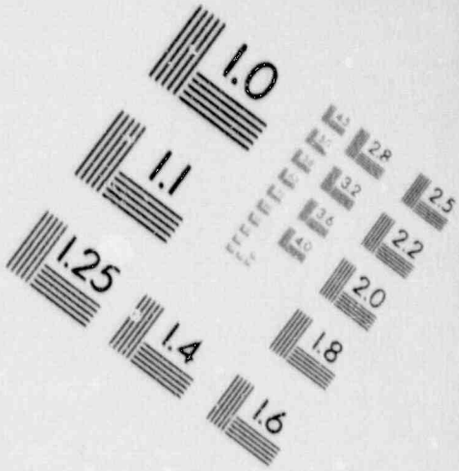

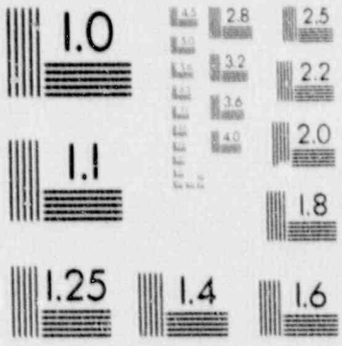

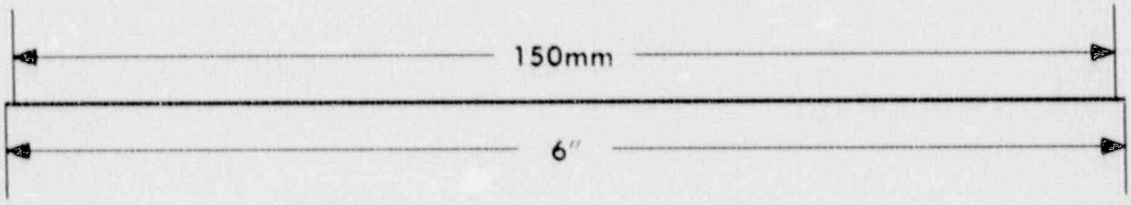

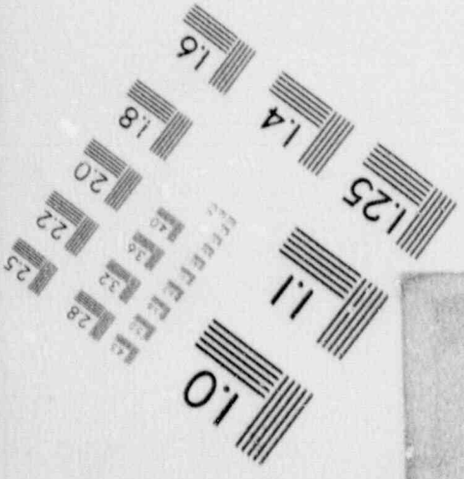

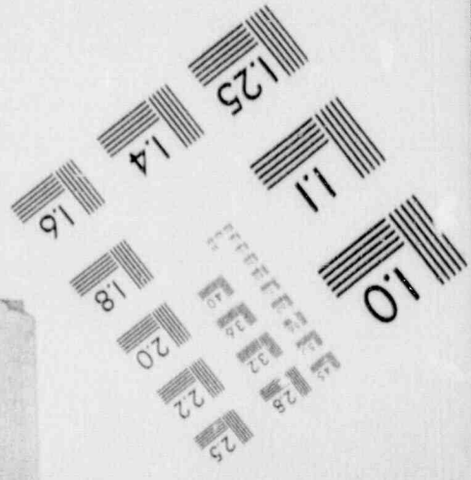

Table 9.1c: OMEGA-BUNDLE, typical input data deck, double break test, steady state run.

```
FREE
*NUMTCR  IEOS  INOPT  NMAT
6        0     1      0
TRAC MOD1 V 14.3 ONB13   25/3/88

TEST 13

STEADY STATE

*****************************************
*   NAMELIST DATA
 $INOPTS  ICFLOW=1  SEND
*  DSTEP  TIMET
      0   0.0
*  STDYST  TRANSI  NCOMP  NJUN  IPAR
      1       0     13     13     0
*  EPSO      EPSI      EPSS
   1.0E-3    1.0E-6    1.0E+4
*  OITMAX  IITMAX  SITMAX  ISOLUT
      10       0      10       0
*  NTSV  NTCB  NTCP  NTBP  NTCP
      1     0     0     0     0
*   COMPONENT
      1     S     *  FILL  :  INLET
      2     S     *  PIPE  :  UPSTREAM JUNCTION
      3     S     *  TEE   :  UPSTREAM VOLUME
      4     S     *  PIPE  :  UPSTREAM SPOOL PIECE
      5     S     *  PIPE  :  UPSTREAM CONNEXION
      6     S     *  CORE  :  ROD BUNDLE
      7     S     *  PIPE  :  DOWNSTREAM CONNEXION
      8     S     *  PIPE  :  DOWNSTREAM SPOOL PIECE
      9     S     *  TEE   :  DOWNSTREAM VOLUME
     10     S     *  PIPE  :  DOWNSTREAM JUNCTION
     11     S     *  FILL  :  OUTLET
     12     S     *  BREAK :  UPSTREAM BREAK
     13     E     *  BREAK :  DOWNSTREAM BREAK
*  IDSV  ISVN  ILCN  ICN1  ICN2
      1     0     0     0     0
*  ()()()()()()()()()()()()()()()()()()()()
    FILL     1     1              INLET
*   JUN1  IFTY  IGPP
      1     S     0
*   IFTB     IFSV    NPTB    NFSV    NFBP
    0        1       6       0       0
*   TWTOLD   BPRN   CONCIN   PELV
    0.       1.E5    0.      0.
*   GXIN     VOLIN      ALPIN   VLIN   TLIN
    0.230    1.38E-3    0.      0.     560.1
*   PIN      PAIN    FLOWIN       VVIN   TVIN
    13.36+6  0.      13.36        0.     560.1
*   VMSCL  = 1.
*   VMTB
      0.00 13.36     2.75 13.36 S
      2.68 17.22     2.68 17.22 S
      2.68  0.00    40.0   6.0  E
*  ::::::::::::::::::::::::::::::::::::::::
   PIPE  2   2            UPSTREAM JUNCTION
*   NCELLS  NODES  JUN1  JUN2  MAT
      3       4     1     2     0
*   ICHF  ICONC  IACC  IPOW
      1     0      0     0
*   IGPSTB  IGPSSV  NGPSTB  NGPSSV  NGPSBP
    0       0       0       0       0
*   RADIN   TH      HSUTL   HSUTV   TSUTL
    .00438  .018    0.0     0.      300.
*   TSUTV   PSUIN   PSUSPP   SPSUSX   PSUSCL
    300.0   0.0     0.0      0.0      0.0
*   GPSIN      GPSSPP   SGPSSX   GPSSCL
    0.         0.       0.       0.
*  ---------------------------------------
*GX   = 0.230 0.210 0.166    E
*VOL  = F =1.                E
*FA   = F =1.                E
*FRIC= F  0.                 E
*GRAV= 0. -0.09 -0.73 -0.86 E
*HD   = F 0.0873 E
*NFF  = F   1    E
*ALFA= F  0.0    E
*VL   = F  4.0   E
*VV   = F  4.0   E
*TL   = F  560.1 E
*TV   = F  560.1 E
*P    = F 13.36E E
*PA   = F  0.    E
*QPPP= F  0.     E
 MATI= F  7      E
*TW   = F  560.1 E
* ::::::::::::::::::::::::::::::::::::::::
   TEE   3   3            UPSTREAM VOLUME
*   JCELL   NODES  MAT  COST  ICHF
      3       4    0     0.    1
*   ICONC1  NCELL1  JUN1  JUN2  IPOW1
    0       S       2     3     0
*   IQPTR1  IQPSV1  NQPTB1  NQPSV1  NQPBP1
    0       0       0       0       0
*   RADIN1  TH1     HSUTL1  HSUTV1  TSUTL1
    0.250   0.048   0.        0.    300.
*   TSUTV1  PVIN1  PVSPP1  SPVSX1  PVSCL1
    300.0   0.      0.      0.      0.
*   GPIN1     GPSPP1  SGPSX1  GPSCL1
    0.        0.      0.      0.
*   ICONC2  NCELL2  JUN2  IPOW2
    0       1       11    0
*   IQPTR2  IQPSV2  NQPTB2  NQPSV2  NQPBP2
    0       0       0       0       0
*   RADIN2  TH2     HSUTL2  HSUTV2  TSUTL2
    0.250   0.048   0.        0.    300.
*   TSUTV2  PVIN2  PVSPP2  SPVSX2  PVSCL2
    300.0   0.      0.      0.      0.
*   GPIN2     GPSPP2  SGPSX2  GPSCL2
    0.        0.      0.      0.
*   PRIMARY SIDE ----------------------------
*GX   = 0.24 0.1878 0.128 0.1678 0.150      E
*VOL  = -1. 2.070666-3          3.403246-3  S
          2.070666-3      -1.               E
*FA   = R2 -1.   R1 0.164078 R2 -1.         E
*FRIC= F 0.                                 E
*GRAV= -0.86 RS -1.                         E
*HD   = R2 0.0873  R3 0.484 R1 0.0873       E
*NFF  = F   1    E
*ALFA= F  0.0    E
*VL   = F  4.0   E
*VV   = F  4.0   E
*TL   = F  560.1 E
*TV   = F  560.1 E
*P    = F 13.36E E
*PA   = F  0.    E
*QPPP= F  0.     E
*MATI= F  7      E
*TW   = F  560.1 E
*   SECONDARY SIDE --------------------------
*GX   = 0.150                               E
*VOL  = 1.13666-4                           E
*FA   = F -1.                               E
*FRIC= F  0.                                E
*GRAV= F  0.                                E
*HD   = 0.0667 0.01388 E
*NFF  = F   1    E
*ALFA= F  0.0    E
*VL   = F  4.0   E
*VV   = F  4.0   E
*TL   = F  560.1 E
*TV   = F  560.1 E
*P    = F 13.36E E
*PA   = F  0.    E
*QPPP= F  0.     E
*MATI= F  7      E
*TW   = F  560.1 E
* ::::::::::::::::::::::::::::::::::::::::
   PIPE  4   4            UPSTREAM SPOOL PIECE
*   NCELLS  NODES  JUN1  JUN2  MAT
      17      4     3     4     0
*   ICHF  ICONC  IACC  IPOW
      1     0      0     0
*   IQPSYB  IQPSSV  NQPSYB  NQPSSV  NQPSBP
    0       0       0       0       0
*   RADIN   TH      HSUTL   HSUTV   TSUTL
    .0438   .018    0.0     0.      300.
*   TSUTV   PSUIN   PSUSPP   SPSUSX   PSUSCL
    300.0   0.0     0.0      0.0      0.0
*   GPSIN      GPSSPP   SGPSSX   GPSSCL
    0.         0.       0.       0.
*  ---------------------------------------
*GX   =          0.300 0.300 0.400 0.400     S
                0.440 0.300 0.400 0.410 0.410 E
                0.400 0.440 0.430 0.430 0.430 S
                0.410 0.410 0.407             E
*VOL  = R7 -1. 2.34706E-3 1.23176E-3 2.23646E-3 S
          2.94176E-3 RS -1. 2.07466E-3          E
*FA   = F -1.                               E
*FRIC= F  0.                                E
*GRAV= R13 -1.  -0.87 -0.18 -0.10 0.08      S
          0.98                              E
*HD   = R6 0.0873 0.0736 0.0768 0.080 R6 0.0873 S
          0.084                             E
*NFF  = F   1    E
*ALFA= F  0.0    E
*VL   = F  4.0   E
*VV   = F  4.0   E
*TL   = F  560.1 E
*TV   = F  560.1 E
*P    = F 13.36E E
*PA   = F  0.    E
*QPPP= F  0.     E
*MATI= F  7      E
*TW   = F  560.1 E
```

Table 9.1c (continued)

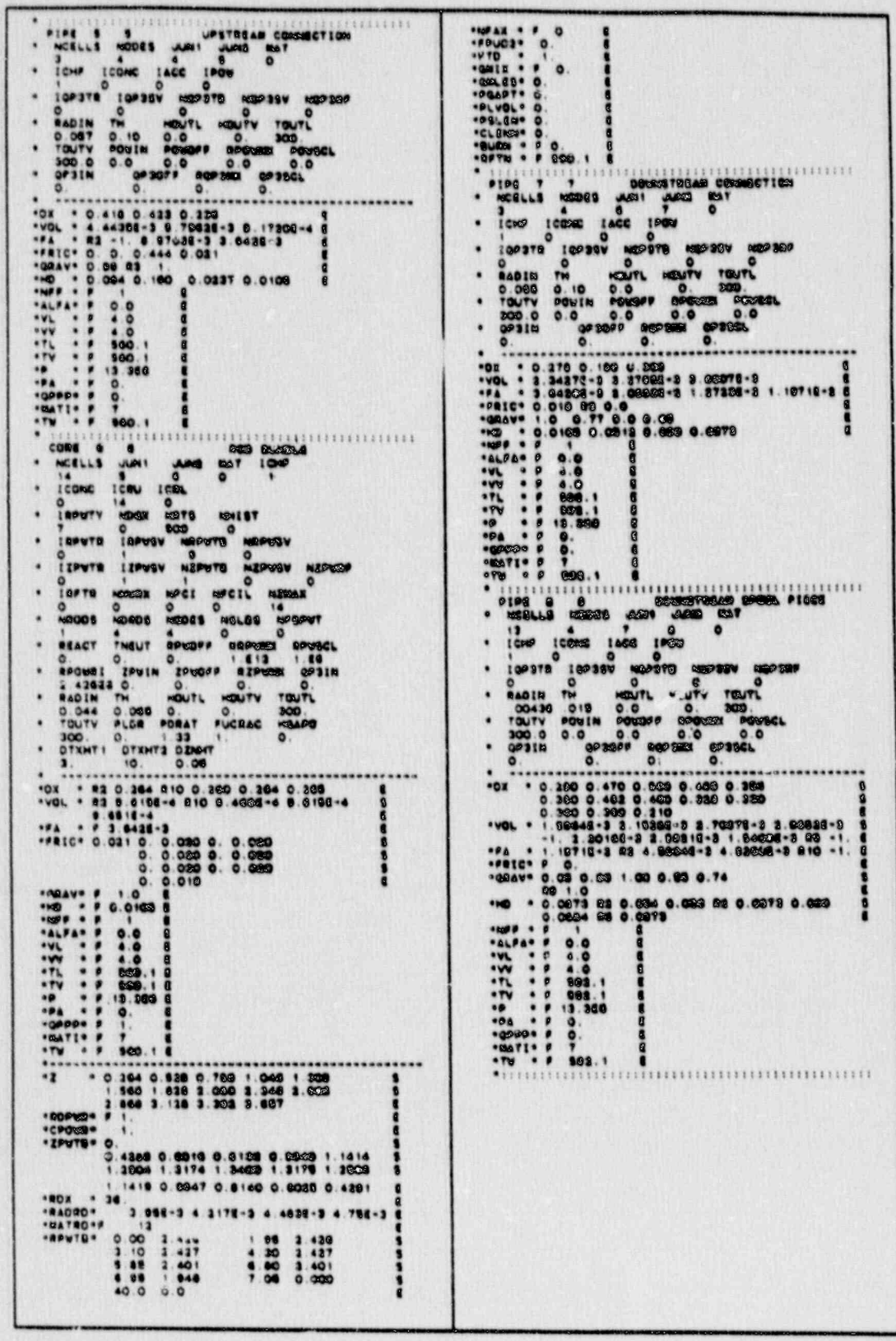

Table 9.ic (continued)

```
  TEE    9   9         DOWNSTREAM VOLUME
*  JCELL   NODES  MAT  COST  ICHF
   3       4      0     0     1
*  ICONC1  NCELL1  JUN1  JUN2  IPOW1
   0       5       8     9     0
*  IQPTR1  IQPSV1  NQPTB1  NQPSV1  NQPRF1
   0       0       0       0       0
*  RADIN1  TH1     HOUTL1  HOUTV1  TOUTL1
   0.280   0.048   0.            0.    300.
*  TOUTV1  PWIN1   PWOFF1  RPWMX1  PWSCL1
   300.0   0.      0.      0.      0.
*  QPIN1     QPOFF1  RQPMX1  QPSCL1
   0.        0.      0.      0.
*  ICONC2  NCELL2  JUN3  IPOW2
   0       1       12    0
*  IQPTR2  IQPSV2  NQPTB2  NQPSV2  NQPRF2
   0       0       0       0       0
*  RADIN2  TH2     HOUTL2  HOUTV2  TOUTL2
   0.280   0.048   0.            0.    300.
*  TOUTV2  PWIN2   PWOFF2  RPWMX2  PWSCL2
   300.0   0.      0.      0.      0.
*  QPIN2     QPOFF12 RQPMX2  QPSCL2
   0.        0.      0.      0.
*  PRIMARY SIDE -----------------------------------
*DX   * 0.15 0.1875 0.125 0.1875 0.230        E
*VOL  * -1. 2.07088E-2              2.40334E-2    S
            3.07088E-2        -1.                 E
*FA   * R2 -1.   R2 0.184075 R2 -1.               E
*FRIC* F 0.                                       E
*GRAV* F  1.                                      E
*HD   * R. 0.0877 R2 0.484 R2 0.131               E
*NFF  * F     1      E
*ALFA* F  0.0        E
*VL   * F  4.0       E
*VV   * F  4.0       E
*TL   * F  583.1     E
*TV   * F  583.1     E
*P    * F 13.360     E
*PA   * F  0.        E
*QPPP* F  0.         E
*MATI* F  7          E
*TW   * F  583.1     E
*  SECONDARY SIDE ---------------------------------
*DX   * 0.186            E
*VOL  * 6.4808E-6        E
*FA   * F -1.            E
*FRIC* F  0.             E
*GRAV* F  0.             E
*HD   * 0.0487 0.00889   E
*NFF  * F    1        E
*ALFA* F  0.0         E
*VL   * F  4.0        E
*VV   * F  4.0        E
*TL   * F  583.1      E
*TV   * F  583.1      E
*P    * F 13.360      E
*PA   * F  0.         E
*QPPP* F  0.          E
*MATI* F  7           E
*TW   * F  583.1      E
* ::::::::::::::::::::::::::::::::::::::::::::::::
  PIPE  10  10        DOWNSTREAM JUNCTION
*  NCELLS  NODES  JUN1  JUN2  MAT
   2       4      9     10    0
*  ICHF  ICONC  IACC  IPOW
   1     0      0     0
*  IQPSTB  IQPSSV  NQPSTB  NQPSSV  NQPSRF
   0       0       0       0       0
*  RADIN   TH      HOUTL   HOUTV   TOUTL
   .0875   .018    0.0     0.      300.
*  TOUTV   POWIN   POWOFF  RPOWMX  POWSCL
   300.0   0.0     0.0     0.0     0.0
*  QPSIN     QPSOFF  RQPSMX  QPSSCL
   0.        0.      0.      0.
*  -----------------------------------------------
*DX   * 0.120 0.280        E
*VOL  * -1. 4.1823E-3      E
*FA   * F -1.              E
*FRIC* F  0.               E
*GRAV* F  1.0              E
*HD   * 0.131 0.1319 0.15  E
*NFF  * F    1      E
*ALFA* F  0.0       E
*VL   * F  4.0      E
*VV   * F  4.0      E
*TL   * F  583.1    E
*TV   * F  583.1    E
*P    * F 13.360    E
*PA   * F  0.       E
*QPPP* F  0.        E
*MATI* F  7         E
*TW   * F  583.1    E
```

```
* ::::::::::::::::::::::::::::::::::::::::::::::::
  FILL   11   11              OUTLET
*  JUN1  IFTY  IOFF
   10    5     0
*  IFTR    IFSV   NFTB   NFSV   NFRF
   0       1      8      0      0
*  TWTOLD  RFMX  CONCIN  FELV
   0.      1.84  0.      0.
*  DXIN   VOLIN     ALPIN  VLIN  TLIN
   0.283  4.18E-3   0.     0.    583.1
*  PIN     PAIN  FLOWIN        VVIN  TVIN
   13.4E+6 0.   -12.38         0.    583.1
*  VMSCL * 1.
*  VMTB
    0.00 -12.30     2.75 -12.30 S
    2.85  13.70     3.15  13.70 S
    3.28   0.00    40.0    0.00 E
* ::::::::::::::::::::::::::::::::::::::::::::::::
  BREAK  12  12       UPSTREAM BREAK
*  JUN  ISTY  ISAT  IVSV  IOFF
   11   1     0     1     0
*  ISTR  ISSV  NBTB  NBSV  NBRF
   0     1     4     0     0
*  DXIN  VOLIN      ALPIN  TIN     PIN
   .188  1.14E-4    0.     583.1   13.5366
*  PAIN  CONCIN  RBMX   POFF  BELV
   0.0   0.      1.E10  0.    0.
*  PSCL *        1.E6
*  PTB * 0.000 13.53 2.75 13.53 S
         2.753 0.10  40.0 0.10  E
* ::::::::::::::::::::::::::::::::::::::::::::::::
  BREAK  13  13       DOWNSTREAM BREAK
*  JUN  ISTY  ISAT  IVSV  IOFF
   12   1     0     1     0
*  ISTR  ISSV  NBTB  NBSV  NBRF
   0     1     4     0     0
*  DXIN  VOLIN      ALPIN  TIN     PIN
   .188  6.408-6    0.     583.1   13.34486
*  PAIN  CONCIN  RBMX   POFF  BELV
   0.0   0.      1.E10  0.    0.
*  PSCL *        1.E6
*  PTB * 0.000 13.344 2.75 13.344 S
         2.753 0.10    40.0 0.10  E
* ()()()()()()()()()()()()()()()()()()()()()()()()(
*              TIME STEP DATA
*  DTMIN  DTMAX  TEND  RTWFP
   1.E-2  5.     30.   10.0
*  EDINT  GFINT  DMPINT  SEDINT
   30.    1.     10.     1000.0
  -10000.
```

Table 9.2: OMEGA-BUNDLE, run statistics.

Test	2	3	9	11	13	18	19
Real time s	40.0	40.3	40.0	40.0	39.5	40.0	40.0
Time step number	495	545	820	585	497	376	667
Mean time step s	9.1 *10-2	7.4 *10-2	4.9 *10-2	6.8 *10-2	7.9 *10-2	1.1 *10-1	6.0 *10-2
CPU time s	50.2	55.3	85.4	62.0	49.0	61.0	67.4
CPU time/ real time	1.3	1.4	2.1	1.5	1.2	1.0	1.7
CPU time/ cell*time step	1.5 *10-3	1.5 *10-3	1.5 *10-3	1.5 *10-3	1.4 *10-3	1.6 *10-3	1.5 *10-3

10 CONCLUSION

10.1 Overall Summary

Independent assessment of the TRAC-PF1/MOD1 version 14.3 has been performed using the separate-effects tests stated hereafter:

Critical flow steady state tests:
MOBY-DICK : tests 403, 408, 455, 79 and 172.
SUPER-MOBY-DICK: tests 1 through 15.

Blowdown tests:
CANON : tests D, L, I.
SUPER-CANON : tests P, X, Q.
VERTICAL-CANON : tests 9, 22, 24.
MARVIKEN : tests 6, 17, 24.
OMEGA-TUBE : tests 3, 6, 8, 9, 29, 30.
OMEGA-BUNDLE : tests 2, 3, 9, 11, 13, 18, 19.

Assessment includes base case simulation and sensitivity studies (among others nodalization sensitivity and runs with natural choking and with the choked flow model). Complete code predictions, comparisons with data and run statistics are given.

10.2 Run Statistics

All the runs were performed on a CRAY-XMP-2200 computer with the code TRAC-PF1/MOD1 version 14.3. The time step was free, except during specified periods of the OMEGA-TUBE and OMEGA-BUNDLE transients, in order to ensure that the experimental events occur at the experimental times. The initial and minimum time step was 1*10-2 s for the MARVIKEN simulations, 1*10-3 s for the MOBY-DICK, VERTICAL-CANON, OMEGA-TUBE and OMEGA-BUNDLE simulations, and 1*10-4 s for the SUPER-MOBY-DICK, CANON and SUPER-CANON simulations.

The extremum CPU time per cell per time step are given hereafter for each experiment (in CPU s *10+3).

MOBY-DICK	: 1.1 - 1.4
SUPER-MOBY-DICK	: 0.6 - 1.2
CANON	: 1.7 - 2.5
SUPER-CANON	: 1.7 - 2.8
VERTICAL-CANON	: 1.1 - 1.2
MARVIKEN	: 1.6 - 1.9
OMEGA-TUBE	: 1.3 - 1.6
OMEGA-BUNDLE	: 1.4 - 1.6

The largest CPU times per cell per time step correspond to the CANON and SUPER-CANON tests with a break equal to the pipe diameter, for which the blowdown transients are very fast (about 1 s from the opening of the break until the atmospheric pressure is reached).

In case of a fine mesh at the break (little cell sizes and large velocities), a Courant stability criterion calculated in subroutine TF1DS1 becomes very limitative. This was not found in the runs performed with version 13.0 of the code, where the value of parameter CSF1D was 1*10+6, instead of 1*10+3 in version 14.3.

10.3 Major Conclusions

The major conclusions derived from the simulations of each experiment are given, followed by an overall conclusion concerning the critical flow and blowdown simulations with TRAC.

10.3.1 MOBY-DICK

No steady state is reached, due to the small size of the throat cell (0.02 m), and, in addition for one test, to the abrupt decrease of the interfacial shear stress at the transition between bubble-slug and annular flow regimes. However, the mass flow rate oscillations are sufficiently low to allow comparisons with data. The pressure at the boiling inception is overpredicted, due to the lack of a delayed boiling model, and the discrepancy is sensitive, due to the low pressure.

The results are very sensitive to the inlet location with regard to the throat, or to the single phase flow length with regard to the total length, and the predicted mass flow rates are therefore relative to a specified inlet location. When the interphase thermal desequilibrium is large, the agreement with the data is worse when the choked flow model (no thermal desequilibrium) is use than with natural choking.

10.3.2 SUPER-MOBY-DICK

The staggered scheme used by TRAC does not respect the Bernoulli equation for single phase flow, and hence a fine meshing (0.004 m) is needed to model properly the inlet convergent of the test section, in order to obtain realistic simulations.

No steady state is reached for two tests among the fifteen for which a simulation was made, and the mass flow rate oscillations are much lower than the data accuracy. This better stability compared to the MOBY-DICK simulations is attributed to the higher pressure of the SUPER-MOBY DICK tests, for which the constitutive laws are probably more suitable.

The agreement between the predicted and measured mass flow rates, is good (discrepancies less than 5 %) for the tests with high entrance subcooling, for which the two phase flow region is short. The agreement is less good (discrepancies up to 10 %) for the tests with positive inlet quality. The largest discrepancies (up to 23 %) between predictions and data correspond to the tests with inlet condition near saturation, for which the boiling model takes a large part.

The data accuracy is not sufficient to predict precisely the boiling inception point. The void fractions are in good agreement with the data even if the agreement concerning the pressures and mass flow rate is poor.

The runs performed with the choked flow model give similar results as the runs performed with natural choking, except for the tests with large inlet subcooling, corresponding to a large thermal desequilibrium.

10.3.3 CANON

The pressure at the end of the initial abrupt decrease is overpredicted, due to the lack of a delayed boiling model, or to the experimental initial temperature stratification. The predicted voidage of the test section is somewhat too fast for the tests with a break diamater equal to the pipe diameter, and somewhat too slow for the test with a break diameter smaller than the pipe diameter.

The simulations performed with natural choking predict too fast blowdowns, far from the data. The lack of a virtual mass term probably takes part in these bad predictions. A Courant stability criterion reduces sharply the time step in case of fine mesh at the break.

10.3.4 SUPER-CANON

The pressure at the end of the initial abrupt pressure decrease is overpredicted, due to the lack of a delayed boiling model, or to the experimental initial temperature stratification. After the boiling inception, the predictions agree well with the data, except in the bottom end of the test section, where the final pressure decrease is anticipated.

The simulations performed with natural choking predict too fast blowdowns, far from the data. The lack of a virtual mass term probably takes part in these bad predictions. A Courant stability criterion reduces sharply the time step in case of fine mesh at the break.

10.3.5 VERTICAL-CANON

Good agreement with the data is obtained, except a too slow liquid level decrease for one test, and pressures at the boiling inception are sligthly overpredicted.

Large void fraction oscillations occur at the transition between bubble-slug and annular flow regime, when the pressure is low, due to the sharp decrease of the interfacial shear stress. Low void fraction oscillations also correspond to the sharp decrease of the interfacial shear stress for the bubble-slug transition. The oscillations vanish when the size of the cells is increased.

The simulations performed with natural choking predict too fast blowdowns. A Courant stability criterion reduces sharply the time step in case of fine mesh at the break. This limitation is not found when the version 13.0 of TRAC is used, where the parameter CSFiD in subroutine TFiDSi had a value 1*10+6 instead of 1*10+3 in version 14.3.

10.3.6 MARVIKEN

The initial pressure undershoot is not predicted, due to the lack of a delayed boiling model.

The mass flow rate predicted with natural choking is in better agreement with the data than the mass flow rate predicted with the choked flow model, for the test with short nozzle, for which the interphase thermal desequilibrium is large. For the test with long nozzle, the results obtained with and without the choked flow model are quite identical.

10.3.7 OMEGA-TUBE

The pressure at the boiling inception is overpredicted, due to the lack of a delayed boiling model. The blowdown of the test section depends mainly on the voidage of the capacities into the test section or towards the break. The voidage of the capacities is not correctly predicted for some tests, for which an adequate model of the capacities was not found.

The Biasi critical heat flux correlation is not suitable for low qualities and for large mass flow rates, which induces anticipated boiling crisis.

The simulation performed with natural choking predicts a too fast blowdown, far from the data. A Courant stability criterion reduces sharply the time step in case of fine mesh at the break.

10.3.8 OMEGA-BUNDLE

The pressure at the boiling inception is overpredicted, due to the lack of a delayed boiling model. The voidage of the spheres into the test section and towards the break is well predicted. The violation of the Bernoulli equation in case of flow area variations induces a systematic initial discrepancy between the predicted and measured pressure drops in the spheres.

The use of a rod wall model with constant thickness prevents the derivation of conclusions concerning the wall temperatures.

The simulation performed with natural choking predicts a too fast blowdown. A Courant stability criterion reduces sharply the time step in case of fine mesh at the break.

10.3.9 Summary

10.3.9.1 General Agreement

The general agreement between the critical flow and blowdown tests and TRAC is moderate: the major trends are correctly predicted, and the thermal hydraulic phenomena are rather properly modelled. However, TRAC values are frequently outside the data uncertainties.

10.3.9.2 Break Flow

The break flow are predicted by TRAC with natural choking or with the choked flow model.

The choked flow model allows the use of large break cells, and is based on the hypothesis of interphase thermal desequilibrium. The choked flow model is convenient for fast transient test, like CANON, SUPER-CANON, VERTICAL-CANON, OMEGA-TUBE and OMEGA-BUNDLE tests, for which it works well.

The runs performed with natural choking are convenient for low transient or steady state tests. The lack of a virtual mass term probably takes a part in the poor agreement between tests and TRAC for fast transients. Furthermore the time step is sharply reduced for fast transients when a fine mesh at the break is used (see hereafter).

The runs performed with the choked flow or with natural choking give similar results for the steady state or low transient test without interphase thermal desequilibrium.

10.3.9.3 Constitutive Laws

No irremediable failure in the constitutive laws of TRAC was found. However some improvements should be made, concerning the CHF correlation, the boiling inception model and the interfacial shear stress coefficient (see hereafter).

10.3.9.4 Courant Stability Criterion

For all the tests with fast transient (CANON, SUPER-CANON, VERTICAL--CANON, OMEGA-TUBE, OMEGA-BUNDLE), a Courant stability criterion reduces sharply the time step, when a fine mesh at the break is used. The value of parameter CSF1D in subroutine TF1DS1 is questionable (see hereafter).

10.4 Recommended Code Improvements

10.4.1 Critical Heat Flux Correlation

The Biasi CHF correlation is used in TRAC. It is not suitable for low qualities and for large mass flow rates. Too early boiling crisis are then obtained for OMEGA-TUBE tests.

A CHF correlation more suitable for low qualities and large mass flow rates is needed.

10.4.2 Critical Flow

The use of the choked flow model gives poor agreement between TRAC and data for steady state or low transient tests with a large interphase thermal desequilibrium. On the other hand, natural choking gives poor agreement in case of fast transients, and the lack of a virtual mass term may take a part in these discrepancies.

Improvements are needed in order to predict break flows without the help of any model. Meanwhile an improvement of the choked flow model is needed in order to take into account the interphase thermal desequilibrium.

10.4.3 Delayed Boiling Model

The predicted boiling inception corresponds to the saturation pressure. The inception of boiling is then predicted too early in the simulation of quite all the tests. For the low pressure steady state tests MOBY-DICK, the experimental liquid overheating is 2 through 3 K, and the discrepancy between the predicted boiling inception pressures is sensi-

tive. For the high pressure steady state tests SUPER-MOBY-DICK, the pressure discrepancy is less sensitive, and the analysis is more difficult because the boiling often beginns in the inlet converging nozzle, where the pressure gradient is large, and because the data accuracy leads to a difficult determination of the experimental boiling inception point. For the blowdown tests (CANON, SUPER-CANON, VERTICAL-CANON, MARVIKEN, OMEGA-TUBE and OMEGA-BUNDLE), the predicted pressure after the first sharp pressure decrease, corresponding to the boiling inception, is too high, with a discrepancy that depends on the test, and may be as high as 0.8 MPa.

A delayed boiling model is needed.

10.4.4 Bernoulli Equation

In case of flow area variations, the predicted pressure drops in liquid single phase flow regime do not follow the Bernoulli equation. The discrepancy between the predicted and measured pressure drops in the inlet convergent of the SUPER-MOBY-DICK test section is then large, and a fine nodalization of the convergent is needed to ensure a valuable comparison with data. This discrepancy is also found between the predicted and measured pressure drops in the spherical capacities of the OMEGA-BUNDLE test section.

The adequacy between the predicted pressure drops and the Bernoulli equation in case of flow area variations is needed.

10.4.5 Interfacial Shear Stress

The sharp decrease of the interfacial shear stress coefficient at the transition between bubble-slug and annular flow leads to large void fraction oscillations at low pressure (less than 1 Mpa), in case of vertical upflow (MOBY-DICK, VERTICAL-CANON). In the same conditions, but at the transition between bubble and slug flow regime, where the interfacial shear stress coeeficient also decreases, low void fraction oscillations may occur (VERTICAL-CANON). However, the oscillations are reduced when the cell size is increased.

More smooth decreases of the interfacial shear stress coefficient at the transitions between bubble and slug flow, and between bubble-slug and annular flow, for low pressures, are needed.

10.4.6 Rod Wall Thickness

The wall thickness of the rods in the test section OMEGA-BUNDLE is axially varying, in order to obtain a cosine heat flux profile. The wall temperature evolution depends on the wall thermal inertia, and the use of a constant thickness instead of a variable thickness is a simplification which prevents the obtention of realistic wall temperatures.

An axially varying rod wall thickness model is needed.

10.4.7 Time Step

In case of a fine mesh at the break (little cell sizes and large velocities), a Courant stability criterion calculated in subroutine TF1DS1 becomes very limitative (CANON, SUPER-CANON, VERTICAL-CANON, OMEGA-TUBE, OMEGA-BUNDLE). This was not found in the runs performed with version 13.0 of the code, where the value of parameter CSF1D was 1*10+6, instead of 1*10+3 in version 14.3.

The value of parameter CFS1D in subroutine TF1DS1 is questionable.

REFERENCES

CHAULIAC, Ch., 1982, Depressurisation d'un ensemble comportant une grappe de 36 barreaux chauffants, campagne d'essais réalisée de février 81 à janvier 82, Commissariat à l'Energie Atomique, Centre d'Etudes Nucléaires de Grenoble, SETh, Note TT/SETRE/82-26 (Tome 1: Présentation de l'expérience, méthode de dépouillement et analyse des résulats, Tome 2: Commentaire détaillé de 3 essais caractéristiques, Tome 3: Ensemble des résultats).

GUIZOUARN, L., PINET, B., BARRIERE, G., PIETRI, D., 1975, Etude expérimentale des débits critiques en écoulements diphasiques eau-vapeur à faible titre dans un canal avec divergent de 7 degrés, à des pressions au col de 2 à 7 bars, Commissariat à l'Energie Atomique, Centre d'Etudes Nucléaires de Grenoble, SETh, Note TT 501.

GULLY, Ph., BLANC, J.P., 1982, Expérience CANON VERTICAL: décompression lente d'une capacité tubulaire verticale par une brèche en partie supérieure, Commissariat à l'Energie Atomique, Centre d'Etudes Nucléaires de Grenoble, SETh, Note TT/SETRE/82-10.

JEANDEY, Ch., GROS D'AILLON, L., BOURGINE, R., BARRIERE, G., 1981, Autovaporisation d'écoulements eau-vapeur, Commissariat à l'Energie Atomique, Centre d'Etudes Nucléaires de Grenoble, SETh, Rapport TT 163.

JEANDEY, Ch., GROS D'AILLON, L., BARRIERE, G., BOURGINE, R., VERDUN, C., 1983, Mesure de débits critiques sur l'installation SUPER-MOBY-DICK dans une section d'essais comportant un divergent ou un élargissement brusque, Commissariat à l'Energie Atomique, Centre d'Etudes Nucléaires de Grenoble, SETh, Note TT/SETRE/82-32.

JEANDEY, Ch., GROS D'AILLON, L., 1983, Débit critique en tuyère courte SUPER-MOBY-DICK, Commissariat à l'Energie Atomique, Centre d'Etudes Nucléaires de Grenoble, SETh, Note TT/SETRE/71.

JUHEL, D., 1980, Boucle OMEGA, Essais de dépressurisation en géométrie tubulaire, résultats de la seconde campagne, Commissariat à l'Energie Atomique, Centre d'Etudes Nucléaires de Grenoble, SETh, Rapport TT 158 (Tome 1: Description du dispositif expérimental, corrections apportées aux mesures, mode de dépouillement, Tome 2: Description détaillée de trois essais caractéristiques, Tome 3: Résultats des 26 essais dépouillés).

MARVIKEN, 1982a, The Marviken Full Scale Critical Flow Tests, Summary Report, MXC-301.

MARVIKEN, 1982b, The Marviken Full Scale Critical Flow Tests, Description of the Test Facility, MXC-101.

MARVIKEN, 1982c, The Marviken Full Scale Critical Flow Tests, Data Accuracy, MXC-104.

MARVIKEN, 1979a, The Marviken Full Scale Critical Flow Tests, Results from Test 17, MXC-217.

MARVIKEN, 1979b, The Marviken Full Scale Critical Flow Tests, Results from Test 24, MXC-224.

REOCREUX, M., 1974, Contribution à l'étude des débits critiques en écoulement diphasique eau vapeur, Thèse de Docteur ès-Sciences Physiques, Université Scientifique et Médicale de Grenoble.

RIEGEL,B., MARECHAL, A., 1977, Expérience CANON: dépressurisation d'une capacité en double phase eau-vapeur, Commissariat à l'Energie Atomique, Centre d'Etudes Nucléaires de Grenoble, SETh, Note TT 547.

RIEGEL,B., 1979, Expérience SUPER-CANON: compte-rendu des essais à 150 bars, Commissariat à l'Energie Atomique, Centre d'Etudes Nucléaires de Grenoble, SETh, Note TT/SETRE/82-10.

NRCM 1102, 3201, 3202

U.S. NUCLEAR REGULATORY COMMISSION

BIBLIOGRAPHIC DATA SHEET

SEE INSTRUCTIONS ON THE REVERSE

1 REPORT NUMBER (Assigned by TIDC, add Vol. No., if any)
NUREG/IA-0023
SETh/LEML/88-138
Vol. 1

2 TITLE AND SUBTITLE
Assessmeht of TRAC-PF1/MOD1 Version 14.3 Using Separate Effects Critical Flow and Blowdown Experiments Volume 1: Text and Tables

3 LEAVE BLANK

4 DATE REPORT COMPLETED
MONTH: September YEAR: 1988

5 AUTHOR(S)
B. Spindler, M. Pellissier

6 DATE REPORT ISSUED
MONTH: April YEAR: 1990

7 PERFORMING ORGANIZATION NAME AND MAILING ADDRESS (Include Zip Code)
Commission of Atomic Energy
CENG/SETH
85X - 38041 Grenoble CEDEX
France

8 PROJECT/TASK/WORK UNIT NUMBER

9 FIN OR GRANT NUMBER

10 SPONSORING ORGANIZATION NAME AND MAILING ADDRESS (Include Zip Code)
Office of Nuclear Regulatory Research
U. S. Nuclear Regulatory Commission
Washington, DC 20555

11a TYPE OF REPORT
Technical Report

b PERIOD COVERED (Inclusive dates)

12 SUPPLEMENTARY NOTES

13 ABSTRACT (200 words or less)

Independent assessment of the TRAC code was conducted at the Centre d'Etudes Nucleaires de Grenoble of the Commissariate a l'Energie Atomique (France) in the frame of the ICAP.

This report presents the results of the assessment of TRAC-PF1/MOD1 version 14.3 using critical flow steady state tests (MOBY-DICK, SUPER-MOBY-DICK), and blowdown tests (CANNON, SUPER-CANNON, VERTICAL-CANON, MARVIKEN, OMEGA-TUBE, OMEGA-BUNDLE).

14 DOCUMENT ANALYSIS - a KEYWORDS/DESCRIPTORS
TRAC-PF1, ICAP Program, Separate Effects

b IDENTIFIERS/OPEN-ENDED TERMS

15 AVAILABILITY STATEMENT
Unlimited

16 SECURITY CLASSIFICATION
(This page)
Unclassified
(This report)
Unclassified

17 NUMBER OF PAGES

18 PRICE

UNITED STATES
NUCLEAR REGULATORY COMMISSION
WASHINGTON, D.C. 20555